arXiv:2611.33997v1 [q-bio.QM] 25 Nov 2026

Milk-removal feedback shapes lactation sustainability and daily output in a model of human lactation

Angelika Manhart*[1] and Tobias Müller[1]

[1]Faculty of Mathematics, University of Vienna, Austria

Abstract

Milk production during lactation is dynamically regulated by milk removal, yet quantitative models linking feeding or pumping schedules to subsequent production remain scarce. We develop a minimal model describing milk accumulation and production between removal sessions, and the stimulation of subsequent production through milk removal.

We compare different assumptions about how stimulation depends on the amount of milk removed or the duration of removal, and consider two removal protocols: prescribing either the removed amount or the removal duration. When stimulation depends on the removed amount, declining production can reduce subsequent stimulation and reinforce the decline. This leads to a critical wait interval beyond which no repeated constant schedule can sustain lactation. If stimulation is inefficient for small removal amounts but more efficient at intermediate amounts, the model can exhibit bistability: depending on the initial conditions, milk production either persists or ceases. In contrast, duration-dependent stimulation does not permit a zero-production state under continued removal, but can generate non-constant long-term dynamics under certain conditions.

We further show that maximizing milk removal per session need not maximize daily output, because increased removal competes with session frequency. The framework provides a basis for testing alternative feedback hypotheses against longitudinal data and for optimizing feeding and pumping schedules.

Keywords: human lactation; milk-removal feedback; hybrid dynamical systems; discrete dynamical systems; long-term behaviour

2020 MSC: 92C30, 37N25, 39A30, 37C25, 92-10.

1 Introduction

Why we need a quantitative understanding of lactation. Human lactation affects a large proportion of mothers and infants, yet difficulties in establishing or maintaining an adequate milk supply are common and are a frequent source of concern during breastfeeding and pumping (Gatti 2008). Human milk provides appropriate nutrition as well as immune and other bioactive components to the infant, making the successful establishment and maintenance of lactation clinically and practically important. This is especially true for prematurely born babies (Haiden and Ziegler 2016). At the same time, the regulation of milk production is inherently dynamic: milk removal alters subsequent production, but much of the practical guidance available to mothers remains

*Corresponding author: angelika.manhart@univie.ac.at, ORCID: 0000-0002-0303-8114

qualitative. A quantitative mechanistic framework could therefore help translate general principles such as frequent and effective milk removal into more precise predictions about how feeding or pumping schedules influence milk supply. Ultimately, such models could be used to address practical questions including how lactation is best established, how supply can be maintained or increased under time and scheduling constraints, how pumping schedules can be optimized, and how lactation can be reduced or stopped in a controlled manner. Before making such predictions, however, it is important to understand which qualitative behaviours arise robustly from the underlying feedback structure and how they depend on specific assumptions about how milk removal stimulates subsequent production.

Removing milk stimulates milk production. Human milk is synthesized and secreted by mammary epithelial cells lining the alveoli of the lactating breast. During breastfeeding or pumping, milk is transported from the alveoli through the ductal system and removed from the breast. Once lactation is established, milk production is strongly regulated by milk removal, allowing supply to adapt to demand (Truchet and Honvo-Houéto 2017; Kent et al. 2012). In particular, short-term measurements in lactating women indicate that the subsequent rate of milk synthesis is associated with the degree to which the breast is emptied during milk removal (Daly et al. 1996). Several mechanisms have been implicated in this local feedback, including mechanical stretching of the mammary epithelium or local biochemical feedback signals within the breast (Weaver and Hernandez 2016; Truchet and Honvo-Houéto 2017; Peaker and Wilde 1996). If milk is not removed for sufficiently long periods, milk synthesis declines and the mammary gland eventually enters involution (Truchet and Honvo-Houéto 2017), the process by which the lactating mammary gland returns toward its non-lactating state.

In addition to the *local* feedback, milk removal also stimulates lactation through neuroendocrine pathways, whereby nipple stimulation triggers neural signals that induce the release of hormones including oxytocin and prolactin (McNeilly et al. 1983). Oxytocin induces contraction of myoepithelial cells surrounding the alveoli and thereby drives milk ejection, whereas prolactin supports milk synthesis and secretory activity of mammary epithelial cells (Truchet and Honvo-Houéto 2017). However, the relationship between stimulation and subsequent milk production is not straightforward: for example, although prolactin is released in response to nipple stimulation, circulating prolactin concentrations during established lactation are not directly correlated with the short-term rate of milk synthesis (Cox et al. 1996). Thus, the physiological feedback from a milk-removal event to subsequent production likely combines neuroendocrine stimulation with local effects associated with the amount of milk removed. In our model we therefore describe this feedback phenomenologically and consider separately stimulation that depends on the duration of milk removal and stimulation that depends on the amount removed.

On the state of lactation modelling. Despite extensive experimental work on human lactation, its dynamic regulation has received relatively little attention from mathematical modelling. Mechanistic models of the human lactating breast have primarily focused on the biomechanics and fluid dynamics of milk removal, including transport through the mammary ductal system and the mechanical processes involved in milk removal by the infant (Mortazavi et al. 2015, 2017; Azarnoosh and Hassanipour 2020). A notable exception is the MSc thesis of Faulkner (2019), which developed ordinary differential equation models coupling milk production and removal with hormonal, neural and local regulatory mechanisms, and used them to investigate the effect of feeding frequency. In other mammalian systems, particularly dairy cattle, mechanistic modelling has a longer history, ranging from models of mammary metabolism and secretory-cell dynamics to models explicitly link-

ing udder filling and milking frequency to milk yield and mammary regression (Dijkstra et al. 1997; Vetharaniam et al. 2003). More recently, data-driven approaches have also been applied to human lactation, for example to predict breastfeeding outcomes or identify low milk supply from milk composition and maternal and infant characteristics (Agudelo-Pérez et al. 2024; Jin et al. 2025). However, these approaches do not describe the dynamic feedback between individual milk-removal events and subsequent milk production.

This work. In Sec. 2, we develop a minimal mechanistic model of the feedback between milk production, milk removal, and the stimulation of subsequent milk production. The model has a hybrid continuous–discrete structure: milk accumulation and changes in the production rate are described continuously between removal sessions, while breastfeeding or pumping sessions are represented as discrete removal and stimulation events (see Rem. 2.1 on impulsive systems). We use this framework to investigate several alternative assumptions about this feedback. First, we ask whether the stimulation of subsequent production depends primarily on the *amount* of milk removed or on the *duration* of the removal session. Second, we consider different possible *shapes* of the stimulation response: in particular, whether even small amounts of milk removal efficiently stimulate production, or whether stimulation is inefficient for small removals and becomes most efficient only at intermediate amounts. Finally, we compare two removal protocols: *set-target* removal, in which removal continues until a prescribed amount of milk has been obtained or the breast is emptied, and *set-duration* removal, in which milk is removed for a prescribed period of time and the amount obtained depends on the milk available. In Sec. 3 we study the resulting models in depth, focusing on long-term behaviour. In particular we determine under which conditions lactation can be sustained, and when the system instead progresses towards zero milk production. We will discuss how these outcomes depend on the initial state, biological parameters, and the removal schedule. In Sec. 4 we further investigate how these factors determine daily milk output and the trade-offs involved in increasing milk production. Finally, Secs. 5 and 6 summarize and discuss the findings. The *Interactive Lactation Explorer* (SI: Online Resource 1) allows readers to vary the model parameters and schedules and to follow the resulting dynamics in phase space and over time.

2 Model

Set-up. The model describes the feedback loop of milk production stimulation and milk removal for one breast. Here *milk removal* can refer to any mode of removing milk via the nipple, which can include breastfeeding, hand expressing or using a breast pump. Individual lobes are not resolved, rather we model the total amount of milk present in the breast m (in ml), and the underlying milk production rate, p (in ml per hour). We refer to the state $(m, p) = (0, 0)$ as the *involution state*, representing a state with no stored milk and zero milk-production rate within the present model. This terminology is used as a modelling shorthand: the model does not resolve the cellular and tissue-remodelling processes of mammary-gland involution.

Time is divided into alternating *wait* phases, during which no milk is removed and *removal* sessions, at which milk is removed and the production rate is updated in response, see Fig. 1. *Wait* intervals are typically much longer (several hours) than *removal* durations (tens of minutes). We therefore describe the wait phase in continuous time using ordinary differential equations, Fig. 1(a). While we account for the fact that removal sessions have a finite removal duration contributing to elapsed schedule time, we do not resolve production or decay during the removal session itself; instead, its effect is represented by discrete-in-time events, Fig. 1(b). We write m_n and p_n for the

milk volume and production rate immediately after the n-th removal session, with (m_0, p_0) denoting the prescribed initial state. For $n \geq 1$, T_n denotes wait interval, which is the length of the wait phase before the n-th removal session.

Remark 2.1 (Relation to impulsive systems). Mathematically, the model belongs to the class of impulsive differential equations (Lakshmikantham and Simeonov 1989): the state evolves according to an ordinary differential equation between sessions and jumps instantaneously at each session. Such systems have been used, for example, to describe pulse vaccination, drug dosing and periodic harvesting, and are typically analysed through the map obtained by composing the flow over one period with the jump. In the language of impulsive harvesting (Clark 1990; Zhang et al. 2003; Lawson and Braverman 2023), set-duration and set-target removal correspond to proportional and constant-quota harvesting, respectively. Unlike in standard harvesting models, however, removal here also stimulates subsequent production.

Removal schedules. A removal schedule specifies the prescribed timing and removal protocol over successive removal cycles (see details in Sec. 2.3). Under a *set-duration protocol*, a schedule is given by the sequence

$$(T_n, \tau_n), \qquad n = 1, 2, \ldots$$

where T_n is the wait interval preceding the n-th removal session and τ_n is its prescribed duration. Under a *set-target protocol*, a schedule is given by the sequence

$$(T_n, M_{\mathrm{tar},n}), \qquad n = 1, 2, \ldots$$

where $M_{\mathrm{tar},n}$ is the prescribed target amount for the n-th removal session. Throughout this work we consider *regular schedules*, meaning that the same schedule is repeated after every removal session:

$$(T_n, \tau_n) \equiv (T, \tau) \quad \text{or} \quad (T_n, M_{\mathrm{tar},n}) \equiv (T, M_{\mathrm{tar}}).$$

Note that the state variables m_n, p_n, the amount actually removed M_n, and, under set-target removal, the resulting session duration τ_n, may nevertheless vary between sessions.

2.1 Wait phase

Consider a wait interval of length $T > 0$ prior to the n-th removal session. During the time $t \in [0, T]$ milk is produced and accumulates in the breast at rate $p(t)$ and decays (e.g. through reabsorption) at rate $\delta > 0$, while, in the absence of stimulation, the production rate itself decays at rate γ:

$$\dot{m} = p - \delta m, \qquad \dot{p} = -\gamma p, \tag{1}$$

for $t \in [0, T]$. The initial conditions are given by the amount of milk in the breast, and the production rate directly after the previous removal event:

$$m(0) = m_{n-1}, \qquad p(0) = p_{n-1}. \tag{2}$$

Solving this system forward to $t = T$ gives $m(T; m_{n-1}, p_{n-1})$ and $p(T; p_{n-1})$, the state of the breast immediately before the next removal session. In the following we define $x_n := m(T; m_{n-1}, p_{n-1})$ to simplify notation.

Remark 2.2. Here we assume that the production rate simply follows exponential decay. However, it has been suggested that there is a negative feedback between the amount of milk in the breast (or breast fullness) and the production rate (Peaker and Wilde 1996). A more general model would therefore have the form $\dot{p} = f(p, m)$ where f is a decreasing function of m.

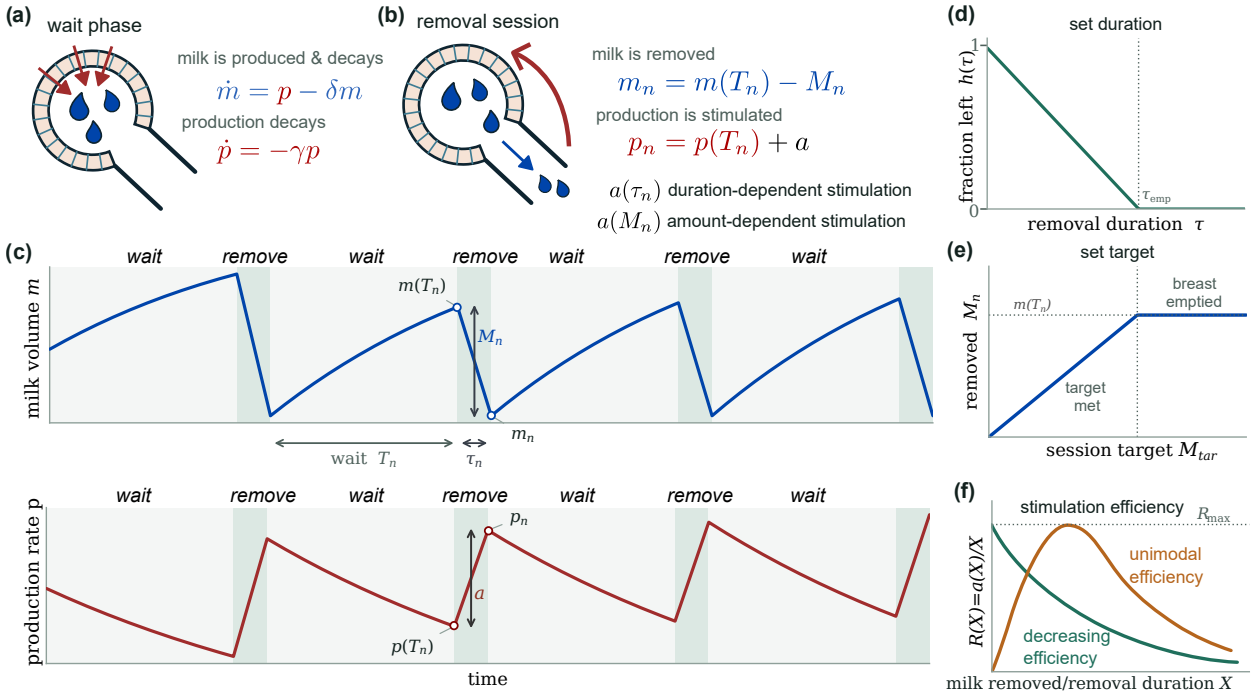

Figure 1: Model. (a),(b) Schematics of the two phases of a cycle. During the wait phase milk is produced and secreted into the lumen of the alveolus. At a removal session milk drains through the duct and the removal stimulates future production. (c) Development of amount of milk in the breast (m, upper panel) and production rate (p lower panel) during wait and removal phases. Note that we model removal sessions as discrete (short) events, while in the figure removal durations are extended for graphical clarity. (d) For a set-duration removal protocol, the fraction of milk left behind is $h(\tau) = \max\{1 - \nu\tau, 0\}$. (e) For a set-target protocol, the removed volume is $\min\{M_{\text{tar}}, m(T_n)\}$. (f) The two stimulation efficiency classes considered.

2.2 Removal session

At a removal session, a volume M_n (in ml) with $0 \le M_n \le x_n$ of milk is removed from the breast. This removal stimulates future production via an increment a (in ml per hour), which can depend on the amount of removed milk M_n and/or the removal duration τ_n. We will discuss the first option in Sec. 3.1, 3.2 and the second option in Sec. 3.3, 3.4,

$$m_n = x_n - M_n, \tag{3}$$

$$p_n = p(T; p_{n-1}) + a(M_n, \tau_n). \tag{4}$$

The removal session is then followed by a new wait phase, starting from m_n, p_n.

2.3 Modelling the removed amount of milk M_n

If x is the amount of milk in the breast directly prior to removal and $\tau > 0$ (in hours) is the length of the removal session, we model the amount of milk removed by

$$M(x, \tau) = x\,(1 - h(\tau))\,, \tag{5}$$

where $h(\tau) \in [0,1]$ the fraction of milk remaining in the breast at the end of a removal session of length τ. We use the linear law, see Fig. 1(d),

$$h(\tau) = \max\{1 - \nu\tau, 0\}.$$

The removal rate parameter is denoted by $\nu > 0$ (per hour), where ν can vary with infant age, pump type, pump setting, etc. Complete emptying occurs at $\tau = \frac{1}{\nu} =: \tau_{\text{emp}}$. One alternative would be to use the exponential removal law $h(\tau) = e^{-\nu\tau}$; we do not consider this alternative further, since it cannot describe complete emptying of the breast.

We consider two possible *removal protocols* of how to decide when to stop a removal session and to determine the volume M_n removed: In the first case, the removal duration τ is set, and the pumping or feeding is stopped after that time. In the second case, the target amount of removed milk is set and the pumping or feeding is stopped when the target is met, or when the breast is emptied.

Set-duration removals. The schedule is given by (T, τ), i.e. in addition to the wait interval T we set the removal duration τ. Then we obtain

$$M_n = x_n \left(1 - h(\tau)\right).$$

Set-target removals. Here the schedule is given by (T, M_{tar}), i.e. in addition to the length of the wait interval, we prescribe a target amount of removed milk M_{tar} (in ml). This can represent infant demand or a pumping goal. The volume actually removed is capped by the milk available in the breast, see Fig. 1(e):

$$M_n = \min\{M_{\text{tar}},\, x_n\}. \tag{6}$$

In this case the associated removal duration τ_n (which now depends on the session index n) is defined using (5) by

$$\tau_n = \begin{cases} \frac{M_{\text{tar}}}{x_n}\tau_{\text{emp}}, & x_n > M_{\text{tar}} \\ \tau_{\text{emp}}, & x_n \le M_{\text{tar}}. \end{cases}$$

2.4 Modelling the stimulation function $a(M, \tau)$

The stimulation function a describes how strongly the removal of milk up-regulates subsequent production. In the following we will focus on two scenarios: 1. Stimulation primarily depends on the amount of milk removed, $a = a(M)$, see Sec. 3.1 and 3.2. 2. Stimulation primarily depends on the duration of milk removal, $a = a(\tau)$, see Sec. 3.4 and 3.3. We do not consider stimulation functions that depend on M and τ simultaneously.

We assume that $a \in \mathcal{C}^1([0,\infty))$, $a(0) = 0$, with a strictly increasing, bounded and with limiting value $a_{\max} > 0$ for large inputs. We also introduce the associated *stimulation efficiencies* $R(X)$, where X can be M or τ,

$$R(X) = \frac{a(X)}{X}, \qquad X > 0,$$

we extend the corresponding efficiency continuously to zero by $a'(0)$.

Table 1: State variables, schedule quantities, model parameters, and derived quantities.

Symbol	Units	Meaning
State variables and schedule quantities		
m	ml	Amount of milk in the breast.
p	$\mathrm{ml\,h^{-1}}$	Milk production rate.
T	h	Wait interval between consecutive removal sessions.
τ	h	Duration of a removal session.
M	ml	Amount of milk removed during a removal session.
M_{tar}	ml	Prescribed amount to be removed under a set-target protocol.
Model parameters and response functions		
δ	$\mathrm{h^{-1}}$	Rate of milk loss from the breast during the wait phase.
γ	$\mathrm{h^{-1}}$	Decay rate of the milk production rate in the absence of stimulation.
ν, $\quad \tau_{\mathrm{emp}} = \frac{1}{\nu}$	$\mathrm{h^{-1}}$, h	ν: Removal-rate parameter. τ_{emp}: Emptying duration.
$h(\tau)$	1	Fraction of the milk available after a removal session of duration τ.
$a(M)$, $a(\tau)$	$\mathrm{ml\,h^{-1}}$	Increase in production rate induced by removing an amount M of milk/a removal session of duration τ.
$a_{\max}$	$\mathrm{ml\,h^{-1}}$	Saturation value of the stimulation response.
μ_M, μ_τ	ml, h	Characteristic amount scale of the amount/duration-dependent stimulation response.
Frequently used derived quantities		
$d(T) = e^{-\delta T}$	1	Fraction of stored milk remaining after a wait interval T in the absence of new production.
$g(T) = e^{-\gamma T}$	1	Fraction of the production rate remaining after a wait interval T.
$G(T)$	h	Factor describing the contribution of milk production during a wait interval T to the milk available before removal.
$x = md(T) + pG(T)$	ml	Amount of milk available immediately before a removal session.

The analysis below considers two structurally different *efficiency classes*, see Fig. 1(f). In a *decreasing-efficiency* response, R is largest for very small arguments and is monotonically decreasing. In a *unimodal-efficiency* response, R is small near zero, rises to a maximum at an intermediate value, and then decreases again. These properties, rather than the particular functional form for a, determine the qualitative dynamics.

Examples. For illustrations and closed-form examples, we use two simple saturating responses. Let $X \in \{M, \tau\}$ for amount-dependent and duration-dependent stimulation respectively and let μ_X have the same units as X.

The *Michaelis–Menten* response (also called a *Type-II functional response*)

$$a(X) = a_{\max} \frac{X}{X + \mu_X} \tag{7}$$

is concave and has strictly decreasing efficiency $a(X)/X = a_{\max}/(X + \mu_X)$.

The *Hill* response (also called a *Type-III functional response*)

$$a(X) = a_{\max}\frac{X^2}{X^2+\mu_X^2} \tag{8}$$

has a sigmoidal form and has unimodal efficiency, with its maximum at $X = \mu_X$.

The explicit forms are used only for examples and figures; the analytical results below are formulated in terms of the shape of the corresponding efficiency function.

2.5 Full Model

An advantage of the model formulation is that the solution to (1),(2) can be determined explicitly using the standard variations-of-constants method for solving differential equations. One obtains for a general time $t \in [0, T]$

$$m(t; m_{n-1}, p_{n-1}) = m_{n-1}d(t) + p_{n-1}G(t), \qquad p(t, p_{n-1}) = p_{n-1}g(t)$$

where

$$g(t) = e^{-\gamma t}, \qquad d(t) = e^{-\delta t}, \qquad G(t) = \frac{e^{-\gamma t} - e^{-\delta t}}{\delta - \gamma}.$$

Note that for $\delta = \gamma$ we have $G(t) = te^{-\gamma t}$. We see that the milk in the breast just prior to removal $x_n = m(T; m_{n-1}, p_{n-1})$ has two contributions: The first term describes the decay of the left-over milk from the previous removal session. The second term describes the new milk produced since the last session.

For a regular schedule, the wait and removal phases therefore define an autonomous discrete dynamical system

$$\begin{pmatrix} m_n \\ p_n \end{pmatrix} = F\begin{pmatrix} m_{n-1} \\ p_{n-1} \end{pmatrix}.$$

where, writing

$$g = g(T), \qquad d = d(T), \qquad G = G(T), \qquad x_n = d\,m_{n-1} + G\,p_{n-1},$$

one cycle is given by

$$m_n = x_n - M_n, \qquad p_n = g\,p_{n-1} + a(M_n, \tau_n).$$

The quantities M_n and τ_n are determined by the chosen removal protocol as described above.

Tab. 1 summarizes the main model variables.

3 Model Analysis

The main goal is to understand how system long-term behaviour depends on the stimulation mechanism (amount-dependent or duration-dependent), the removal protocol (set-target or set-duration) and the efficiency class (decreasing efficiency or unimodal efficiency). In order to make the main narrative and insights easier to follow, the main text focuses on results and interpretation. Technical details and proofs are collected in the Appendix. For the same reason, non-generic boundary cases are generally excluded in the statements. We encourage readers to follow the analysis below with the *Interactive Lactation Explorer* (Online Resource 1), in which phase planes, orbits and schedule spaces can be recomputed for any parameter choice.

We define the key quantity

$$\Gamma = \Gamma(T) := \frac{1-g}{G}. \tag{9}$$

The quantity $\Gamma(T)$ will repeatedly arise as the stimulation efficiency required to balance the decay of the production rate over one removal cycle.

Here is an overview over the analysis sections of the four discussed cases:

	Set-target protocol	**Set-duration protocol**
Amount-dependent stimulation	Sec. 3.1 (Proofs in App. 8.1)	Sec. 3.2 (Proofs in App. 8.2)
Duration-dependent stimulation	Sec. 3.4 (Proofs in App. 8.4)	Sec. 3.3 (Proofs in App. 8.3)

Then in Sec. 3.5 we discuss in more detail how protocol choice affects the long-term dynamics. We start by analysing amount-dependent stimulation under a set-target removal protocol.

3.1 Amount-dependent stimulation, set-target protocol

Preliminaries. Throughout this section we assume that production stimulation depends on the amount of milk removed during removal sessions, i.e. $a = a(M)$ with $a : [0,\infty) \to [0, a_{\max})$ is C^1, strictly increasing, bounded, satisfies $a(0) = 0$, and has finite saturation level $a_{\max}$.

Further the schedule (T, M_{tar}) is fixed with $T > 0$ and $M_{\text{tar}} > 0$, and we use a set-target removal protocol: The amount of removed milk is the minimum of the session target M_{tar} and the available milk.

We abbreviate

$$a_{\text{tar}} = a(M_{\text{tar}}), \quad R_{\text{tar}} = R(M_{\text{tar}}), \tag{10}$$

where $R(M) = a(M)/M$ is the stimulation efficiency as defined and discussed in Sec. 2.4. The state space is $X = [0,\infty)^2$ and the dynamics is generated by the map $F : X \to X$,

$$F(m,p) = \Big(\max\{x - M_{\text{tar}},\, 0\},\ \ p\,g + a\big(\min\{M_{\text{tar}},\, x\}\big)\Big), \tag{11}$$

where $x = md + pG$ is the amount of milk in the breast just prior to removal. Lem. 8.1 and Lem. 8.2 in App. 8.1 establish basic monotonicity and boundedness results.

We call $E = \{z \in X :\ x(z) \le M_{\text{tar}}\}$ the *emptying region*: on E all milk available immediately before the session is removed. If $x < M_{\text{tar}}$ the target cannot be met, while on the boundary $x = M_{\text{tar}}$ the target is met exactly and the breast is emptied. We call $E^c := X \setminus E$ the *target-met region*: Here the target is met with milk left behind. See also Fig. 3 and Fig. 5.

Fixed points in the target-met region E^c. On E^c the map F reduces to the affine map

$$F(m,p) = \big(x - M_{\text{tar}},\ p\,g + a(M_{\text{tar}})\big). \tag{12}$$

Solving the fixed point equation $F(z) = z$ gives a unique fixed point $z_{\text{tar}} = (m_{\text{tar}}, p_{\text{tar}})$, the *target-met fixed point*, given by

$$p_{\text{tar}} = \frac{a(M_{\text{tar}})}{1-g} = \frac{M_{\text{tar}} R_{\text{tar}}}{G\Gamma}, \qquad m_{\text{tar}} = \frac{p_{\text{tar}} G - M_{\text{tar}}}{1-d} = \frac{M_{\text{tar}}}{1-d}\left(\frac{R_{\text{tar}}}{\Gamma} - 1\right). \tag{13}$$

For z_{tar} to lie in E^c it has to fulfill $z_{\text{tar}} \in X$ and $x(z_{\text{tar}}) > M_{\text{tar}}$. It is easy to see that this is equivalent to

$$R_{\text{tar}} > \Gamma(T). \tag{14}$$

Fixed points in the emptying region E. On E the map F becomes

$$F(m,p) = \big(0,\ p\,g + a\big(x(m,p)\big)\big).$$

We see that the first component of F vanishes, so every point of E is mapped onto the p-axis. While an orbit lies on the p-axis within the emptying region, its dynamics reduces to the scalar map

$$\Phi(p) = gp + a(Gp),$$

with

$$\Phi(p) - p = pG\big(R(Gp) - \Gamma\big).$$

Hence the sign of $R-\Gamma$ determines whether production increases or decreases along the p-axis. The resulting scalar dynamics for the decreasing- and unimodal-efficiency cases is used in the proofs of the global results and is detailed in App. 8.1 in Lem. 8.6 and Lem. 8.7.

Fixed points in E all have $m = 0$ and are given by $z_0 = (0,0)$ and $(0,p)$ with $p > 0$ a solution to

$$R(pG) = \Gamma(T). \tag{15}$$

For the resulting fixed point to lie in E, we need the associated volume of removed milk $x = pG$ to fulfil

$$pG \le M_{\text{tar}}. \tag{16}$$

Stimulation efficiency vs inter-session production loss. Eqs. (14) and (15) show that the key to understanding fixed point existence is the relation of two central quantities: $\Gamma(T)$, and the stimulation efficiency $R(M)$. Straight-forward calculations show that $\Gamma(T)$ is strictly increasing with $\lim_{T\to 0^+}\Gamma(T) = \gamma$ and $\lim_{T\to\infty}\Gamma(T) = \infty$. For R, we define

$$R_{\max} = \sup_{M>0} R(M). \tag{17}$$

Therefore, if $\gamma < R_{\max}$, there exists a unique $T_{\text{crit}} > 0$ defined by

$$\Gamma(T_{\text{crit}}) = R_{\max}. \tag{18}$$

For $T < T_{\text{crit}}$ there exists at least one solution $p > 0$ to (15) and a range of M_{tar} values that fulfil (14), see also Fig. 2(a) and Fig. 4(a). If $\gamma \ge R_{\max}$ then $\Gamma(T) > R_{\max}$ for all $T > 0$ and both (14) and (15) can never be fulfilled. In this case $z_0 = (0,0)$ is the only fixed point and we define $T_{\text{crit}} = 0$.

Thus T_{crit} represents the critical wait threshold below which sustained lactation can in principle be achieved. For $T_{\text{crit}} = 0$ no positive wait interval can sustain lactation. If $0 < T < T_{\text{crit}}$, there exists a range of removed volumes for which stimulation exceeds inter-session production loss. These considerations also show that $\Gamma(T)$ can be interpreted as the wait-interval dependent stimulation efficiency required to balance between-session production loss. Next we will discuss how the existence of the fixed points depend on the shape of R.

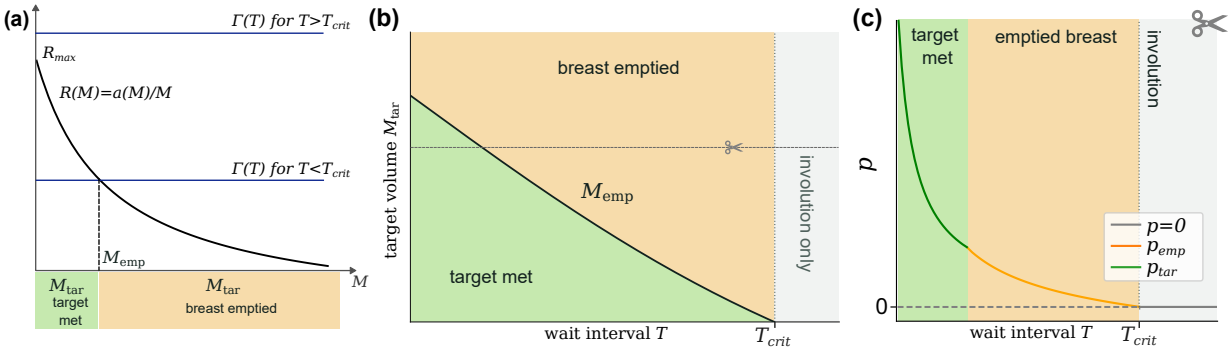

Figure 2: Decreasing-efficiency stimulation, illustrated with the Michaelis–Menten response in (7) with $\gamma < R_{\max}$. (a) The stimulation efficiency $R(M)$ and its intersection with $\Gamma(T)$ for $T > T_{\text{crit}}$ (no intersection) and $T < T_{\text{crit}}$ (one intersection). (b) The corresponding schedule space (T, M_{tar}). For $T < T_{\text{crit}}$ the maximal achievable target curve $M_{\text{emp}}(T)$, defined in (19), separates the schedule space: for $M_{\text{tar}} > M_{\text{emp}}$ the target is not met at the attractor and the breast is always emptied (orange), for $M_{\text{tar}} < M_{\text{emp}}$ the target is met with milk left behind (green), and for $T > T_{\text{crit}}$ the involution state is globally attracting (grey). The horizontal dashed-grey line indicates the slice shown in (c). (c) Slice through schedule space for a fixed value of M_{tar}. Shown are the steady state values of p as functions of T with solid lines indicating stable fixed points and dashed lines unstable ones.

Decreasing stimulation efficiency. We first consider responses for which stimulation efficiency $R(M) = a(M)/M$ is largest at small removed volumes and decreases thereafter, see also Sec. 2.4. We assume $R(M)$ is defined for $M \geq 0$ and fulfils $R'(M) < 0$ for $M > 0$, and $R(M) \to 0$ as $M \to \infty$. Then $R_{\max} = R(0) = a'(0)$, see Fig. 2(a).

We see that for $T < T_{\text{crit}}$, there exists a unique $M_{\text{emp}}(T) > 0$, such that

$$R(M_{\text{emp}}(T)) = \Gamma(T), \qquad R(M) > \Gamma(T) \quad \Longleftrightarrow \quad 0 < M < M_{\text{emp}}(T). \tag{19}$$

We write $p_{\text{emp}} = M_{\text{emp}}/G$, see (15), and call $(0, p_{\text{emp}})$ the *emptying fixed point*. Holding T fixed, we can now inspect how the existence of fixed points depend on the second scheduling parameter M_{tar}: If $M_{\text{emp}} < M_{\text{tar}}$ the emptying fixed point exists/lies in the emptying region, see (16). If $M_{\text{emp}} > M_{\text{tar}}$ the emptying fixed point does not exist, but the target-met fixed points exists, see (14). This is summarized in Fig. 2(a),(b).

Example: concave Michaelis–Menten response. For the Michaelis–Menten response from (7), i.e.

$$a(M) = a_{\max} \frac{M}{M + \mu_M},$$

one has $R(M) = a_{\max}/(M + \mu_M)$ and $R_{\max} = a_{\max}/\mu_M$. Hence for $T < T_{\text{crit}}$ we find, see Fig. 2(b),(c),

$$p_{\text{emp}} = \frac{\mu_M}{G}(\kappa - 1), \qquad M_{\text{emp}} = \mu_M(\kappa - 1), \qquad \kappa := \frac{R_{\max}}{\Gamma}. \tag{20}$$

This example of a decreasing-efficiency response is used in the figures, but the theorem below does not depend on this particular choice.

The following theorem establishes how system long-term behaviour depends on the scheduling parameters (T, M_{tar}):

Theorem 3.1. *Let $R(M) = a(M)/M$ be a decreasing-efficiency response as above.*

(i) If $T > T_{\text{crit}}$, then $z_0 = (0, 0)$ is the unique fixed point of F in X and it is globally asymptotically stable.

(ii) If $T < T_{\text{crit}}$ and $M_{\text{tar}} \neq M_{\text{emp}}$, then F has exactly two fixed points, namely z_0 and

$$z_2 = \big(m_{\text{tar}}, p_{\text{tar}}\big) \quad \text{with } m_{\text{tar}} > 0 \quad \text{if } M_{\text{tar}} < M_{\text{emp}}, \qquad z_2 = \big(0, p_{\text{emp}}\big) \quad \text{if } M_{\text{tar}} > M_{\text{emp}}.$$

The state z_0 is unstable, and z_2 attracts every other initial condition, i.e. the basin of attraction of z_2, $B(z_2) = X \setminus \{z_0\}$.

For proof see App. 8.1, for visualisations see Fig. 2 and Fig. 3.

Interpretation. Thm. 3.1 gives the following conclusion: whenever stimulation efficiency $R(M) = a(M)/M$ decreases with the removed volume, the schedule alone decides the long-term outcome. If $\gamma \geq R_{\max}$ sustained lactation is impossible for any schedule (T, M_{tar}) and involution occurs. In this case even the maximal stimulation efficiency cannot overcome the minimal production loss. If $\gamma < R_{\max}$, there exists a critical wait interval $T_{\text{crit}} > 0$. For wait intervals with $T > T_{\text{crit}}$, again lactation cannot be sustained, since stimulation cannot compensate for the intersession loss. However for wait intervals with $T < T_{\text{crit}}$, the system converges to a sustained lactation state from every nonzero starting state.

For such sufficiently short wait intervals $T < T_{\text{crit}}$ the sustained state can have two different forms depending on whether the session target M_{tar} lies below or above the maximal achievable target $M_{\text{emp}}(T)$. If $M_{\text{tar}} < M_{\text{emp}}$ the session target is met with milk left behind. If $M_{\text{tar}} > M_{\text{emp}}$, every session empties the available milk, and the target is not met. The shorter the intersession wait time T, the larger the maximal achievable target M_{emp}. These regimes are summarized in Fig. 2(b),(c).

Although the initial milk amount and production rate do not affect the long-term outcome, they can affect the transient route to the attractor. For example, Fig. 3(a) shows an orbit that initially undergoes complete emptying before production increases sufficiently for the session target to be met. The unimodal response considered next shows that a different efficiency profile can instead make the long-term outcome itself initial-state dependent.

Unimodal stimulation efficiency. Next we consider responses for which stimulation efficiency is weak for very small removals, maximal at an intermediate volume, and decreases again for large removals. Specifically, assume that $R(M) = a(M)/M$ extends continuously to $M = 0$ with $R(0) = 0$, has a unique maximum at $M = M_{\text{peak}} > 0$, satisfies $R'(M) > 0$ for $0 < M < M_{\text{peak}}$ and $R'(M) < 0$ for $M > M_{\text{peak}}$, and tends to zero as $M \to \infty$. Then $R_{\max} = R(M_{\text{peak}})$, see Fig. 4(a).

For $0 < T < T_{\text{crit}}$ $R(M) = \Gamma$ (compare (15) and see Fig. 4(a)) has exactly two positive solutions M_{sep} and M_{emp} with

$$M_{\text{sep}} < M_{\text{peak}} < M_{\text{emp}}, \qquad p_{\text{sep}} = M_{\text{sep}}/G, \quad p_{\text{emp}} = M_{\text{emp}}/G,$$

and

$$R(M) > \Gamma \qquad \Longleftrightarrow \qquad M_{\text{sep}} < M < M_{\text{emp}}. \tag{21}$$

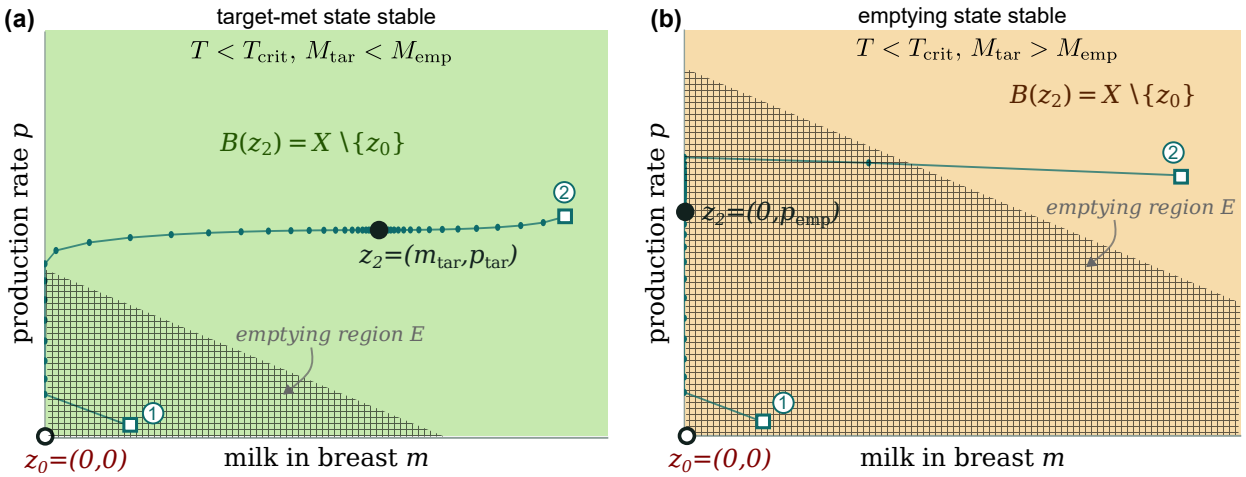

Figure 3: Phase planes for the set-target map (11) with a decreasing-efficiency response, illustrated with the Michaelis–Menten example of Fig. 2. The grey lattice pattern marks the emptying region E. The filled circle is the stable state z_2; the open circle at the origin is the unstable involution state z_0. In (a) z_2 is a target-met state in E^c, in (b) z_2 is an emptying state on the p-axis. Orbits (1),(2) show example behaviours.

Holding T fixed, we can now inspect how the existence of fixed points depend on the second scheduling parameter M_{tar}: The fixed point $z_0 = (0, 0)$ always exists. We see that for $M_{\mathrm{sep}} < M_{\mathrm{tar}} < M_{\mathrm{emp}}$ the target-met fixed point exists, see (14). Additionally the fixed point $(0, p_{\mathrm{sep}})$ in the emptying region exists, see (16). For $M_{\mathrm{emp}} < M_{\mathrm{tar}}$ the target-met fixed point does not exist, but the two fixed points in the emptying region exist, $(0, p_{\mathrm{sep}})$ and $(0, p_{\mathrm{emp}})$, see (16). If $M_{\mathrm{tar}} < M_{\mathrm{sep}}$ only $z_0 = (0, 0)$ exists. This is summarized in Fig. 4(a),(b).

Example: Sigmoidal Hill response. For the Hill response (8), i.e.

$$a(M) = a_{\max}\frac{M^2}{M^2 + \mu_M^2},$$

one has unimodal efficiency with $M_{\mathrm{peak}} = \mu_M$ and $R_{\max} = a_{\max}/(2\mu_M)$. For $T < T_{\mathrm{crit}}$, and defining $\kappa := R_{\max}/\Gamma$, the two thresholds are explicit, see Fig. 4(b),(c):

$$p_{\mathrm{sep}} = \frac{\mu_M}{G}\left(\kappa - \sqrt{\kappa^2 - 1}\right), \qquad p_{\mathrm{emp}} = \frac{\mu_M}{G}\left(\kappa + \sqrt{\kappa^2 - 1}\right), \tag{22}$$

$$M_{\mathrm{sep}} = \mu_M\left(\kappa - \sqrt{\kappa^2 - 1}\right), \qquad M_{\mathrm{emp}} = \mu_M\left(\kappa + \sqrt{\kappa^2 - 1}\right).$$

These closed forms are specific to the example; the global results below use only the shape of R.

The following definitions are useful for formulating the next theorem: The state space $X = [0, \infty)^2$ is equipped with the component-wise partial order: $(m, p) \le (\tilde{m}, \tilde{p})$ iff $m \le \tilde{m}$ and $p \le \tilde{p}$. A set $S \subseteq X$ is a *lower set* if $z \le w \in S$ implies $z \in S$, and an *upper set* if $z \ge w \in S$ implies $z \in S$.

The following theorem and corollary describe how the long-term dynamics depend on the scheduling parameters (T, M_{tar}) and the initial conditions.

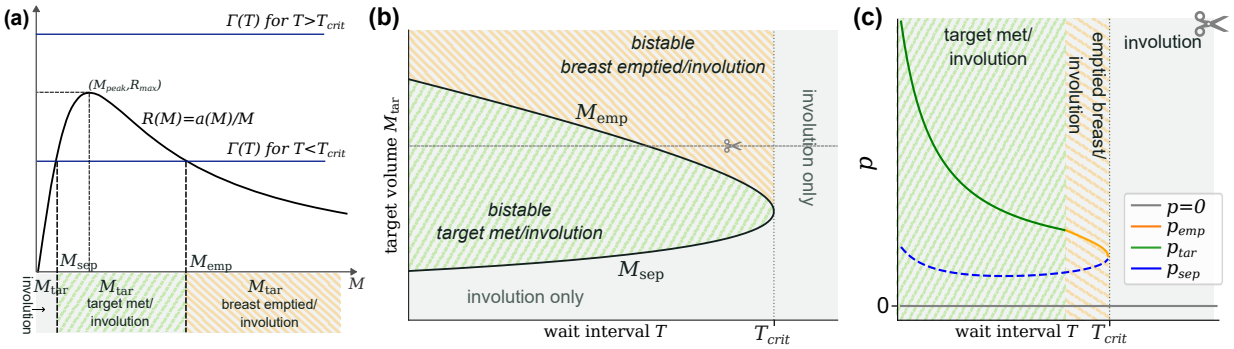

Figure 4: Unimodal-efficiency stimulation, illustrated with sigmoidal Hill response (8) for $\gamma < R_{\max}$. (a) The stimulation efficiency $R(M)$ and its intersection with $\Gamma(T)$ for $T > T_{\text{crit}}$ (no intersection) and $T < T_{\text{crit}}$ (two intersections). (b) The corresponding schedule space (T, M_{tar}). A globally attracting involution state is shown in grey, bistable regions are shown in two colours: green/grey whenever the target-met and the involution state are both stable, and orange/grey whenever the emptying state and the involution state are both stable. The horizontal dashed-grey line indicates the slice shown in (c). (c) Slice through schedule space for a fixed value of M_{tar}. Shown are the steady state values of p as functions of T. Solid lines indicate stable states, dashed lines unstable ones.

Theorem 3.2. *Let $R = a(M)/M$ be a unimodal-efficiency response as above. Assume $0 < T < T_{\text{crit}}$, $M_{\text{tar}} > M_{\text{sep}}$ and $M_{\text{tar}} \neq M_{\text{emp}}$. Then the following hold.*

(i) Fixed points. *F has exactly three fixed points in X: the involution state $z_0 = (0, 0)$; the state $z_1 = (0, p_{\text{sep}})$; and a third state*

$$\begin{cases} z_2 = (m_{\text{tar}},\, p_{\text{tar}}) \quad \text{with } m_{\text{tar}} > 0 & \text{if } M_{\text{tar}} < M_{\text{emp}}, \\ z_2 = (0,\, p_{\text{emp}}) & \text{if } M_{\text{tar}} > M_{\text{emp}}. \end{cases}$$

The states z_0 and z_2 are locally asymptotically stable, and z_1 is unstable.

(ii) Global behaviour. *Writing $B(z)$ for the basin of attraction of a fixed point z, we can write the state space in terms of the disjoint union*

$$X = B(z_0) \sqcup \Sigma \sqcup B(z_2), \qquad \Sigma = W^s(z_1),$$

where $W^s(z_1)$ is the stable set of the unstable fixed point z_1. Thus every orbit converges to one of the three fixed points. The set $B(z_0)$ is an open lower set and $B(z_2)$ is an open upper set.

(iii) Separatrix. *The separatrix Σ is the graph of a continuous, strictly decreasing function $\sigma : [0, \bar{m}_{\text{sep}}] \to [0, p_{\text{sep}}]$ with $\sigma(0) = p_{\text{sep}}$ and $\sigma(\bar{m}_{\text{sep}}) = 0$. Its explicit construction is detailed in App. 8.1.*

Corollary 3.3. *If $T > T_{\text{crit}}$, or if $0 < T < T_{\text{crit}}$ and $M_{\text{tar}} < M_{\text{sep}}$, then z_0 is the unique fixed point of F in X, and it is globally asymptotically stable.*

For proofs see App. 8.1, for visualisations see Fig. 4 and Fig. 5.

Interpretation

The critical-wait threshold T_{crit} and the distinction between target-met and emptying lactation states are unchanged from the decreasing-efficiency case. However, the unimodal efficiency response introduces two additional features:

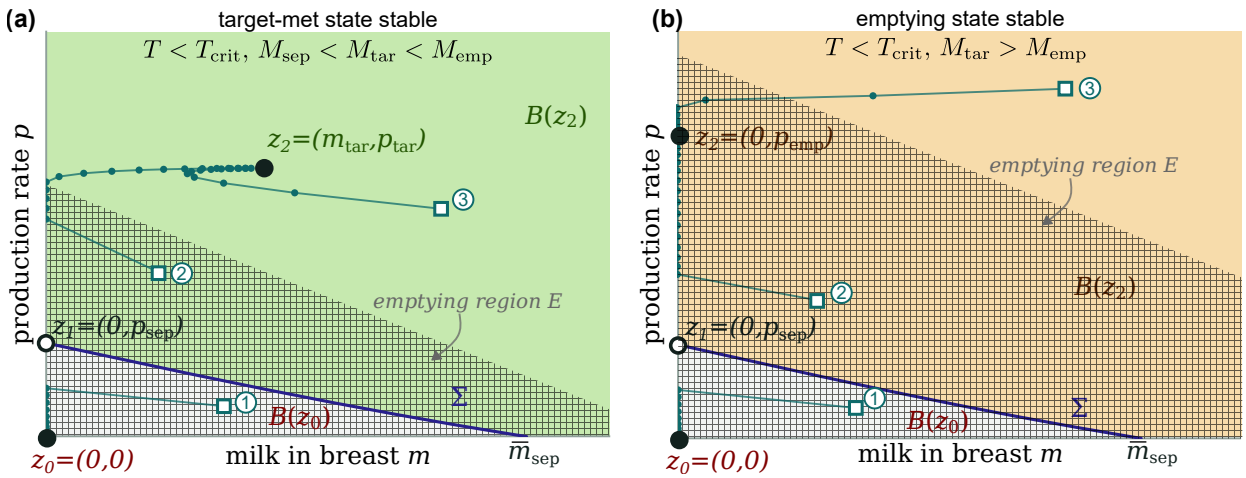

Figure 5: Phase planes for the set-target map (11) with a unimodal-efficiency response, illustrated with the Hill example (8). The grey lattice pattern indicates the emptying region E, filled circles denote the stable states z_0 and z_2, the open circle the unstable state z_1. The separatrix Σ (blue) runs from $(0, p_{\text{sep}})$ to $(\bar{m}_{\text{sep}}, 0)$ and separates the two basins $B(z_0)$ (grey) and $B(z_2)$ (green for the target-met state, orange for the emptying state). In (a) the attractor z_2 lies in the interior, in (b) it lies on the p-axis. Orbits (1)-(3) show example behaviours.

First, for $T < T_{\text{crit}}$ in addition to the maximal achievable target amount M_{emp} (beyond which stable lactation is possible, but the session target cannot be met), there is also a lower threshold M_{sep}. For session targets M_{tar} below this value, the amount removed does not provide sufficient stimulation to maintain production, which leads to involution. Together these thresholds define a range of session targets that can be sustainably met $M_{\text{sep}}(T) < M_{\text{tar}} < M_{\text{emp}}(T)$, see Fig. 4(b).

Second, Theorem 3.2 says that, for a unimodal stimulation efficiency, whether stable lactation can be achieved is not determined by the schedule alone. For $M_{\text{tar}} > M_{\text{sep}}$ the schedule admits two outcomes, involution and stable lactation, and which one is realised depends on initial milk in the breast and the initial production rate. The model therefore separates two questions: what state a schedule can sustain, and whether that state can be reached from the current condition.

Whenever a positive lactation state exists, the (m, p) state space is divided into two regions representing the possible initial states that lead to involution or sustained lactation, which is shown in Fig. 5. The dividing separatrix is a decreasing curve, quantifying the trade-off between initially stored milk and initial production rate: Starting from an empty breast, production must exceed p_{sep}; starting from zero production, stored volume must exceed $\bar{m}_{\text{sep}}$. Between these Σ interpolates monotonically.

3.2 Amount-dependent stimulation, set-duration protocol

We continue to assume that stimulation depends on the amount of milk removed, but now prescribe the removal duration $\tau > 0$ rather than a target amount. Writing $h = h(\tau)$ for the fraction of milk remaining after the session and $x = md + pG$ for the available milk immediately before removal, the removed amount is

$$M = x(1 - h).$$

We use the linear removal law introduced in Sec. 2, $h(\tau) = \max\{1 - \nu\tau, 0\}$ and define $\tau_{\text{emp}} = 1/\nu$. Removal durations $\tau \geq \tau_{\text{emp}}$ produce no additional removal or stimulation, so we analyse $0 < \tau <$

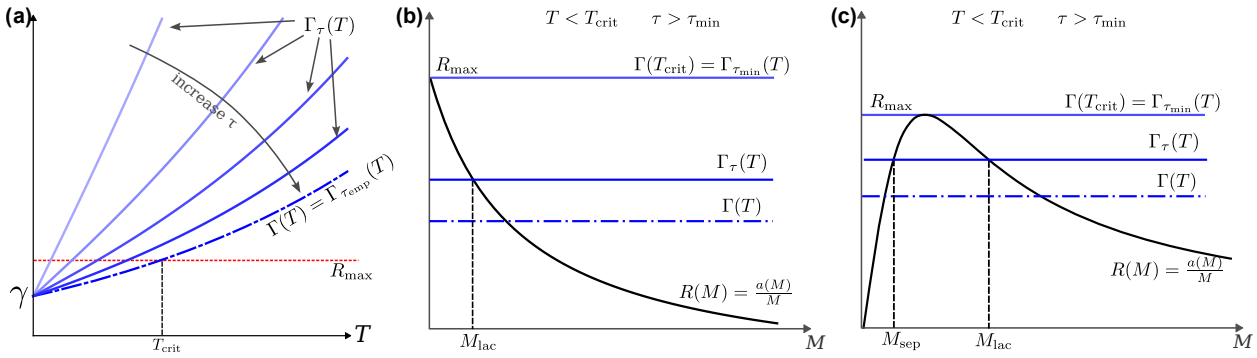

Figure 6: (a) Behaviour of $\Gamma(T)$ and $\Gamma_\tau(T)$ as functions of T. (b),(c) Determination of M_{lac} and M_{sep} for a decreasing-efficiency response (b) and a unimodal-efficiency response (c).

τ_{emp} and treat $\tau = \tau_{\text{emp}}$ as the complete-emptying endpoint. For $\tau \geq \tau_{\text{emp}}$ the map reduces to $F(m,p) = \big(0,\, pg + a(x)\big)$, which we have already analysed as the emptying scenario in Sec. 3.1.

Hence, if $0 < \tau < \tau_{\text{emp}}$ we have $0 < h < 1$, and the dynamics is generated by

$$F(m,p) = \Big(x\,h,\;\; p\,g + a\big(x(1-h)\big)\Big). \tag{23}$$

A fixed point (m_*, p_*) will satisfy

$$m_* = \frac{p_* G h}{1 - dh}, \qquad p_*(1-g) = a\,(p_* G r) \tag{24}$$

with r defined as

$$r = r(T,\tau) := \frac{1 - h(\tau)}{1 - h(\tau)d(T)} \in (0,1). \tag{25}$$

Since $a(0) = 0$, there always exists the zero fixed point $z_0 = (0,0)$.

Steady-state condition and minimum removal duration. Writing the fixed-point condition (24) in terms of the amount removed at steady state $M_* = p_* G r$ gives

$$R(M_*) = \Gamma_\tau(T,\tau), \tag{26}$$

where

$$\Gamma_\tau(T,\tau) := \frac{\Gamma(T)}{r(T,\tau)}. \tag{27}$$

Thus Γ_τ is the stimulation efficiency required to balance production loss for a set-duration schedule. As τ increases from 0 to τ_{emp}, $r(\tau)$ increases from 0 to 1. Hence, for each fixed $T > 0$, $\Gamma_\tau(T)$ decreases from ∞ to $\Gamma(T)$ as τ increases from 0 to τ_{emp}. Thus longer removal sessions reduce the stimulation efficiency required for maintenance.

The following can be shown using basic monotonicity properties of Γ_τ and Γ, see Fig. 6: There exists at least one solution $M_* > 0$ to (26) if and only if the following three, nested conditions hold (ignoring equality cases)

$$\gamma < R_{\max}, \quad T < T_{\text{crit}}, \quad \tau > \tau_{\min}(T).$$

A positive wait-interval threshold $T_{\text{crit}} > 0$ only exists for $\gamma < R_{\max}$ and is defined (as in Sec. 3.1) as solution to

$$\Gamma(T_{\text{crit}}) = R_{\max}.$$

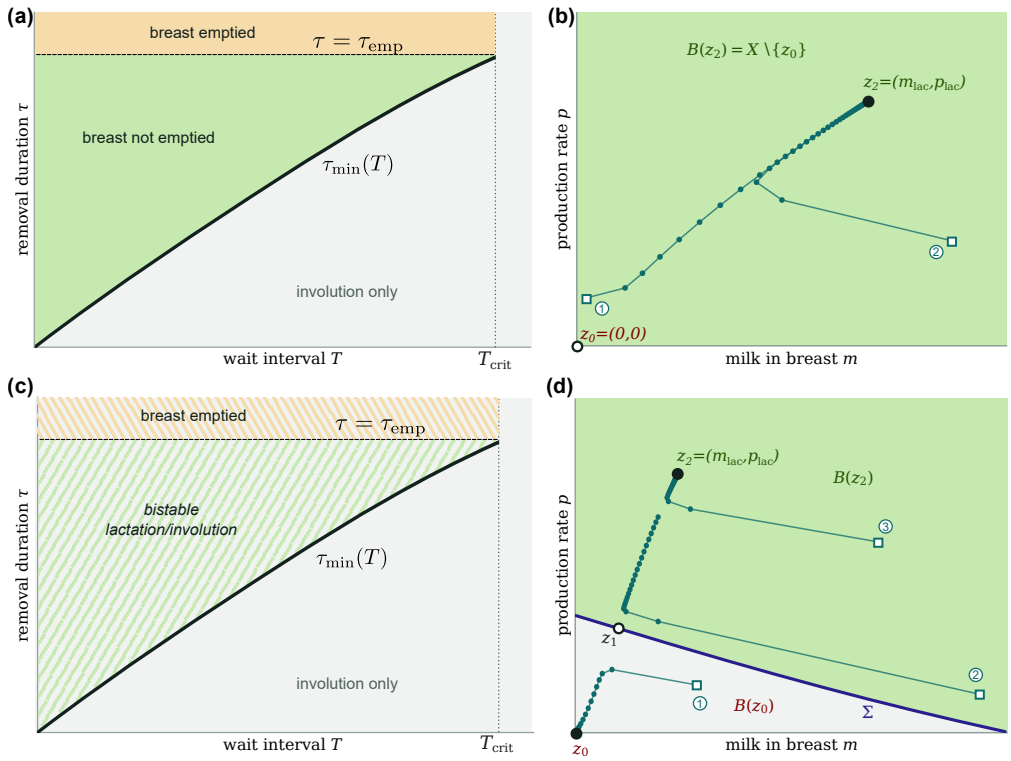

Figure 7: (a),(c) Partition of schedule space (T, τ) for a set-duration protocol using the same coloring conventions as in Fig. 2 and Fig. 4. Shown is a Michaelis-Menten response (7) as example for a decreasing efficiency response in (a) and a Hill-response (8) as example for a unimodal efficiency response in (c). The line $\tau_{\min}$ separates the schedule space and the line $\tau = \tau_{\text{emp}}$ marks complete emptying of the breast. (b),(d) Phase plane for the decreasing efficiency response in (a) (b) and the unimodal response of (c) (d) for the case $\tau_{\min}(T) < \tau < \tau_{\text{emp}}$. The color conventions are the same as in Fig. 3 and Fig. 5. Shown are fixed points, the basins of attraction for the lactation state z_2 in green and for the involution state z_0 in grey, as well as example orbits (1)-(3).

The minimal removal duration $0 < \tau_{\min}(T) < \tau_{\text{emp}}$ only exists for $T < T_{\text{crit}}$ and is defined as solution to

$$\Gamma_{\tau_{\min}}(T) = R_{\max}.$$

This equation can be solved for $\tau_{\min}$, yielding

$$\tau_{\min}(T) = \tau_{\text{emp}} \frac{\Gamma(T)(1 - d(T))}{R_{\max} - d(T)\Gamma(T)}. \tag{28}$$

We see that as T increases from 0 to T_{crit}, $\tau_{\min}(T)$ increases from 0 to τ_{emp}. Note that $\tau_{\min}(T)$ depends on the stimulation-response only through $R_{\max}$, compare curves in Fig. 7(a),(c).

The analysis in App. 8.2 in Lem. 8.10 and Lem. 8.11 shows two general facts used below: A positive steady state on a decreasing branch of R, i.e. for $R'(M_*) < 0$, is locally asymptotically stable, whereas one on an increasing branch, i.e. for $R'(M_*) > 0$, is a saddle. Moreover, every orbit converges to a fixed point.

Decreasing stimulation efficiency. Assume that R decreases strictly from $R(0) = R_{\max}$ to zero. For $0 < T < T_{\text{crit}}$, $R(M) = \Gamma_\tau$ has a unique positive solution M_{lac} exactly when $\tau_{\min}(T) < \tau < \tau_{\text{emp}}$, see Fig. 6(b), and the corresponding production rate is

$$p_{\text{lac}} = \frac{M_{\text{lac}}}{Gr}.$$

Example: concave Michaelis–Menten response. For $a(M) = a_{\max}M/(M + \mu_M)$ (see (7)) this root is explicit:

$$M_{\text{lac}} = \mu_M(\kappa_\tau - 1), \quad \kappa_\tau = \frac{R_{\max}}{\Gamma_\tau}. \tag{29}$$

See Fig. 7(a),(b) for a summary of the results of the following theorem:

Theorem 3.4. *Let $R(M) = a(M)/M$ be a decreasing-efficiency response as above and write $z_0 = (0, 0)$.*

(i) If $T > T_{\text{crit}}$, or if $0 < T < T_{\text{crit}}$ and $\tau < \tau_{\min}(T)$, then z_0 is the unique fixed point of F in X and it is globally asymptotically stable.

(ii) If $0 < T < T_{\text{crit}}$ and $\tau_{\min}(T) < \tau < \tau_{\text{emp}}$, then F has exactly two fixed points, z_0 and the interior state $z_2 = (m_{\text{lac}}, p_{\text{lac}})$, where M_{lac} is the unique solution of $R(M) = \Gamma_\tau$,

$$p_{\text{lac}} = \frac{M_{\text{lac}}}{Gr}, \quad m_{\text{lac}} = \frac{p_{\text{lac}}Gh}{1 - dh}.$$

The state z_0 is unstable and the basin of attraction of z_2, $B(z_2) = X \setminus \{z_0\}$.

For a proof see App. 8.2.

Unimodal stimulation efficiency. Assume that $R(0) = 0$, increases to a unique maximum and then decreases to zero. For $0 < T < T_{\text{crit}}$ and $\tau_{\min}(T) < \tau < \tau_{\text{emp}}$, the equation $R(M) = \Gamma_\tau$ has two positive roots $M_{\text{sep}} < M_{\text{lac}}$, see Fig. 6(c).

Example: sigmoidal Hill response. For $a(M) = a_{\max}M^2/(M^2 + \mu_M^2)$ as in (8), the two steady-state removed amounts are

$$M_{\text{sep}} = \mu_M\left(\kappa_\tau - \sqrt{\kappa_\tau^2 - 1}\right), \quad M_{\text{lac}} = \mu_M\left(\kappa_\tau + \sqrt{\kappa_\tau^2 - 1}\right), \quad \kappa_\tau = \frac{R_{\max}}{\Gamma_\tau} \tag{30}$$

See Fig. 7(c),(d) for a summary of the results of the following theorem and corollary:

Theorem 3.5. *Let $R(M) = a(M)/M$ be a unimodal-efficiency response as above and assume $0 < T < T_{\text{crit}}$ and $\tau_{\min}(T) < \tau < \tau_{\text{emp}}$. Let*

$$M_{\text{sep}} < M_{\text{lac}}$$

be the two solutions of $R(M) = \Gamma_\tau$ and define

$$p_{\text{sep}} = \frac{M_{\text{sep}}}{Gr}, \quad m_{\text{sep}} = \frac{p_{\text{sep}}Gh}{1 - dh}, \qquad p_{\text{lac}} = \frac{M_{\text{lac}}}{Gr}, \quad m_{\text{lac}} = \frac{p_{\text{lac}}Gh}{1 - dh}.$$

Set $z_0 = (0, 0)$, $z_1 = (m_{\text{sep}}, p_{\text{sep}})$ and $z_2 = (m_{\text{lac}}, p_{\text{lac}})$.

(i) ***Fixed points and stability.*** *The map F has exactly the three fixed points z_0, z_1, z_2. The states z_0 and z_2 are locally asymptotically stable, whereas z_1 is a hyperbolic saddle.*

(ii) ***Global dynamics.*** *Every orbit in X converges to one of the three fixed points. Hence*

$$X = B(z_0) \sqcup \Sigma \sqcup B(z_2), \qquad \Sigma := W^s(z_1),$$

where $B(z)$ and $W^s(z)$ denotes the basin of attraction and stable manifold of a fixed point z respectively. Moreover, $B(z_0)$ is an open lower set and $B(z_2)$ is an open upper set with respect to the componentwise order on X.

(iii) ***Separatrix.*** *The stable set Σ is a one-dimensional forward-invariant curve. It can be written as the graph of a continuous, strictly decreasing function*

$$p = \sigma(m), \qquad m \in I_\Sigma,$$

where $I_\Sigma \subset [0, \infty)$ is an interval containing m_{sep}.

For a proof, see App.8.2.

Corollary 3.6. *Let R be a unimodal-efficiency response. If $T > T_{\text{crit}}$, or if $0 < T < T_{\text{crit}}$ and $\tau < \tau_{\min}(T)$, then $z_0 = (0, 0)$ is the unique fixed point and is globally asymptotically stable.*

Interpretation. The critical wait threshold T_{crit} is unchanged by the removal protocol (compare Sec. 3.1): if $T > T_{\text{crit}}$, no removal duration can sustain lactation. For $0 < T < T_{\text{crit}}$, set-duration removal introduces a second threshold, the minimum session duration $\tau_{\min}(T)$. Sessions shorter than this threshold remove too little milk to generate sufficient stimulation, whereas longer sessions admit positive lactation states. Since $\tau_{\min}(T)$ increases from 0 to τ_{emp} as T increases from 0 to T_{crit}, longer waits must be compensated by longer removal sessions. As under set-target removal, decreasing stimulation efficiency produces a unique positive attractor whenever maintenance is possible, whereas unimodal efficiency creates bistability between involution and sustained lactation.

3.3 Duration-dependent stimulation, set-duration protocol

Next we examine the case in which stimulation depends on the length of a session rather than on the volume removed, so that each session contributes a fixed increment $a(\tau)$ to the production rate. Note that since we modelled the milk remaining in the breast as

$$\text{available milk} \times h(\tau),$$

$1 - h(\tau)$ is the fraction of available milk removed and can therefore be interpreted as a measure of the degree of breast emptying. Since h is a function of τ, *duration-dependent stimulation* can also be interpreted as *degree-of-emptying-dependent stimulation* as long as $\tau < \tau_{\text{emp}}$. For larger values $\tau > \tau_{\text{emp}}$, i.e. if the session duration and therefore stimulation continues past complete emptying, this equivalence no longer holds.

The map becomes affine. Retaining the fixed removal duration for the milk equation, the model is

$$F(m, p) = \Big(x\,h, \;\; p\,g + a(\tau)\Big), \qquad x = x(m, p) = m\,d + p\,G. \tag{31}$$

Only the second component has changed from (23). Since it no longer refers to the state, the resulting map is *affine*,

$$F(z) = Lz + b, \qquad L = \begin{pmatrix} dh & Gh \\ 0 & g \end{pmatrix}, \qquad b = \begin{pmatrix} 0 \\ a(\tau) \end{pmatrix}, \tag{32}$$

with the zero in the lower-left corner showing that there is no feedback from the milk present to production. This causes the dynamics to be particularly easy to understand.

Theorem 3.7. *Assume $a(\tau) > 0$. Then the map (31) has a unique fixed point $z_{\mathrm{lac}} = (m_{\mathrm{lac}}, p_{\mathrm{lac}})$ in X, given by*

$$p_{\mathrm{lac}} = \frac{a(\tau)}{1-g}, \qquad m_{\mathrm{lac}} = \frac{p_{\mathrm{lac}}\, G\, h}{1-dh}, \qquad M_{\mathrm{lac}} = Gr\, p_{\mathrm{lac}}, \tag{33}$$

where r is defined in (25) and z_{lac} is globally asymptotically stable on X for every $T > 0$ and removal duration τ with $a(\tau) > 0$. The involution state is not a steady state.

Interpretation. When the production stimulation depends on the removal duration (and not the amount removed), and a set-duration protocol is used, the milk production becomes an autonomous linear recursion with a globally attracting positive equilibrium, and the involution state $(m, p) = (0, 0)$ ceases to exist. Thus, under the exponential decay assumptions of the baseline model, every finite wait interval and every initial condition lead to convergence to a lactation state. In particular, unlike the amount-dependent stimulation models, there is no threshold in removal frequency below which involution occurs. The mechanism is the loss of state-dependent feedback: When stimulation depends on the removed amount, a supply that has fallen supplies less milk, hence receives less stimulation, and may fall further; that self-reinforcement is what allows involution to be an attractor.

3.4 Duration-dependent stimulation, set-target protocol

We finally consider duration-dependent stimulation under a set-target removal protocol with schedule (T, M_{tar}). As we will see, this combination can lead to a long-term behaviour that is qualitatively different from the ones observed in the preceding three sections.

As previously, we let $M_{\mathrm{tar}} > 0$ denote the prescribed target and write $x = dm + Gp$ for the milk available immediately before a removal session. We use the linear removal law $h(\tau) = \max\{1 - \tau/\tau_{\mathrm{emp}}, 0\}$.

If $x > M_{\mathrm{tar}}$, the target is reached before emptying and the required session duration, see also Sec. 2, is

$$\tau(x) = \tau_{\mathrm{emp}} \frac{M_{\mathrm{tar}}}{x} < \tau_{\mathrm{emp}}.$$

If $x \le M_{\mathrm{tar}}$, the target cannot be reached and we assume that the session continues until complete emptying, so that $\tau = \tau_{\mathrm{emp}}$.

The overall resulting map is therefore

$$F(m,p) = \begin{cases} \left(x - M_{\mathrm{tar}},\ gp + a\left(\tau_{\mathrm{emp}} \dfrac{M_{\mathrm{tar}}}{x}\right)\right), & x > M_{\mathrm{tar}}, \\ \left(0,\ gp + a(\tau_{\mathrm{emp}})\right), & x \le M_{\mathrm{tar}}. \end{cases} \tag{34}$$

Unlike the corresponding duration-dependent stimulation under a set-duration protocol, the map is non-linear since the duration needed to reach the prescribed target depends on the current state through x. As in Sec. 3.1, we can define the emptying region $E = \{z \in X : \ x(z) \leq M_{\text{tar}}\}$ and the target-met region as $E^c = X \setminus E$.

Fixed points in the emptying region E. On E the map F becomes

$$F(m,p) = \big(0,\ p\,g + a(\tau_{\text{emp}})\big).$$

The *emptying fixed point* $z_{\text{emp}} = (0, p_{\text{emp}})$ with associated removed amount M_{emp}, is uniquely given by

$$m_{\text{emp}} = 0, \qquad p_{\text{emp}} = \frac{a(\tau_{\text{emp}})}{1-g}, \qquad M_{\text{emp}}(T) = \frac{a(\tau_{\text{emp}})}{\Gamma(T)}. \tag{35}$$

It exists in the emptying region precisely when $x = p_{\text{emp}}G = M_{\text{emp}}(T) \leq M_{\text{tar}}$. Note that since $a(\tau_{\text{emp}}) > 0$, the involution state $(m,p) = (0,0)$ is not a steady state.

Fixed points in the target-met region E^c. On E^c the map F becomes

$$F(m,p) = \Big(x - M_{\text{tar}},\ p\,g + a\bigg(\tau_{\text{emp}}\frac{M_{\text{tar}}}{x}\bigg)\Big).$$

It is useful to characterize a target-met steady state by its associated session duration $\tau \in (0, \tau_{\text{emp}})$. Using $M_{\text{tar}} = x(1-h)$, we can rewrite the fixed point equations for m and p,

$$m = x - M_{\text{tar}}, \qquad p = gp + a\left(\tau_{\text{emp}}\frac{M_{\text{tar}}}{x}\right)$$

in terms of τ and p, giving

$$(1-g)p = a(\tau), \qquad M_{\text{tar}} = G\,r(T,\tau)\,p, \tag{36}$$

where $r(T,\tau) = \frac{1-h}{1-dh}$ as in (25). Eliminating p, we can write a single equation for τ

$$M_{\text{tar}} = \frac{r(T,\tau)a(\tau)}{\Gamma(T)}. \tag{37}$$

Note that this equation is related to (26). The resulting solution τ depends on the scheduling parameters (T, M_{tar}). Since both $a(\tau)$ and $r(T,\tau)$ are strictly increasing in τ, the right-hand side of (37) is strictly increasing from 0 to $M_{\text{emp}}(T) = \frac{a(\tau_{\text{emp}})}{\Gamma(T)}$ as τ increases from 0 to τ_{emp}, see also Fig. 10(d). Hence for

$$M_{\text{tar}} < M_{\text{emp}}(T) \tag{38}$$

a unique target-met steady state exist and, once τ is determined, is given by

$$p_{\text{tar}} = \frac{a(\tau)}{1-g(T)}, \qquad x_{\text{tar}} = \frac{a(\tau)}{\Gamma(T)(1-d(T)h(\tau))}, \qquad m_{\text{tar}} = h(\tau)\,x_{\text{tar}}. \tag{39}$$

Notice that (37) is precisely the steady removed amount obtained under set-duration removal with duration τ. We discuss how steady states under different protocols are connected in detail in Sec. 3.5.

To formulate the following theorem, which characterizes fixed point stability, we define the *elasticity of the stimulation response* E_a and the corresponding *critical elasticity* E_{crit} by

$$E_a(\tau) := \frac{\tau a'(\tau)}{a(\tau)}, \qquad E_{\text{crit}}(T,\tau) := \frac{1+d(T)}{1-d(T)h(\tau)}\frac{1+g(T)}{1-g(T)}. \tag{40}$$

Theorem 3.8 (Set-target removal with duration-dependent stimulation)**.** *Assume that* $a(0) = 0$ *and that* a *is continuously differentiable and strictly increasing.*

(i) If

$$0 < M_{\text{tar}} < M_{\text{emp}}(T) = \frac{a(\tau_{\text{emp}})}{\Gamma(T)},$$

there exists a unique target-met steady state. It is parameterized by the unique $\tau \in (0, \tau_{\text{emp}})$ *satisfying* (37) *and given by* (39)*.*

(ii) The target-met steady state is locally asymptotically stable if

$$E_a(\tau) < E_{\text{crit}}(T, \tau), \tag{41}$$

and unstable if $E_a(\tau) > E_{\text{crit}}(T, \tau)$*. At* $E_a(\tau) = E_{\text{crit}}(T, \tau)$ *one eigenvalue of the Jacobian is* -1*, while the second equals* $-dg$*. The fixed point is then nonhyperbolic, and its stability cannot be determined from the linearization alone. Moreover,* $\lambda = -1$ *is the only possible local stability-loss mechanism of the target-met steady state.*

(iii) If $M_{\text{tar}} > M_{\text{emp}}(T)$*, the unique steady state is the emptied state* (35)*, which is locally asymptotically stable.*

The proof is given in App. 8.4.

Stimulation efficiency and the possibility of instability. It is easy to check that $E_{\text{crit}} > 1$ and, for fixed τ, decreases as a function of T with limits ∞ for $T \to 0^+$, and 1 for $T \to \infty$. Therefore, if $E_a(\tau) > 1$ for some value of τ, we can fix τ and define $T_{\text{thresh}} > 0$ by $E_a(\tau) = E_{\text{crit}}(T_{\text{thresh}}, \tau)$. Then for all $T > T_{\text{thresh}}$ it holds that $E_a(\tau) > E_{\text{crit}}(T, \tau)$, i.e. (41) is violated and hence the target-met state is unstable for such pairs (T, τ). One can then use (37) to obtain the corresponding schedule variables (T, M_{tar}).

Next, we connect $E_a(\tau)$ with the shape of the stimulation efficiency: In analogy to the amount-dependent models, we can define the *stimulation efficiency* (which is now the production stimulation per removal duration)

$$R_d(\tau) := \frac{a(\tau)}{\tau}. \tag{42}$$

Unlike in the amount-dependent models, R_d does not directly determine steady-state existence. However, since it connects to the elasticity of the stimulation response via

$$E_a(\tau) = 1 + \frac{\tau R_d'(\tau)}{R_d(\tau)}$$

it provides a simple criterion for whether unstable target-met steady states can occur. This allows to formulate the following corollary.

Corollary 3.9. *An unstable target-met steady state exists for some schedule* (T, M_{tar}) *if and only if*

$$R_d'(\tau) > 0$$

for some $\tau \in (0, \tau_{\text{emp}})$*. In particular, if* R_d *non-increasing on* $(0, \tau_{\text{emp}})$*, every target-met steady state is locally asymptotically stable.*

This shows that only responses where the duration efficiency R_d increasing on some interval, can create this type of instability.

Example: Michaelis-Menten response. For the Michaelis–Menten response of (7) taking durations as an argument

$$a(\tau) = a_{\max}\frac{\tau}{\tau + \mu_\tau},$$

we have

$$R_d(\tau) = \frac{a_{\max}}{\tau + \mu_\tau},$$

which is strictly decreasing. Hence every target-met steady state is locally asymptotically stable.

Example: Hill response. For the Hill response of (8)

$$a(\tau) = a_{\max}\frac{\tau^2}{\tau^2 + \mu_\tau^2}, \tag{43}$$

we have

$$R_d(\tau) = a_{\max}\frac{\tau}{\tau^2 + \mu_\tau^2},$$

which increases for $\tau < \mu_\tau$ and decreases for $\tau > \mu_\tau$.

Consequently, instability is possible only on the increasing-efficiency branch $\tau < \mu_\tau$. Furthermore, since the increasing-efficiency branch always intersects the admissible interval $(0, \tau_{\text{emp}})$, Corollary 3.9 implies that unstable target-met steady states exist for some schedules for every Hill response of this form.

For the Hill response the stability boundary $E_a = E_{\text{crit}}$ can be evaluated explicitly; the resulting expression is given in App. 8.4 in (65). Mapping this boundary through (37) gives the stability boundary in (T, M_{tar})-space shown as dark red line in Fig. 8(a). Since we have determined the existence of a region where no stable fixed point exists, we next discuss non-constant long-term behaviours.

Non-constant long-term behaviour. The occurrence of an eigenvalue $\lambda = -1$ at the stability boundary suggests a possible flip (period-doubling) bifurcation. We do not pursue a formal bifurcation classification here, but use numerical simulations to explore the long-term dynamics for the Hill example above. The found behaviour is indeed consistent with a supercritical flip, with a stable period-2 orbit appearing beyond the fixed-point stability boundary: Fig. 8(b) and Fig. 9(b)-(e) show that the period-2 attractor can either consist of two target-met states, Fig. 9(b),(d), or contain one target-met and one emptying state, Fig. 9(c),(e).

Further numerical exploration revealed a striking result: For small targets M_{tar}, the system appears to undergo a series of period-doubling events as T increases. We also observed apparent chaotic behaviour, see Fig. 8(c). In App. 8.4 we derive the system's small target limit. The resulting approximation is the Maynard Smith-Slatkin population model (Smith and Slatkin 1973), which shows structural similarities with the logistic map, which is known to have the Feigenbaum-cascade as bifurcation diagram.

Remark 3.10 (Timescales and non-constant dynamics). The instability described above cannot occur at arbitrarily short wait intervals: We assume $E_{\max} > 1$ (otherwise the instability cannot occur). If the stimulation elasticity is bounded by $E_a(\tau) \leq E_{\max}$ and since

$$E_{\text{crit}}(T, \tau) = \frac{(1+d)(1+g)}{(1-dh)(1-g)} > \frac{1+g}{1-g}.$$

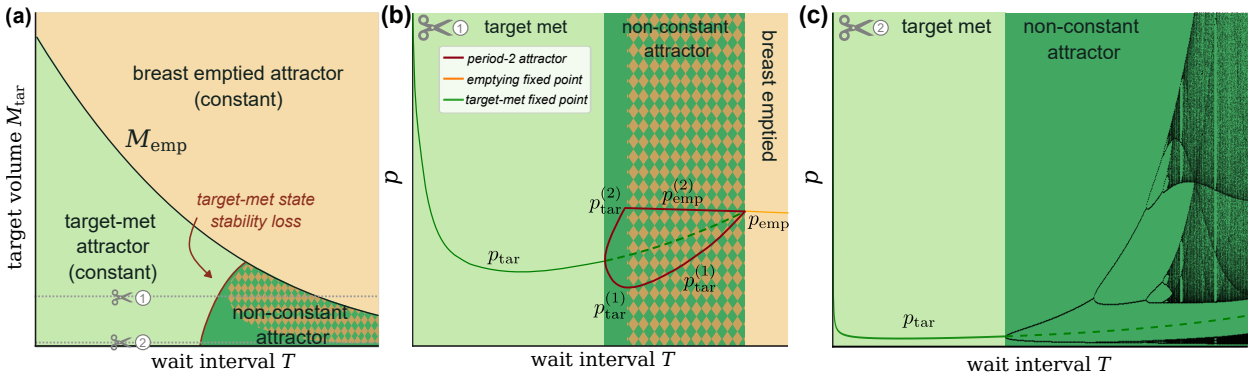

Figure 8: Duration-dependent stimulation under a set-target protocol with a unimodal-efficiency response, Hill response (8). (a) Long-term behaviour in schedule space (T, M_{tar}). The curve $M_{\mathrm{emp}}(T)$ separates schedules for which a target-met fixed point exists from those for which it does not. For $M_{\mathrm{tar}} > M_{\mathrm{emp}}(T)$, the emptied fixed point is stable (orange). For $M_{\mathrm{tar}} < M_{\mathrm{emp}}(T)$, the dark red line separates the region where the target-met fixed point is stable (pale green) and the region where it is not. In the region, where the target-met fixed point exists, but is unstable, dark green denotes schedules for which a non-constant target-met attractor is observed numerically. The chequered region denotes schedules for which the observed non-constant attractor contains at least one emptying state. The horizontal dashed-grey lines indicate the slices shown in (b) and (c). (b),(c) Numerical bifurcation diagrams. Slices through schedule space at fixed M_{tar}. Shown are the target-met fixed point, the emptied fixed point, and the numerically observed asymptotic values of p as functions of T. Solid and dashed portions of the green curve indicate stable and unstable parts of the target-met fixed-point. In (b), the two members of the observed period-2 orbit are marked by superscripts (1) and (2). Parameters used (not calibrated to data): $\delta = \gamma = 0.15/\mathrm{h}$, $a_{\max} = 50\mathrm{ml/h}$, $\mu_\tau = 0.5\mathrm{h}$, $\tau_{\mathrm{emp}} = 1/3\mathrm{h}$ with slice position $M_{\mathrm{tar}} = 12.5\mathrm{ml}$ (b) and $M_{\mathrm{tar}} = 0.01\mathrm{ml}$ (c). For (c), 720 regularly spaced T-values between 0 and 30 were used with starting values close to the unstable target-met fixed point. In each case 4000 iterations were performed and the last 2000 iterates were kept for plotting. The transition to non-constant dynamics can be explored interactively in Online Resource 1.

instability requires

$$T > \frac{1}{\gamma} \log\left(\frac{E_{\max}+1}{E_{\max}-1}\right).$$

For the Hill response considered here, $E_{\max} = 2$, giving the necessary condition

$$T > \frac{\log 3}{\gamma}.$$

Thus instability requires waits that are sufficiently long relative to the decay timescale of the production rate. Whether this regime is physiologically relevant is a separate question. The period-doubling cascade observed numerically for very small targets should therefore primarily be interpreted as demonstrating a possible dynamical consequence of the proposed feedback mechanism, rather than as a prediction that such behaviour occurs in human lactation.

Interpretation. The non-steady dynamics arise from a feedback that is absent under set-duration removal. If more milk is available before a set-target session, the prescribed target is reached more

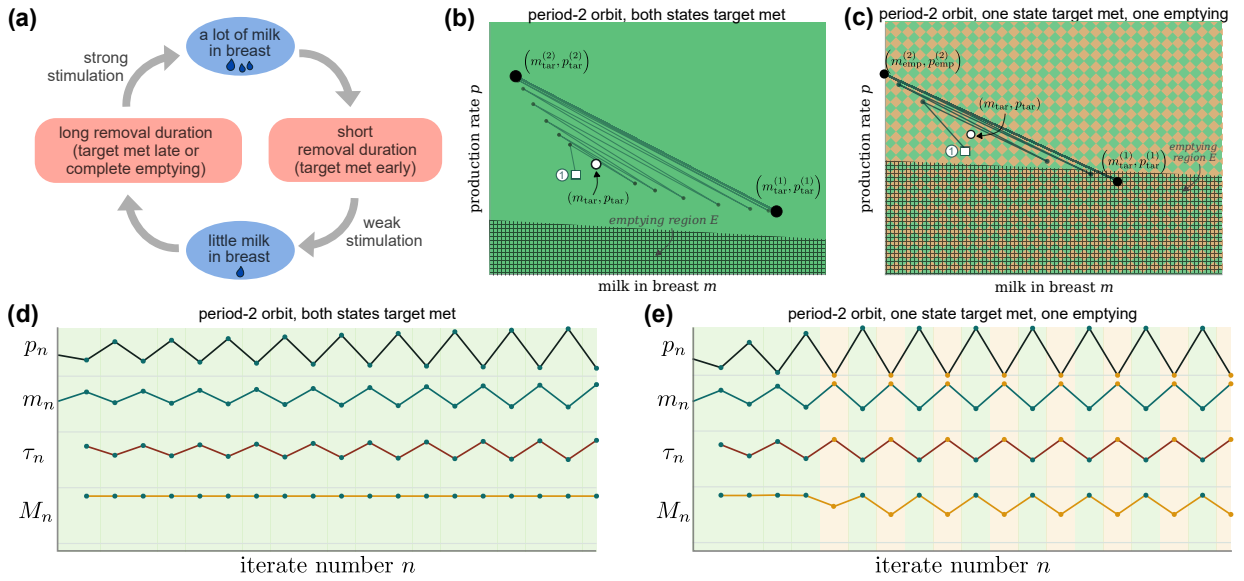

Figure 9: Duration-dependent stimulation under a set-target protocol with a unimodal-efficiency response, illustrated with the Hill response in (8). (a) Schematic explanation of the feedback mechanism that can generate stable period-2 dynamics. (b),(c) Phase planes. The grey lattice pattern indicates the emptying region E. Filled circles denote the numerically observed stable period-2 orbit, open circle denotes the unstable target-met fixed point. In (b), both members of the attracting period-2 orbit are target-met. In (c), one member is target-met and the other is an emptying state. Representative trajectories illustrate convergence towards the period-2 attractor. (d),(e) Qualitative behaviour of m_n, p_n, τ_n and milk removed M_n as a function of iteration number n of the orbits shown in (b) (panel (d)) and in (c) (panel (e)). Background shading and dot color indicate target-met or emptying behaviour.

quickly. This shortens the session and, under duration-dependent stimulation, reduces the stimulation of subsequent production. Conversely, a lower available amount produces a longer and more strongly stimulating session. If stimulation increases sufficiently strongly with session duration, this negative feedback can overshoot, causing the production and milk amounts to alternate between successive sessions, see Fig. 9(a).

Thus the two duration-dependent protocols generate the same family of positive steady states but can have qualitatively different dynamics. Under set-duration removal the map is affine and its positive steady state is always globally stable under the baseline exponential decay assumptions. Under set-target removal the state-dependent session duration makes the map non-linear, and increasing duration efficiency can destabilize the steady state and generate persistent non-steady behaviour. See also the discussion in Sec. 3.5.

3.5 Steady-state correspondence and differences between removal protocols

In the preceding sections, we analysed the long-term behaviour under two removal protocols: setting the target session output and setting the removal duration. Although these protocols define different dynamical maps, their positive steady states can be compared through the realised session output M_* and removal duration τ_*. A target-met fixed point under set-target removal with $M_{\mathrm{tar}} = M_*$

can be associated with the set-duration schedule that prescribes its realised duration $\tau = \tau_*$. Conversely, a set-duration fixed point with $\tau \leq \tau_{\text{emp}}$ corresponds to a target-met set-target fixed point with $M_{\text{tar}} = M_*$. This correspondence concerns the location of fixed points; their stability and resulting long-term dynamics need not be preserved between protocols.

The correspondence follows from a general balance relation.

Lemma 3.11 (Steady-state balance)**.** *Consider any positive steady state of the model, and let $M_* > 0$, τ_*, and a_* denote the amount of milk removed, the removal duration, and the resulting stimulation per session, respectively. Then*

$$\frac{a_*}{M_*} = \frac{\Gamma(T)}{r(T, \tau_*)}. \tag{44}$$

In particular, at complete emptying $r(T, \tau_*) = 1$, so that

$$\frac{a_*}{M_*} = \Gamma(T).$$

For a proof see App. 8.5.

The lemma allows the fixed points of the two removal protocols to be represented in the common (T, M_*)-plane. Next, we will discuss what this means for the two stimulation mechanisms.

Amount-dependent stimulation. For amount-dependent stimulation, where $a_* = a(M_*)$, the balance relation (44), solved for τ_*, gives

$$\tau_*(T, M_*) = \tau_{\text{emp}} \frac{1 - d(T)}{\frac{R(M_*)}{\Gamma(T)} - d(T)}, \qquad R(M_*) \geq \Gamma(T). \tag{45}$$

Equality $R(M_*) = \Gamma(T)$ corresponds to complete emptying, $\tau_* = \tau_{\text{emp}}$.

For a decreasing efficiency response, Eq. (45) shows that the positive pre-emptying steady states of the two protocols are in one-to-one correspondence and have the same qualitative stability. Thus, although the protocols use different schedule variables, they describe the same family of attracting positive states.

For amount-dependent stimulation with a unimodal efficiency response however, there are fundamental differences: Fig. 10(a) shows the relation between removal duration and fixed-point session output at fixed T. We see that the steady-state correspondence is not one-to-one. For a range of removal durations, one fixed point lies below M_{peak} and one above it. Fig. 10(b), (c) compare the existence and stability of the corresponding fixed points under set-target and set-duration removal: Under set-target removal, the target-met positive fixed points on both sides of M_{peak} are stable (Fig. 10(b)). Under set-duration removal, however, the lower branch $M_* < M_{\text{peak}}$ is unstable, whereas the upper branch $M_* > M_{\text{peak}}$ is stable (Fig. 10(c)). The two protocols therefore permit the same fixed-point outputs over this range, but do not assign the same stability to them.

Duration-dependent stimulation. For duration-dependent stimulation, where $a_* = a(\tau_*)$, we obtain from (44) for M_*

$$M_*(T, \tau_*) = \frac{r(T, \tau_*) a(\tau_*)}{\Gamma(T)}. \tag{46}$$

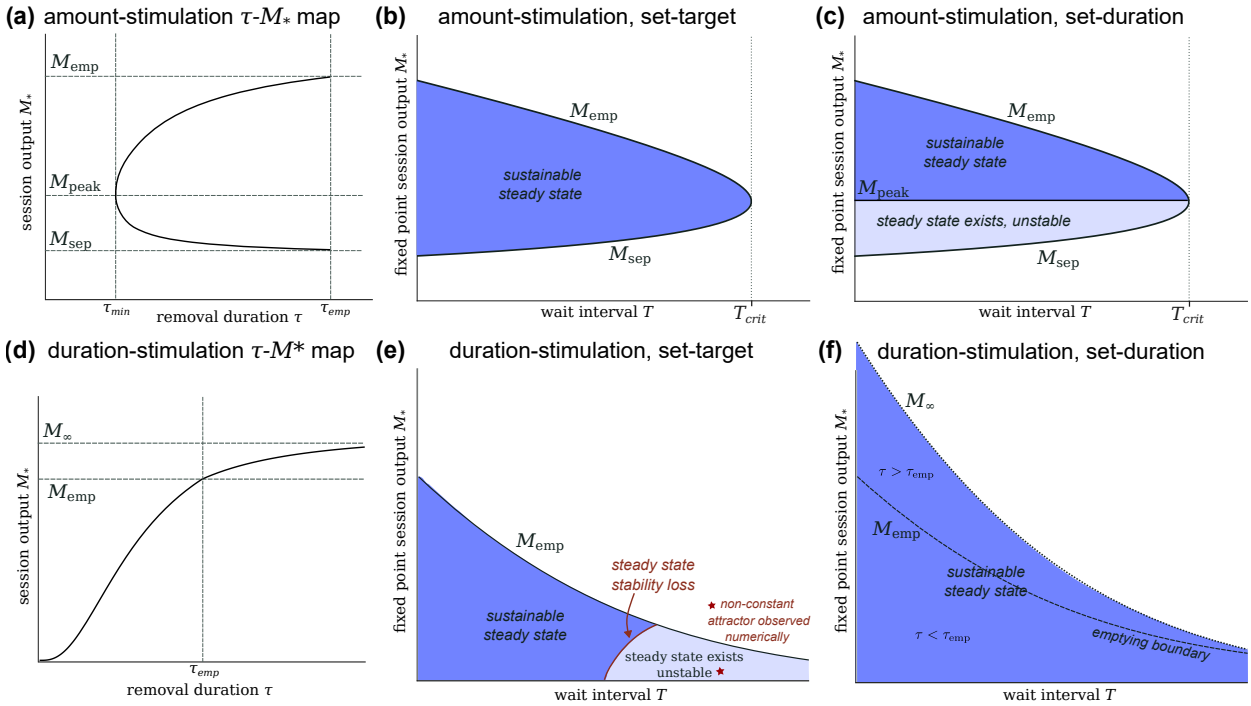

Figure 10: Effect of protocol for unimodal stimulation efficiency. (a),(d) Shown are the maps between τ and M_* given by (45) and (46). (b)-(c) and (e)-(f): The existence and stability of positive fixed points in (T, M_*)-space for different stimulation mechanisms and removal protocols. Dark blue denotes an existing, stable state, light blue an existing, unstable state. In (f) M_∞ is defined as $M_\infty = a_{\max}/\Gamma(T)$.

At complete emptying,

$$\tau_* = \tau_{\text{emp}} \qquad \Longleftrightarrow \qquad M_* = M_{\text{emp}}(T) = \frac{a(\tau_{\text{emp}})}{\Gamma(T)}.$$

Here, a different distinction occurs: Fig. 10(d) shows how the right-hand side of (46) increases monotonically with τ_*. However, set-duration removal permits prescribed durations $\tau > \tau_{\text{emp}}$. The breast is then already emptied, but increasing τ can continue to increase stimulation, so that the fixed-point output extends beyond $M_{\text{emp}}(T)$ and approaches $M_\infty(T) := a_{\max}/\Gamma(T)$. Set-target removal has no corresponding post-emptying duration regime because its realised duration cannot exceed τ_{emp}. This is a consequence of the modelling assumption that for under a set-target protocol the removal is stopped, once the breast is emptied. For decreasing efficiency these states (whenever they exist) remain stable under both protocols. For unimodal efficiency, however, the set-target fixed point can lose stability (Fig. 10(e)); numerical simulations reveal non-constant long-term dynamics in this regime. The corresponding set-duration fixed point remains stable (Fig. 10(f)).

Interpretation. It is an interesting and perhaps surprising observation that given a steady state, the choice of removal protocol affects the state's stability, and hence whether it would be observable as long-term behaviour. To understand this, one has to view the protocols through the lens of perturbations. We will use the amount-dependent stimulation as an example: For the set-target protocol, as long as the dynamics stay in the target-met region, the amount pumped and therefore the stimulation stay constant at M_{tar} and $a(M_{\text{tar}})$. Therefore there is no feedback from the amount

of milk in the breast m to the production rate p (hence a zero in the lower-left corner of the Jacobian in App. 8.1). Both p and m have a stabilizing effect on themselves (hence the entries $d < 1$ and $g < 1$ on the diagonal of the Jacobian in App. 8.1), leading to overall stability. For the set-duration protocol the situation is different: Changes in m and p *do* affect the amount pumped during a set duration τ and feed back onto the production rate (hence the terms involving $a'(M)$ in the lower row of the Jacobian in App. 8.2). Then, if $R'(M) > 0$, this causes the instability.

4 Daily Output

Having characterised the possible long-term states, we next ask how these translate into milk obtained over time. For this we move away from per session behaviour and rather ask the question of how the schedule (T, M_{tar}) or (T, τ) influences the *daily milk output*. Guiding questions are: Which schedules lead to the same daily milk output? How can daily milk output be maximized under certain constraints?

If M_n and τ_n are the session output and session duration of the n-th removal session, the long-term average daily milk output is defined as

$$M_{\text{DAY}} = 24 \lim_{N\to\infty} \frac{\sum_{n=1}^{N} M_n}{\sum_{n=1}^{N}(T+\tau_n)},$$

whenever this limit exists.

If the system converges to a steady state with session duration τ_* and session output M_*, the formula simplifies to

$$M_{\text{DAY}} = \frac{24}{T+\tau_*} M_*. \tag{47}$$

For cases of bistability, we assume the convergence was to the non-trivial state.
Similarly, for a general period-k orbit with session durations $(\tau_*^{(1)}, \dots \tau_*^{(k)})$ and session outputs $(M_*^{(1)}, \dots M_*^{(k)})$ we obtain

$$M_{\text{DAY}} = \frac{24}{T + \frac{1}{k}\sum_{j=1}^{k} \tau_*^{(j)}} \frac{1}{k} \sum_{j=1}^{k} M_*^{(j)}. \tag{48}$$

Interpretation. For both (47) and (48) the first factor represents the average number of sessions per day and the second factor the average session output. In general both factors can depend on the scheduling parameters. This can create a trade-off between the amount removed per session and the number of daily sessions. For example, increasing the target amount or removal duration may increase the milk obtained in an individual session, but it may also increase the duration of each removal cycle and therefore reduces the number of sessions possible per day. This trade-off is the focus of the analysis below.

On the treatment of the two removal protocols. As discussed in Sec. 3.5, before complete emptying the two removal protocols, set-target and set-duration, describe the same positive steady states, although their stability can differ. To make the following analysis more readable, we formulate the main results for the set-duration protocol and then state explicitly how they translate to set-target removal. The main exception is Sec. 4.4, where non-constant long-term dynamics under set-target removal are considered directly.

4.1 Universal properties of steady-state daily output

Unless stated otherwise, we assume a set-duration protocol and consider daily output at a stable steady state. In models with bistability, we assume convergence to the positive lactation state. The daily output is given by

$$M_{\mathrm{DAY}}(T,\tau) = \frac{24 M_*(T,\tau)}{T+\tau}, \tag{49}$$

where the session output $M_*(T,\tau)$ is given by (26) for amount-dependent stimulation and by (33) for duration-dependent stimulation.

We start by inspecting how the *session* output $M_*(T,\tau)$ depends on the schedule parameters.

Lemma 4.1 (Monotonicity of steady-state session output)**.** *Consider a stable steady-state under a set-duration protocol. Let $M_*(T,\tau) > 0$ be the associated session output. Then the following hold.*

(i) The session output decreases with T,

$$\frac{\partial M_*}{\partial T} < 0.$$

(ii) The session output increases with τ,

$$\frac{\partial M_*}{\partial \tau} \geq 0.$$

More precisely, $\partial_\tau M_* > 0$ before complete emptying. Beyond complete emptying, M_* is constant for amount-dependent stimulation and continues to increase for duration-dependent stimulation.

For a proof see App. 8.6.

A simple consequence of this Lemma is that

$$\frac{\partial M_{\mathrm{DAY}}}{\partial T} < 0.$$

Interpretation. The two monotonicity results in Lem. 4.1 show the different effects of the schedule parameters T and τ. Increasing the wait interval T lengthens the removal cycle while decreasing the session output, so it always has a negative effect on daily output. In contrast, increasing τ before complete emptying increases the amount removed per session, but also lengthens the removal cycle. The resulting effects oppose each other, leading to a trade-off. Next we inspect this trade-off in more detail, i.e. we investigate how the function $\tau \mapsto M_{\mathrm{DAY}}(T,\tau)$ behaves. A particularly interesting question is whether a maximum is reached before, at, or after emptying the breast.

By differentiating $M_{\mathrm{DAY}}(T,\tau)$ with respect to τ, it follows directly that

$$Q > 1 \iff M_{\mathrm{DAY}} \text{ increases with } \tau \tag{50}$$

where we have defined,

$$Q(T,\tau) = (T+\tau)\frac{\partial_\tau M_*(T,\tau)}{M_*(T,\tau)}.$$

Q can be interpreted as the ratio

$$Q := \frac{\text{relative increase in session output}}{\text{relative increase in cycle duration}}.$$

The guiding principle for the next sections is therefore

$$Q > 1:\ M_{\mathrm{DAY}} \text{ increases}, \qquad Q = 1:\ \text{critical point}, \qquad Q < 1:\ M_{\mathrm{DAY}} \text{ decreases}.$$

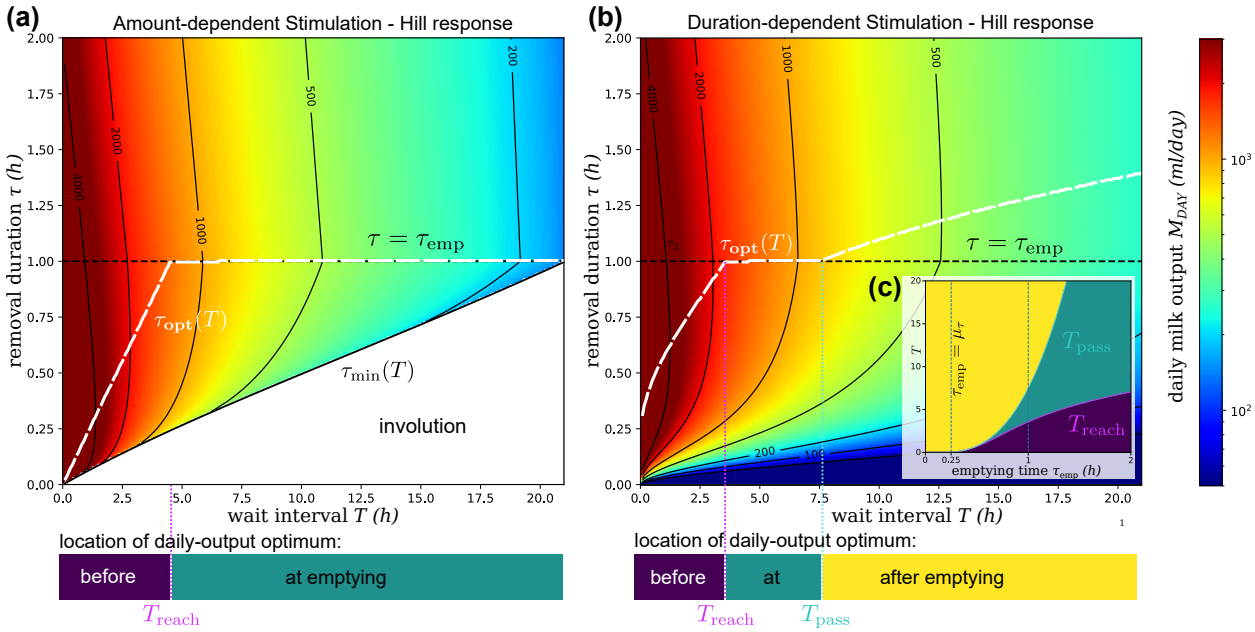

Figure 11: Daily milk output under set-duration removal. (a),(b): Steady-state M_{DAY} as a function of wait interval (T) and removal duration (τ) for the Hill response with amount-dependent (a) and duration-dependent stimulation (b). Colours and contours show M_{DAY}; the white dashed curve marks the maximizing duration $\tau_{\mathrm{opt}}(T)$, and the black dashed line complete emptying, $\tau = \tau_{\mathrm{emp}}$. In (a), the solid black curve marks the lower boundary $\tau_{\mathrm{min}}(T)$ of positive steady states. Bars below (a),(b) indicate whether the maximum occurs before, at, or after complete emptying, with transitions at T_{reach} and T_{pass}. (c) Regime diagram for duration-dependent stimulation in the (T, τ_{emp})-plane; the curves T_{reach} and T_{pass} separate the three regimes, the vertical line marks $\tau_{\mathrm{emp}} = \mu_\tau$. Parameters: $\delta = 0.03$/h, $\gamma = 0.1$/h, $a_{\mathrm{max}} = 37.5$ml/h, $\mu_M = 125$ml, $\mu_\tau = 0.25$h, $\tau_{\mathrm{emp}} = 1$h (in (a), (b))

Level sets and constrained schedules. The level sets of $M_{\mathrm{DAY}}(T, \tau)$ in Fig. 11, show which schedules (T, τ) produce the same long-term daily output. The figure also shows $\tau_{\mathrm{opt}}(T)$, the removal duration maximizing $M_{\mathrm{DAY}}(T, \tau)$ for fixed T. Characterizing $\tau_{\mathrm{opt}}(T)$ is the main focus of the next sections. What can we learn from the level sets and why is $\tau_{\mathrm{opt}}(T)$ such as a useful quantity?

The level sets and $\tau_{\mathrm{opt}}(T)$ can be used to answer several natural scheduling questions:

- For a given daily output target, which schedule (T, τ) allows for the maximum wait interval T between sessions? *Answer: Intersect $T \mapsto \tau_{\mathrm{opt}}(T)$ with the corresponding level set. The intersection point gives the wanted schedule.*

- For a given wait interval T, what is the maximal achievable daily output?
  Answer: $M_{\mathrm{DAY}}(T, \tau_{\mathrm{opt}}(T))$.

- For a given wait interval T and a given daily output target, what is the minimal removal duration possible? *Answer: Intersect the level set with the vertical line $T = const$. If there are several possible removal durations, pick the smallest one. If the daily output target is bigger than $M_{\mathrm{DAY}}(T, \tau_{\mathrm{opt}}(T))$, there is no such schedule.*

These are just some examples of how the level sets and the function $\tau_{\text{opt}}(T)$ can be used to answer practical questions about scheduling. In particular, they show that the optimal removal duration $\tau_{\text{opt}}(T)$ is a useful quantity for comparing schedules. Next, we characterize $\tau_{\text{opt}}(T)$, starting with amount-dependent stimulation.

4.2 Amount-dependent stimulation

In this section we consider amount-dependent stimulation $a = a(M)$. To determine the location of the maximum of $\tau \mapsto M_{\text{DAY}}(T, \tau)$ for fixed T, it is useful to characterize its growth or decay behaviour near $\tau = \tau_{\text{min}}$, and near $\tau = \tau_{\text{emp}}$. The following Lemma shows what happens near τ_{min}.

Lemma 4.2 (Daily output near τ_{min})**.** *Fix $0 < T < T_{\text{crit}}$. Along a stable positive steady state under set-duration removal, $\tau \mapsto M_{\text{DAY}}(T, \tau)$ is strictly increasing for $\tau > \tau_{\text{min}}(T)$ sufficiently close to $\tau_{\text{min}}(T)$.*

For a proof see App. 8.6.

Thus the daily output $M_{\text{DAY}}(T, \tau)$ initially increases as τ moves away from τ_{min}. To determine whether it reaches a maximum before complete emptying, we inspect its growth or decay as τ approaches τ_{emp}. This is characterized by the value of Q just before emptying. We obtain

$$Q_A^{\text{pre}}(T) := \lim_{\tau \to \tau_{\text{emp}}^-} Q(T, \tau) = -\frac{(1 + T/\tau_{\text{emp}})(1 - d(T))\Gamma(T)}{M_{\text{emp}}(T) R'(M_{\text{emp}}(T))}. \tag{51}$$

Now (50) tells us that

$$Q_A^{\text{pre}}(T) > 1 \iff \partial_\tau M_{\text{DAY}}(T, \tau) > 0 \quad \text{for } \tau < \tau_{\text{emp}} \text{ sufficiently close to } \tau_{\text{emp}}.$$

We are now ready to state the main result of this section, which answers the question of when a pre-emptying maximum of $\tau \mapsto M_{\text{DAY}}(T, \tau)$ exists and how it is characterized. Note that the proposition contains a concavity assumption on $\tau \mapsto M_*(T, \tau)$, which ensures that the sign of $\partial_\tau M_{\text{DAY}}$ can change at most once. Fig. 11(a) demonstrates the main statements of Prop. 4.3 and Cor. 4.4.

Proposition 4.3 (Maximal daily output under amount-dependent stimulation)**.** *Assume that R is a decreasing, or unimodal-efficiency response, and that $R_{\text{max}} > \gamma$. Fix $0 < T < T_{\text{crit}}$ and consider positive stable steady states under a set-duration protocol. Further assume that before emptying*

$$\partial_\tau^2 M_*(T, \tau) < 0.$$

Then $\tau \mapsto M_{\text{DAY}}(T, \tau)$ has a unique maximum τ_{opt}. Its position relative to complete emptying is determined as follows:

$$\begin{aligned} Q_A^{\text{pre}}(T) < 1 &\implies \text{the maximum occurs before complete emptying, } \tau_{\text{opt}} < \tau_{\text{emp}}, \\ Q_A^{\text{pre}}(T) \geq 1 &\implies \text{the maximum occurs at complete emptying, } \tau_{\text{opt}} = \tau_{\text{emp}}. \end{aligned}$$

Whenever the maximum occurs before complete emptying, τ_{opt} is given as solution to

$$Q(T, \tau_{\text{opt}}) = 1.$$

The proof is given in App. 8.6.

Corollary 4.4 (Dependence of the maximum on the wait interval)**.** *Under the assumptions of Prop. 4.3,*

$$Q_A^{\mathrm{pre}}(T) < 1$$

for all sufficiently small $T > 0$*, whereas*

$$Q_A^{\mathrm{pre}}(T) > 1$$

for $T < T_{\mathrm{crit}}$ *sufficiently close to* T_{crit}*. Consequently, the daily-output maximum lies before complete emptying for sufficiently short wait intervals and is attained at complete emptying for wait intervals sufficiently close to* T_{crit}*. In particular, there exists at least one* $T_{\mathrm{reach}} \in (0, T_{\mathrm{crit}})$ *satisfying*

$$Q_A^{\mathrm{pre}}(T_{\mathrm{reach}}) = 1,$$

at which the maximum reaches the complete-emptying boundary.

Corresponding result for set-target removal. Before complete emptying, the set-target and set-duration protocols describe the same steady states, although their stability can differ; see Sec. 3.5 and Fig. 10(a)-(c).

Consider first stable set-target steady states whose corresponding set-duration steady states are also stable. These are precisely the states satisfying $R'(M_*) < 0$. For such states, the realized removal duration $\tau_*(T, M_{\mathrm{tar}})$ increases with the session target; see Fig. 10(a). Hence $M_{\mathrm{tar}} = M_*(T, \tau)$ provides an order-preserving reparametrization of the set-duration steady states, and the results above for M_{DAY} transfer directly to the set-target protocol.

Stable set-target steady states whose corresponding set-duration states are unstable, i.e. states satisfying $R'(M_*) > 0$ do not generate an additional daily-output maximum. The reason is that for these states, the realized removal duration $\tau_*(T, M_{\mathrm{tar}})$ *decreases* as M_{tar} increases; see Fig. 10(a). This also follows directly by differentiating the relation (45). Thus increasing M_{tar} simultaneously increases the amount removed per session and shortens the removal session, so M_{DAY} increases with M_{tar}.

Consequently, whenever the set-duration maximum occurs before complete emptying, the corresponding set-target maximum is attained at

$$M_{\mathrm{tar},opt} = M_*(T, \tau_{\mathrm{opt}}).$$

If the set-duration maximum occurs at complete emptying, then under set-target removal the daily output first reaches its maximum at

$$M_{\mathrm{tar}} = M_{\mathrm{emp}}(T) = M_*(T, \tau_{\mathrm{emp}})$$

and remains constant for all $M_{\mathrm{tar}} \geq M_{\mathrm{emp}}(T)$.

Examples. For both the Michaelis–Menten and Hill responses, the function $\tau \mapsto M_*(T, \tau)$ is strictly concave. This can be seen by differentiating the steady state session output M_{lac}, given in (29) and (30), with respect to τ, and using that before emptying $\partial_\tau r > 0$ and $\partial_\tau^2 r < 0$. Hence Prop. 4.3 applies.

Michaelis–Menten response: We have $R(M) = a_{\max}/(M + \mu_M)$ and $R_{\max} = a_{\max}/\mu_M$. A direct calculation using $R(M_{\text{emp}}) = \Gamma(T)$ gives

$$M_{\text{emp}}(T)R'(M_{\text{emp}}(T)) = -\Gamma(T)\left(1 - \frac{\Gamma(T)}{R_{\max}}\right).$$

Hill response: We have $R(M) = a_{\max}M/(M^2 + \mu_M^2)$ and $R_{\max} = a_{\max}/(2\mu_M)$. We obtain

$$M_{\text{emp}}(T)R'(M_{\text{emp}}(T)) = -\Gamma(T)\sqrt{1 - \left(\frac{\Gamma(T)}{R_{\max}}\right)^2}.$$

Substituting these results into (51) and using Cor. 4.4 shows that T_{reach} is characterized by

$$(1 + T_{\text{reach}}/\tau_{\text{emp}})(1 - d(T_{\text{reach}})) = \begin{cases} 1 - \dfrac{\Gamma(T_{\text{reach}})}{R_{\max}}, & \text{Michaelis–Menten,} \\ \sqrt{1 - \left(\dfrac{\Gamma(T_{\text{reach}})}{R_{\max}}\right)^2}, & \text{Hill.} \end{cases} \tag{52}$$

Examining the monotonicity of the right and the left hand sides as functions of T, we see that there always exists a unique $T_{\text{reach}} \in (0, T_{\text{crit}})$. Thus, for $0 < T < T_{\text{reach}}$ the daily-output optimum occurs before complete emptying, whereas for $T_{\text{reach}} < T < T_{\text{crit}}$ it is attained at complete emptying, compare Fig. 11(a).

4.3 Duration-dependent stimulation

Suppose now that stimulation depends on the removal duration, $a = a(\tau)$. Under the set-duration protocol, the steady-state balance lemma, Lem. 3.11, gives

$$M_*(T, \tau) = \frac{r(T, \tau)a(\tau)}{\Gamma(T)}. \tag{53}$$

We know from Lem. 4.1 that session output $M_*(T, \tau)$ increases with removal duration τ. At the same time, increasing the removal duration also decreases the number of sessions per day.

As before, the quantity $Q(T, \tau)$ defined above determines whether $M_{\text{DAY}}(T, \tau)$ is increasing or decreasing, see (50). We characterize the behaviour of Q with respect to τ in the following Lemma. Note that the condition on the stimulation elasticity $E_a(\tau)$ plays a role analogous to the concavity assumption in Prop. 4.3; it ensures that the sign of $\partial_\tau M_{\text{DAY}}$ can change at most once.

Lemma 4.5 (Behaviour of Q under duration-dependent stimulation)**.** *Fix $T > 0$ and let $M_*(T, \tau) > 0$ be the session output as a stable positive steady state. Define the stimulation elasticity as*

$$E_a(\tau) := \frac{\tau a'(\tau)}{a(\tau)},$$

and suppose that $E_a(\tau) > 0$ is strictly decreasing, with $\lim_{\tau\to\infty} E_a(\tau) = 0$.
Then $Q(T, \tau)$ is strictly decreasing with τ both before and after complete emptying. Moreover,

$$\lim_{\tau\to 0^+} Q(T, \tau) = \infty, \qquad \lim_{\tau\to\infty} Q(T, \tau) = 0.$$

At complete emptying, the one-sided limits are

$$Q_D^{\mathrm{pre}}(T) := \lim_{\tau \to \tau_{\mathrm{emp}}^-} Q(T,\tau) = (1 + T/\tau_{\mathrm{emp}}) \left[E_a(\tau_{\mathrm{emp}}) + 1 - d(T)\right], \tag{54}$$

$$Q_D^{\mathrm{post}}(T) := \lim_{\tau \to \tau_{\mathrm{emp}}^+} Q(T,\tau) = (1 + T/\tau_{\mathrm{emp}}) E_a(\tau_{\mathrm{emp}}). \tag{55}$$

In particular,

$$Q_D^{\mathrm{post}}(T) < Q_D^{\mathrm{pre}}(T).$$

For a proof see App. 8.6.

Interpretation. The two quantities Q_D^{pre} and Q_D^{post} describe the growth or decay of daily output immediately before and after complete emptying. Their difference arises because increasing the removal duration before emptying increases both the amount removed and the stimulation, whereas after emptying it can only increase stimulation.

The following proposition now characterizes the maximum of $\tau \mapsto M_{\mathrm{DAY}}(T,\tau)$. See also Fig. 11(b) for a demonstration of its main results.

Proposition 4.6 (Maximal daily output under duration-dependent stimulation)**.** *Fix $T > 0$ and suppose the assumptions of Lem. 4.5 hold. Then $\tau \mapsto M_{\mathrm{DAY}}(T,\tau)$ has a unique maximum. Its position relative to complete emptying is determined as follows:*

$$\begin{aligned}
&Q_D^{\mathrm{pre}}(T) < 1 &&\implies \text{the maximum occurs before complete emptying, } \tau_{\mathrm{opt}} < \tau_{\mathrm{emp}},\\
&Q_D^{\mathrm{post}}(T) \le 1 \le Q_D^{\mathrm{pre}}(T) &&\implies \text{the maximum occurs at complete emptying, } \tau_{\mathrm{opt}} = \tau_{\mathrm{emp}},\\
&Q_D^{\mathrm{post}}(T) > 1 &&\implies \text{the maximum occurs after complete emptying, } \tau_{\mathrm{opt}} > \tau_{\mathrm{emp}}.
\end{aligned}$$

Whenever the maximum occurs away from the emptying boundary, it is attained at the unique τ_{opt} satisfying

$$Q(T, \tau_{\mathrm{opt}}) = 1.$$

The proof is given in App. 8.6.

Corollary 4.7 (Dependence of the maximum on the wait interval)**.** *Under the assumptions of Prop. 4.6, both $Q_D^{\mathrm{pre}}(T)$ and $Q_D^{\mathrm{post}}(T)$ are strictly increasing with T, and $Q_D^{\mathrm{post}}(T) < Q_D^{\mathrm{pre}}(T)$ for all $T > 0$. Moreover,*

$$\lim_{T \to 0^+} Q_D^{\mathrm{pre}}(T) = \lim_{T \to 0^+} Q_D^{\mathrm{post}}(T) = E_a(\tau_{\mathrm{emp}}),$$

whereas

$$\lim_{T \to \infty} Q_D^{\mathrm{pre}}(T) = \lim_{T \to \infty} Q_D^{\mathrm{post}}(T) = \infty.$$

Case: *$E_a(\tau_{\mathrm{emp}}) < 1$. There exist unique wait intervals*

$$T_{\mathrm{reach}} < T_{\mathrm{pass}}$$

satisfying

$$Q_D^{\mathrm{pre}}(T_{\mathrm{reach}}) = 1, \qquad Q_D^{\mathrm{post}}(T_{\mathrm{pass}}) = 1.$$

Consequently, the location of the maximum is

$$\begin{cases}
\text{before complete emptying}, & T < T_{\mathrm{reach}},\\
\text{at complete emptying}, & T_{\mathrm{reach}} \le T \le T_{\mathrm{pass}},\\
\text{after complete emptying}, & T > T_{\mathrm{pass}}.
\end{cases}$$

Case: *$E_a(\tau_{\mathrm{emp}}) \ge 1$. The maximum lies after complete emptying for every $T > 0$.*

Corresponding result for set-target removal. All of the above refers to steady states, however we know from Sec. 3.4 that duration-dependent stimulation under a set-target protocol can lead to non-constant long-term dynamics. We will discuss daily output for non-constant long-term dynamics in the next section, and restrict our discussion here to the case of stable fixed points.

Before complete emptying, set-target and set-duration removal describe the same positive steady states, see Sec. 3.5. For duration-dependent stimulation, $M_*(T,\tau)$ is strictly increasing with τ, so the corresponding session target $M_{\mathrm{tar}} = M_*(T,\tau)$ provides an equivalent parametrization, see Fig. 10(d). Hence a pre-emptying fixed-point daily maximum at τ_{opt} under set-duration removal corresponds to a unique set-target maximum at

$$M_{\mathrm{tar},opt} = M_*(T,\tau_{\mathrm{opt}}).$$

The protocols differ once complete emptying is reached. Under set-duration removal, the prescribed duration can exceed τ_{emp} (compare Fig. 10(d)), and continued stimulation can therefore shift the maximum beyond complete emptying. Under the set-target formulation, the session terminates at complete emptying. Consequently, if $E_a(\tau_{\mathrm{emp}}) < 1$, the set-target fixed-point daily maximum lies before complete emptying for $T < T_{\mathrm{reach}}$, whereas for $T \geq T_{\mathrm{reach}}$ the fixed-point daily output first reaches its maximum at $M_{\mathrm{tar}} = M_{\mathrm{emp}}(T)$ and remains constant for $M_{\mathrm{tar}} \geq M_{\mathrm{emp}}(T)$. If $E_a(\tau_{\mathrm{emp}}) \geq 1$, this latter case applies for every $T > 0$.

Examples. For the *Michaelis–Menten* duration response,

$$a(\tau) = a_{\max}\frac{\tau}{\tau+\mu_\tau}, \qquad E_a(\tau) = \frac{\mu_\tau}{\tau+\mu_\tau},$$

so E_a fulfils the assumptions of Prop. 4.6, and $E_a(\tau_{\mathrm{emp}}) < 1$. Hence, for set-duration removal, the maximum moves from before, to at, and finally to after complete emptying as T increases. For set-target removal, sufficiently short wait intervals have a pre-emptying maximum with respect to the session target, whereas for sufficiently long wait intervals the daily output is maximized at complete emptying.

For the *Hill* duration response,

$$a(\tau) = a_{\max}\frac{\tau^2}{\tau^2+\mu_\tau^2}, \qquad E_a(\tau) = \frac{2\mu_\tau^2}{\tau^2+\mu_\tau^2},$$

which again fulfils the assumptions of Prop. 4.6, with

$$E_a(\tau_{\mathrm{emp}}) < 1 \iff \mu_\tau < \tau_{\mathrm{emp}}.$$

If $\mu_\tau < \tau_{\mathrm{emp}}$ the same sequence of optimization regimes occurs as for the Michaelis–Menten response. If $\mu_\tau \geq \tau_{\mathrm{emp}}$, complete emptying is optimal for all set-target schedules, whereas under set-duration removal the optimum always lies after complete emptying. See Fig. 11(b),(c) for a visual summary of these results.

4.4 Daily output on non-constant attractors.

As shown in Sec. 3.4, under duration-dependent stimulation with set-target removal, the target-met fixed point may lose stability, giving rise to non-constant attractors. However, so far all results above are based on fixed points.

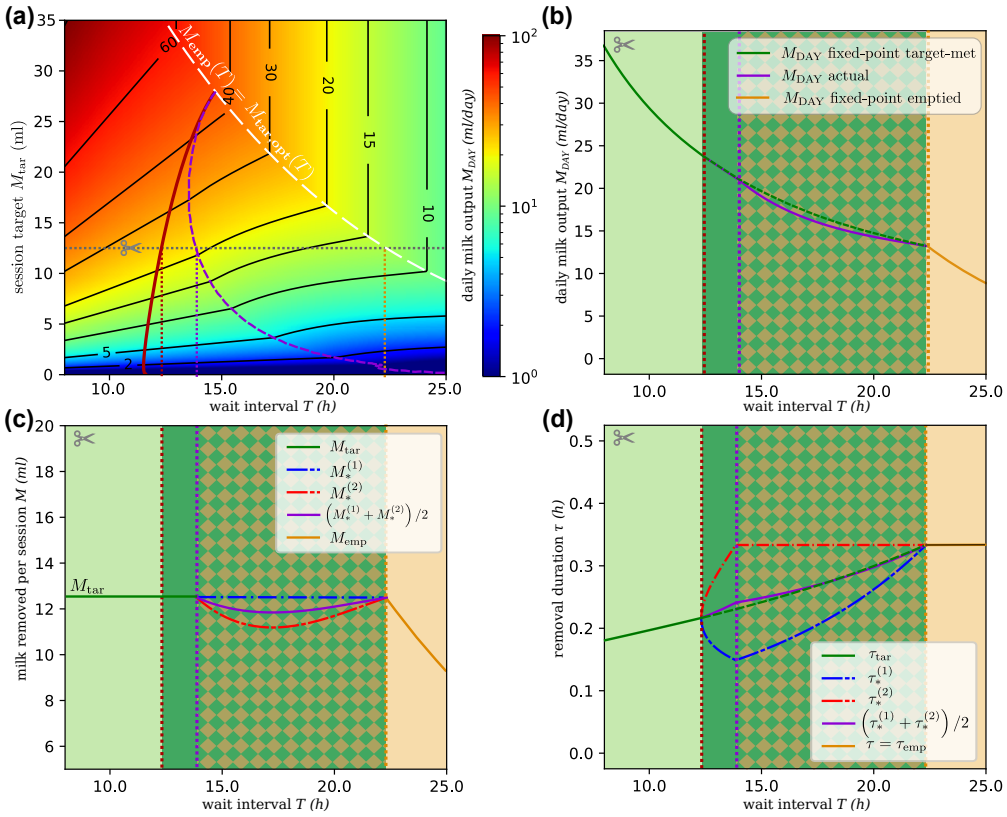

Figure 12: Daily milk output on non-constant attractors under duration-dependent stimulation and set-target removal. (a) Numerically determined long-term daily milk output $M_{\rm DAY}$ in $(T, M_{\rm tar})$-schedule space for the Hill response. Colours and black contours indicate $M_{\rm DAY}$. The black curve $M_{\rm emp}(T)$ separates target-met and emptied fixed-point branches. The red curve marks the instability boundary of the target-met fixed point, the dashed-purple curve the (numerically determined) boundary at which the attracting orbit first contains an emptying state. The horizontal dotted line indicates the slice $M_{\rm tar} = 12.5$ml used in (b)-(d). (b) Daily milk output along this slice, comparing the numerically realized attractor with the unstable target-met fixed-point and the emptying fixed-point. (c) Milk removed per session along the same slice. $M^{(1)}$ and $M^{(2)}$ denote the two period-2 values and the additional curve their mean. (d) Corresponding removal durations $\tau^{(1)}$ and $\tau^{(2)}$, their mean, the target-met fixed-point duration, and the complete-emptying duration $\tau_{\rm emp}$. Vertical dotted lines in (b)-(d) mark, from left to right, the period-doubling point, the first occurrence of an emptying state on the attracting orbit, and the transition to the emptied fixed point. Parameters used: $\delta = 0.15$/h, $\gamma = 0.15$/h, $a_{\max} = 50$ml/h, $\mu_\tau = 0.5$h, $\tau_{\rm emp} = 1/3$h.

Pre-emptying maxima are always stable. We start by discussing how the position of the fixed-point daily output maximum with respect to M_{tar} relates to the instability boundary of the target-met fixed point. The following Lemma gives an answer.

Lemma 4.8 (Stability of a pre-emptying daily-output maximum)**.** *Fix $T > 0$ and consider duration-dependent stimulation under a set-target protocol. Suppose that the fixed-point daily output*

$$M_{\text{tar}} \mapsto M_{\text{DAY}}(T, M_{\text{tar}})$$

has a pre-emptying maximum, i.e.

$$0 < M_{\text{tar},opt}(T) < M_{\text{emp}}(T).$$

Then the corresponding target-met fixed point is locally asymptotically stable.

For a proof see App. 8.6.

Interpretation. The above Lemma shows that a pre-emptying maximum of the daily output never lies in the region, where the target-met fixed point is unstable.

Numerical exploration of daily output under non-constant attractors. We next examine numerically the daily output under non-constant attractors. We chose a Hill response using the parameters given in Fig. 12. For the chosen parameters, $E_a(\tau_{\text{emp}}) > 1$. Hence the previous results imply that the fixed-point daily-output maximum lies at complete emptying for all $T > 0$, while part of the target-met fixed-point region is unstable. Beyond the fixed-point stability boundary, daily output is evaluated numerically from the asymptotic attractor. For this example, accounting for the non-constant attractors does not change the maximizing set-target schedule: daily output is still first maximized at complete emptying.

In the example in Fig. 12 we consider the behaviour of the daily output along a slice through schedule space with constant M_{tar}. Along this slice the only observed non-constant long-term behaviour is a 2-periodic attractor. In this case (48) gives

$$M_{\text{DAY}} = \frac{24}{T + \frac{1}{2}\left(\tau_*^{(1)} + \tau_*^{(2)}\right)} \frac{1}{2}\left(M_*^{(1)} + M_*^{(2)}\right).$$

Fig. 12 shows the resulting output and the numerically determined maximizing schedule. We observe that the daily output under the non-steady dynamics is qualitatively similar to the daily output corresponding to the unstable target-met fixed point, Fig. 12(a),(b). Inspecting how the individual and mean session outputs, and individual and mean session durations are affected, Fig. 12(c) and (d) respectively, we see that the observed (small) difference in daily output is mainly driven by periodic attractors that involve emptied-breast states: Here the mean session output is lowered, and the mean session duration is increased, compared to the unstable target-met fixed point. This leads to the observed small reduction in daily output.

4.5 Interpretation

In this section, we shifted the focus from milk removed per session to the long-term daily milk output M_{DAY}, and asked how this quantity depends on the removal schedule. For set-target removal, the schedule is controlled by (T, M_{tar}), whereas for set-duration removal it is controlled by (T, τ).

The effect of the wait interval T is consistent across all model variants: Holding the second schedule parameter fixed, increasing T decreases steady-state daily milk output. Increasing the amount or duration of removal can creates a trade-off. Longer removal sessions, or larger removal targets, can increase the amount of milk obtained per session, but also tends to lengthen the removal cycle and thereby reduce the number of sessions per day. As a result, M_{DAY} can be non-monotone in the second schedule parameter.

Fig. 11 illustrates how the location of this optimum depends on the stimulation mechanism. For amount-dependent stimulation, sufficiently short wait intervals favour removal that stops before complete emptying. As T increases, the optimum reaches complete emptying and remains there. Duration-dependent stimulation can show an additional regime: after the optimum has reached complete emptying, sufficiently long wait intervals can favour continuing the removal session beyond the time required to empty the breast. In this regime no additional milk is removed during the extended part of the session, but the additional removal duration continues to stimulate subsequent production. For Hill-type duration responses, the existence of a pre-emptying optimum also depends on the emptying time τ_{emp}; for sufficiently short emptying times, this regime disappears.

The preceding results describe daily output for stable steady-states. Duration-dependent stimulation under set-target removal can, however, lose fixed-point stability and generate non-constant attractors. Fig. 12 shows that the onset of period-doubling need not produce a substantial change in daily milk output. In the numerical example examined, while both points of the period-2 attractor remain target-met, daily output remains close to the value obtained from the formal fixed-point continuation. A clearer reduction occurs once one point of the attractor reaches complete emptying. However, these changes did not affect the maximum of the daily output with respect to the second scheduling variable.

Taken together, the results show that maximizing output per session and maximizing output per day are distinct objectives. Inspecting the level-sets of M_{DAY} in Fig. 11(a),(b) and Fig. 12(a) we see that for a given M_{DAY}, there can be several schedules with different wait intervals, removal targets, and removal durations that produce similar long-term output. One can therefore choose among these schedules based on additional criteria, such as the time spent removing milk or the frequency of removal sessions.

5 Comparison and summary of model predictions

After analysing the individual model variants, we now compare which qualitative predictions are robust and which depend on the assumed stimulation mechanism, stimulation-efficiency response, or removal protocol. Fig. 13 provides an overview of the resulting long-term behaviour and daily milk output. In particular, we distinguish whether a model predicts a critical wait interval, dependence of the long-term outcome on the initial state, and non-constant long-term dynamics.

Duration-dependent stimulation lacks direct state-dependent feedback. A principal distinction is whether stimulation depends on the amount of milk removed or on removal duration. With amount-dependent stimulation, a reduction in milk production leads to less milk being available for removal, which in turn reduces stimulation of subsequent production. This feedback allows low-production states to reinforce themselves and ultimately permits involution. For duration-dependent stimulation this direct coupling between the amount removed and subsequent stim-

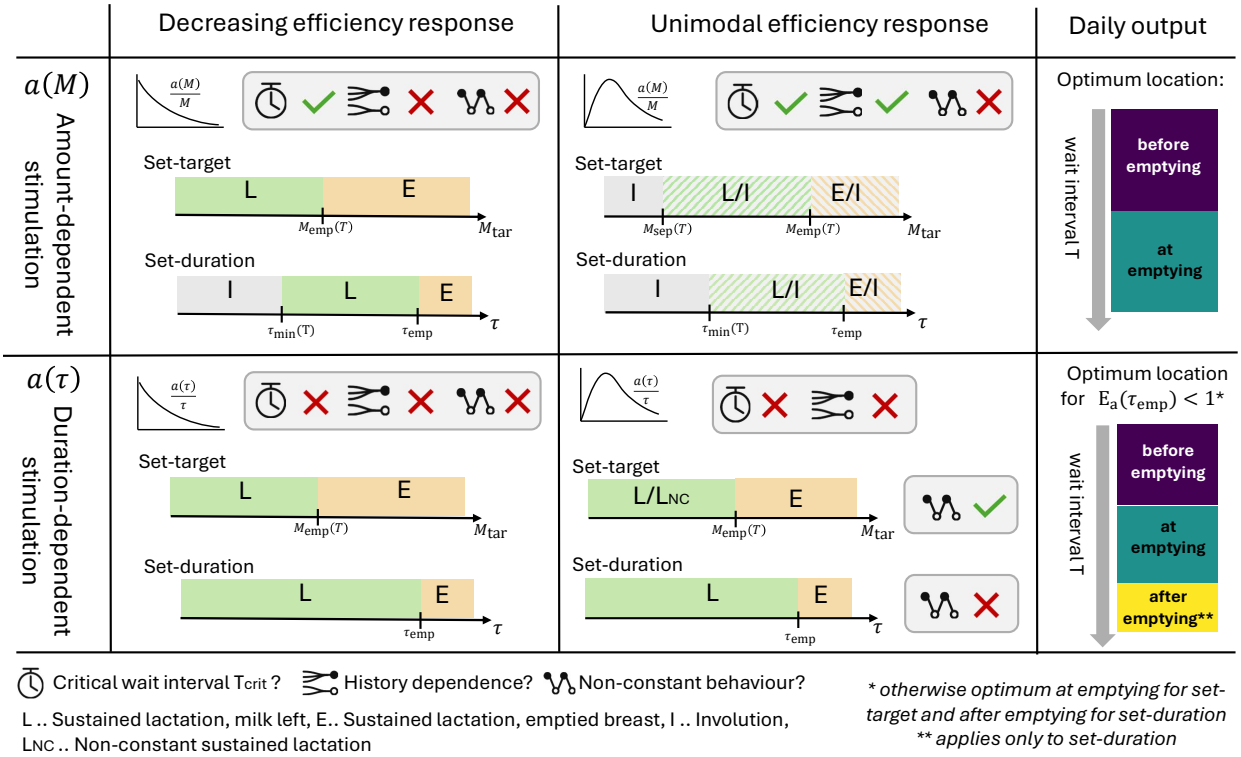

Figure 13: Comparison of long-term model behaviour and daily milk output across the dimensions: Stimulation-dependence, removal protocol and stimulation efficiency response.

ulation is absent. Consequently, for the regular positive-removal schedules considered here, the duration-dependent models do not admit the involution state as a long-term outcome.

Amount-dependent stimulation yields a critical wait interval. For amount-dependent stimulation, sustained lactation requires the stimulation generated per unit milk removed to compensate for the loss of production between removal sessions. This gives a robust result: the same critical wait interval T_{crit} for both removal protocols and for both efficiency classes. If the maximal stimulation efficiency is smaller than the rate of production loss, no positive wait interval can sustain lactation. Otherwise, positive sustained states are possible only for wait intervals with $0 < T < T_{\text{crit}}$. The critical wait interval shortens if production loss or milk loss between sessions is large, and lengthens if the maximal stimulation efficiency is large.

History dependence requires a unimodal efficiency response. The distinction between decreasing and unimodal efficiency for amount-dependent stimulation is particularly important at small removals. For a decreasing efficiency response, stimulation is most efficient for small amounts and whenever the wait interval is below T_{crit} every nonzero initial condition converges to sustained lactation. For a unimodal efficiency response, efficiency is small at small removals, increases before reaching its maximum and only then decays. In the amount-dependent models this has two effects: First, a minimal amount of milk has to be removed per session to allow for a sustained lactation

state to exist. Second, even if the sustained lactation state exists, the long-term outcome depends on the initial milk amount and production rate: If these are too low, the system will converge to the involution state. In contrast, duration-dependent stimulation does not produce bistability between involution and sustained lactation, since the involution state is absent under continued stimulation.

Set-target and set-duration protocols are qualitatively similar for decreasing efficiency, but can differ substantially for unimodal efficiency. In this work we compared two removal protocols, setting the session target or setting the removal duration. For decreasing efficiency responses, changing between the two protocols has relatively little effect on the sustained long-term states predicted by the model. One distinction arises for duration-dependent stimulation, where prescribed removal durations can extend beyond complete emptying and thereby support larger steady-state session outputs. The differences become more pronounced for unimodal efficiency responses. For amount-dependent stimulation, some steady states that are stable under set-target removal are unstable under set-duration removal. For duration-dependent stimulation, corresponding steady states can likewise differ in stability, and set-target removal can additionally generate non-constant long-term dynamics. Thus, prescribing an amount or a duration can change how deviations from a sustained state feed back into subsequent removal sessions, even when the corresponding steady-state session output and removal duration are the same.

Non-constant long-term behaviour occurs only for duration-dependent stimulation with unimodal efficiency under a set-target protocol. Within the model variants analysed here, all amount-dependent models converge to steady states. Duration-dependent stimulation under set-duration removal likewise has a stable steady state. Non-constant long-term dynamics arise only when duration-dependent stimulation with a unimodal efficiency response is combined with set-target removal. In this case the realised removal duration depends on the amount of milk available at the start of the session, and this state-dependent duration feeds back into subsequent stimulation. Numerical simulations then revealed attracting non-constant solutions, including period-doubled states.

Daily output reflects a trade-off between session output and session frequency. Across all model variants, increasing the wait interval decreases daily milk output, since it lengthens the removal cycle without increasing the amount obtained per session. In contrast, increasing the removal target or removal duration can increase session output, but simultaneously reduces the number of sessions that can be performed per day. Consequently, for sufficiently short wait intervals the daily-output maximum can occur before complete emptying, see the right column of Fig. 13: the gain from extracting more milk per session is then outweighed by the additional time required for removal. As the wait interval increases, the optimum shifts towards complete emptying. For duration-dependent stimulation, continued removal after emptying can still increase subsequent production, so that under set-duration removal the optimum can shift further, from before to at and eventually after complete emptying. Thus, the stimulation mechanism determines not only whether lactation can be sustained, but also how the competing benefits of more intensive removal and more frequent removal affect long-term milk output.

6 Discussion

6.1 Comparing model predictions to reality

The big picture. We developed and analysed a hybrid model of the feedback between milk removal and subsequent production. For repeated constant schedules, we characterised the long-term behaviour and identified which qualitative predictions depend on the assumed stimulation mechanism and removal protocol (see Sec. 5 and Fig. 13 and *Interactive Lactation Explorer* - Online Resource 1). The predictions are broadly consistent with the physiology of established lactation, where milk removal regulates production and prolonged milk stasis can lead to involution (Truchet and Honvo-Houéto 2017; Daly et al. 1996; Kent et al. 2012). However, the underlying physiology involves hormonal, mechanical and local regulatory mechanisms. Our stimulation function therefore represents the combined effect of a removal session rather than any specific physiological pathway. The models distinguish between amount- and duration-dependent stimulation, decreasing and unimodal stimulation efficiency, and two alternative removal protocols. These distinctions lead to several potentially testable predictions.

Amount-dependent versus duration-dependent stimulation. Amount-dependent stimulation introduces a direct state-dependent feedback: declining production reduces the milk available for removal and hence subsequent stimulation, potentially reinforcing the decline. This allows for involution and leads to a critical wait interval T_{crit}. In contrast, duration-dependent stimulation lacks this coupling in our formulation and does not permit involution under continued stimulation. Observations of self-reinforcing production loss despite continued removal, or of a critical wait interval beyond which more intensive removal cannot sustain lactation, would therefore favour the amount-dependent models.

However, this distinction should be interpreted cautiously. First, removal amount and duration are intrinsically correlated, making the two mechanisms difficult to distinguish experimentally. Second, our removal law assumes a state-independent emptying time τ_{emp}. If emptying duration depended on the available milk, duration-dependent stimulation could itself become state dependent and potentially alter the low-production dynamics.

Decreasing and unimodal stimulation efficiency. The two efficiency classes differ primarily in their response to small inputs: decreasing efficiency is maximal at small removal amounts or durations, whereas unimodal efficiency reaches its maximum at an intermediate scale. Distinguishing these alternatives requires measurements spanning small and intermediate inputs, ideally through longitudinal data relating removal to subsequent production.

For amount-dependent stimulation, unimodal efficiency additionally permits bistability: whether lactation is sustained can depend on the initial milk amount and production rate. This is consistent with the idea that lactation must first be sufficiently established before a given schedule can maintain it. However, our model does not describe postpartum establishment or its endocrine regulation. Bistability therefore demonstrates that an establishment-like threshold can arise from the feedback structure, but does not establish unimodal stimulation efficiency as the underlying physiological mechanism. History dependence could also arise from additional physiological variables absent from the model.

Further predictions may help distinguish the models. For amount-dependent stimulation, the maximal sustainable session output decreases with increasing wait interval. Non-constant long-term

dynamics, on the other hand, occur only for duration-dependent stimulation with unimodal efficiency under a set-target protocol. Observing persistent oscillations under approximately repeated schedules would therefore be of interest, although distinguishing them from biological variability may be difficult.

Parameter estimates. Available estimates suggest a characteristic decline timescale of milk production of about 48 h (Truchet and Honvo-Houéto 2017), which we use as an order-of-magnitude proxy for $\gamma^{-1} \approx 48\,\mathrm{h}$. Further, Meier et al. (2016) reported that efficient breast pumps remove approximately 85% of the available milk within 15 min. Under our linear removal law, this corresponds to $\nu \approx 3.4\,\mathrm{h}^{-1}$ and hence to a model emptying time of $\tau_{\mathrm{emp}} = 1/\nu \approx 18$ min. Kent et al. (1999) measured a production rate of about 18 ml/h per breast during exclusive breastfeeding. During established lactation, exclusively breastfed infants typically consume approximately 700–800 mL of milk per day, distributed over roughly 7–8 feeding occasions, although substantial variation exists (Kent et al. 2006; Rios-Leyvraz and Yao 2023).

To estimate the stimulation parameters, we assume that the milk-loss timescale is of similar order to the production-loss timescale, $\delta \sim \gamma$, and use the steady state of a session that empties the breast, for which $M^* = G(T)\,p^*$ and $a(M^*) = p^*\big(1 - e^{-\gamma T}\big)$. For $p^* \approx 18\,\mathrm{ml/h}$ and $T \approx 3\,\mathrm{h}$, this gives $M^* \approx 51\,\mathrm{ml}$, consistent with the intake data above, and $a(M^*) \approx 1.1\,\mathrm{ml/h}$. Assuming $\mu_M \approx 100\,\mathrm{ml}$, this yields $a_{\max} \approx 3$–$5\,\mathrm{ml/h}$ and $R_{\max} \approx 0.032\,\mathrm{h}^{-1}$ for the Michaelis–Menten response and $R_{\max} \approx 0.027\,\mathrm{h}^{-1}$ for the Hill response. Both exceed $\gamma \approx 0.021\,\mathrm{h}^{-1}$, so a sustained lactation state exists, with critical wait intervals T_{crit} of roughly one to two days. Eq. (52) then gives $T_{\mathrm{reach}} \approx 2$–$3\,\mathrm{h}$: for shorter wait intervals, terminating removal before complete emptying maximizes daily milk output. Consistently with our assumption of an emptying steady state at $T \approx 3\,\mathrm{h}$, this lies just below typical feeding intervals. Thus, this non-trivial model prediction may occur in a physiologically and practically relevant regime.

In contrast, for the Hill duration-response model the necessary condition for loss of fixed-point stability, $T > \log(3)/\gamma$, gives $T \gtrsim 53\,\mathrm{h}$. Thus, with these order-of-magnitude estimates, the non-constant dynamics found in the duration-dependent set-target model are unlikely to occur under typical feeding or pumping schedules. A quantitative assessment will require parameter estimation from longitudinal data, in particular for the stimulation-response parameters that are not currently constrained.

6.2 Milk output and schedule design

Maximising daily milk output. Sustaining lactation is only one possible objective of a removal schedule; in practice, the amount of milk obtained over time is also important. Increasing the session target or removal duration may increase the amount of milk obtained per session, but at the cost of lengthening the full wait–removal cycle and thereby reducing session frequency. The resulting trade-off can make daily output non-monotone with respect to removal intensity. In the examples analysed here, schedules that maximise daily output involve either complete emptying of the breast or, for sufficiently short wait intervals, terminating individual sessions before the breast is emptied. This mirrors a familiar distinction in impulsive harvesting, where maximising the yield of a single harvest and maximising sustained yield per unit time are likewise different objectives (Zhang et al. 2003; Lawson and Braverman 2023); in contrast to harvesting, however, removal here also stimulates future production. These results depend on model assumptions and should not be interpreted as direct breastfeeding or pumping recommendations. They do, however, illustrate

why maximising milk obtained per session, maximising milk obtained per day, and minimising the practical burden of removal are different objectives.

Schedule choice depends on objective. More generally, a given daily milk output can be achieved by different removal schedules. This flexibility may be as relevant in applications as maximizing output itself. Depending on the practical objective, one might choose a schedule that achieves an adequate output while minimizing the number of sessions or total pumping time, allowing longer uninterrupted intervals, limiting prolonged breast fullness, or satisfying constraints imposed by work, sleep, or other activities. The present analysis provides a mechanistic basis for such schedule-design problems, but quantitatively meaningful optimization will require physiological parameterization and extension to non-constant schedules.

6.3 Model assumptions and limitations

Model structure. The simplicity that makes the model analytically tractable also imposes important limitations. We represent each breast independently, and by only two state variables, total milk volume and an effective production rate, without resolving individual lobes, alveoli, or spatial variation. We separate each cycle into a comparatively long continuous wait phase and a short removal phase represented as a discrete update. Production and milk loss during removal are neglected. This approximation is appropriate only when removal sessions occur on a substantially shorter timescale than the intervals between them.

Stimulation. The biological mechanisms connecting milk removal to future production are represented phenomenologically through a single stimulation function. In particular, the present formulation does not explicitly include the proposed negative feedback of breast fullness on ongoing milk production (Peaker and Wilde 1996). Further we let stimulation depend either on the amount removed or on the session duration, but not on both. For duration-dependent stimulation we additionally assume that stimulation can continue after complete emptying; whether post-emptying nipple or pump stimulation has a comparable effect on subsequent milk synthesis is not established.

Removal law. Milk removal itself is described by a simple linear removal law. The removal law further assumes a state-independent removal-rate parameter, so that complete emptying occurs after the fixed duration $\tau_{\text{emp}} = 1/\nu$. In reality, removal rate and the time required to empty the breast may depend on the amount of milk available, milk-ejection dynamics, infant or pump characteristics, and other state-dependent factors. Moreover, actual breastfeeding and pumping sessions can contain multiple milk-ejection events, variable flow rates and interruptions.

Variable schedules. The present paper analyses repeated identical schedules. Real breastfeeding and pumping behaviour is highly variable: intervals between sessions differ throughout the day, night-time schedules differ from daytime schedules, individual sessions differ in duration and effectiveness, and both schedules and parameters can change systematically during establishment, maintenance, and weaning. Constant schedules provide a useful first step because they reveal fixed points, thresholds, bistability, and the dependence of long-term output on model assumptions in a form that can be analysed explicitly. They are best viewed as building blocks for studying realistic sequences of non-identical removal events.

6.4 Outlook

Model selection and parameter estimation. To determine the most likely stimulation mechanism, a natural next step is to fit the alternative model variants to longitudinal pumping data and use model-selection and predictive criteria to assess which stimulation mechanisms are supported by the data. This would also allow estimation of the physiological timescales, stimulation-response parameters, and removal characteristics required for quantitative predictions. In particular, distinguishing amount- from duration-dependent stimulation will require datasets with sufficient independent variation in removed amount and removal duration.

Analysis of variable schedules. Analytically, the next step is to extend the analysis from constant to variable schedules. The hybrid formulation already allows the wait interval, removal duration, and removal target to vary from one session to the next, so realistic daily or multi-day schedules can be represented without changing the underlying model structure. This will make it possible to study questions that cannot be addressed by constant schedules, including whether occasional long gaps can be compensated by more intensive removal at other times, how rapidly the system responds to changes in schedule, and how the timing and ordering of sessions influence long-term production.

Practical impact. Combined with parameter estimation from longitudinal human data, the same framework can ultimately be used to formulate practical optimisation problems. Relevant objectives include increasing production from a low-output state, maintaining a prescribed daily output with minimal pumping burden, adapting schedules to external constraints, and deliberately reducing production during weaning. The present theory does not yet provide individual recommendations for these questions. Rather, it identifies the dynamical mechanisms and thresholds that must be understood before such recommendations can be made and provides an analytically tractable foundation for subsequent data-driven and practice-oriented work. Such applications will require both model calibration and validation on independent longitudinal data.

7 Statements and Declarations

Competing interests

The authors declare no competing interests.

Supplementary Information

Online Resource 1. *Interactive Lactation Explorer*: A stand-alone html file with which the analytical and numerical results can be tested, visualised and explored, see also *Data and Code availability.*

Data and Code availability

No experimental data were generated or analysed during the current study. A Jupyter notebook for numerical simulation of the model, as well as the *Interactive Lactation Explorer* are available on Github `https://github.com/angelikamanhart/Lactation_model_analytical_paper`. For a direct link to the *Interactive Lactation Explorer* follow `https://angelikamanhart.github.io/Lactation_model_analytical_paper/interactive_lactation_explorer.html`.

Author contribution

AM designed the project and developed the models. AM and TM analysed the models. AM wrote and edited the paper.

Acknowledgements

The authors thank Dominik Stürzer for helpful discussions and feedback.

LLM disclosure

During the preparation of this manuscript, the authors used ChatGPT (OpenAI) and Claude (Anthropic) for language editing and to assist in discussing, checking, and presenting mathematical arguments. In particular ChatGPT was used for the creation of the interactive *Lactation Explorer*. All resulting text and mathematical content were reviewed and verified by the authors, who take full responsibility for the manuscript.

Funding

No funding was received for conducting this study.

8 Appendix

Throughout this appendix, $\leq$ denotes the componentwise order on $X = [0, \infty)^2$.

8.1 Amount-dependent stimulation, set-target protocol: Auxiliary results and proofs

Auxiliary results. The following facts are independent of the particular shape of R, and apply to both the decreasing efficiency response class and the unimodal efficiency response class. Throughout $F : X \to X$ is given by (11),

$$F(m, p) = \Big(\max\{x - M_{\text{tar}},\, 0\},\;\; p\, g + a\big(\min\{M_{\text{tar}},\, x\}\big)\Big),$$

where $x(m, p) = md + pG$.

Lemma 8.1 (Monotonicity)**.** *F is order-preserving: $z \leq \tilde{z}$ implies $F(z) \leq F(\tilde{z})$.*

Proof. Both components of (11) are nondecreasing in m and in p, since $x(m, p) = md + pG$ is, a is increasing, and min and max preserve monotonicity. □

Lemma 8.2 (Boundedness)**.** *Every orbit of F is bounded. More precisely, for every $z \in X$,*

$$\limsup_{n\to\infty} p_n \leq \frac{a_{\max}}{1-g}, \qquad \limsup_{n\to\infty} m_n \leq \frac{1}{1-d} \max\left\{0,\; \frac{a_{\max}}{\Gamma} - M_{\text{tar}}\right\}.$$

Proof. Since $a \leq a_{\max}$, the second component of (11) gives $p_{n+1} \leq p_n g + a_{\max}$, so $p_n \leq g^n p_0 + a_{\max}(1 - g^n)/(1 - g)$, which yields the first bound and shows (p_n) is bounded. Fix $\varepsilon > 0$ and n_0 with $p_n \leq a_{\max}/(1 - g) + \varepsilon$ for $n \geq n_0$. Then, for $n \geq n_0$, the first component satisfies $m_{n+1} \leq \max\{m_n d + \frac{a_{\max}}{\Gamma} + \varepsilon G - M_{\text{tar}}, 0\}$, and iterating this recursion from n_0 gives the second bound as $\varepsilon \downarrow 0$. □

Lemma 8.3 (Sandwich)**.** *Assume $R_{\mathrm{tar}} > \Gamma$ and set $z^* = (0, M_{\mathrm{tar}}/G)$. Then $F(z^*) \geq z^*$, and every $z \geq z^*$ satisfies $F^n(z) \to z_{\mathrm{tar}}$.*

Proof. We have $F(z^*) = \big(0,\, gM_{\mathrm{tar}}/G + a_{\mathrm{tar}}\big)$, and $R_{\mathrm{tar}} > \Gamma$ directly implies $F(z^*) \geq z^*$. By Lem. 8.1 the sequence $\big(F^n(z^*)\big)_n$ is nondecreasing, and it is bounded by Lemma 8.2, so it converges to a fixed point $w \geq z^*$. Any fixed point with $m = 0$ lies in E and therefore has $p \leq M_{\mathrm{tar}}/G$; combined with $w \geq z^*$ this would force $p = M_{\mathrm{tar}}/G$ and hence $R_{\mathrm{tar}} = \Gamma$, which the hypothesis excludes. Since w has $m > 0$, it lies in the target-met region and hence $w = z_{\mathrm{tar}}$, the unique fixed point of F.

Let now $z \geq z^*$ and put $P = \max\{p,\, a_{\max}/(1-g)\}$, $M = \max\{m,\, (PG - M_{\mathrm{tar}})/(1-d)\}$ and $z^{**} = (M, P)$. Then $z^{**} \geq z$ and $F(z^{**}) \leq z^{**}$: the second component is at most $Pg + a_{\max} \leq P$ by the choice of P, and the first is at most $\max\{Md + PG - M_{\mathrm{tar}}, 0\} \leq M$ by the choice of M. Hence $\big(F^n(z^{**})\big)_n$ is nonincreasing and converges to a fixed point w'. Since $z^{**} \geq z^*$, monotonicity gives $F^n(z^{**}) \geq F^n(z^*) \to z_{\mathrm{tar}}$, so $w' \geq z_{\mathrm{tar}}$. Since $m_{\mathrm{tar}} > 0$, this implies that the first component of w' is positive and w' therefore lies in the target-met region. Hence $w' = z_{\mathrm{tar}}$. Finally $F^n(z^*) \leq F^n(z) \leq F^n(z^{**})$ for all n, and both bounds converge to z_{tar}. □

Lemma 8.4 (Linearisation)**.** *Let z be a fixed point of F with $p > 0$.*

(i) If z lies in the interior of E, then $z = (0, p)$ with $p = pg + a(pG)$, and $DF(z)$ has eigenvalues 0 and $g + a'(pG)G$. Writing $M = pG$ for the volume removed at z, the state is asymptotically stable if $R'(M) < 0$ and unstable if $R'(M) > 0$.

(ii) If z lies in the interior of $X \setminus E$, then $DF(z)$ has eigenvalues d and g, both in $(0, 1)$, and z is asymptotically stable.

Proof. On the interior of E the map is $(m, p) \mapsto \big(0, pg + a(x)\big)$, with Jacobian

$$\begin{pmatrix} 0 & 0 \\ a'(x)\, d & g + a'(x)\, G \end{pmatrix},$$

whose eigenvalues are 0 and $g + a'(x)G$. A fixed point there has $m = 0$ and $x = pG$ with p fulfilling $p = pg + a(pG)$. Setting $M = pG$ and using $R(M) = \Gamma$, we can rewrite $g + a'(x)\, G - 1 = G(a'(M) - \Gamma) = G\, M\, R'(M)$ showing that the condition $g + a'(pG)G < 1$ is therefore precisely $R'(M) < 0$. On the interior of $X \setminus E$ the map is the affine map (12), whose linear part is upper triangular with diagonal entries d and g. □

Further we define $E_0 = \{0\} \times \big[0,\, M_{\mathrm{tar}}/G\big]$ so that E_0 is the part of the p-axis lying in E.

Lemma 8.5 (Entry into the emptying region)**.** *(i) If $R_{\mathrm{tar}} < \Gamma$, then every orbit enters E in finite time. Moreover, if $R_{\mathrm{tar}} \leq \Gamma$, then*

$$F(E) \subseteq E_0.$$

(ii) If $R_{\mathrm{tar}} > \Gamma$, then the target-met fixed point $z_{\mathrm{tar}} = (m_{\mathrm{tar}}, p_{\mathrm{tar}})$ lies in the interior of E^c, and every orbit that never enters E converges to z_{tar}.

Proof. Eq. (13) shows that $m_{\mathrm{tar}} < 0$ if $R_{\mathrm{tar}} < \Gamma$ and $m_{\mathrm{tar}} > 0$ if $R_{\mathrm{tar}} > \Gamma$.

Suppose an orbit never enters E. It is then generated entirely by the now affine target-met map F. Since the linear part of F has eigenvalues $d, g \in (0, 1)$,

$$F^n(z) \to z_{\mathrm{tar}}.$$

If $R_{\mathrm{tar}} < \Gamma$, this is impossible for an orbit contained in X, since $m_{\mathrm{tar}} < 0$. Hence every orbit enters E in finite time.

If $R_{\mathrm{tar}} \le \Gamma$ and $(m,p) \in E$, then $p \le M_{\mathrm{tar}}/G$ and $x(m,p) \le M_{\mathrm{tar}}$. Therefore

$$pg + a(x) \le g\frac{M_{\mathrm{tar}}}{G} + a(M_{\mathrm{tar}}) \le \frac{M_{\mathrm{tar}}}{G},$$

so $F(E) \subseteq E_0$.

Finally, if $R_{\mathrm{tar}} > \Gamma$, then $m_{\mathrm{tar}} > 0$. Since at a target-met fixed point

$$m_{\mathrm{tar}} = x(z_{\mathrm{tar}}) - M_{\mathrm{tar}},$$

we have $x(z_{\mathrm{tar}}) > M_{\mathrm{tar}}$, so $z_{\mathrm{tar}} \in \mathrm{int}(E^c)$. Any orbit which never enters E is an orbit of F and therefore converges to z_{tar}. □

Lemma 8.6 (Dynamics on the p-axis, decreasing-efficiency case)**.** *Let $q \in [0, M_{\mathrm{tar}}/G]$. While the orbit of $(0,q)$ remains in $E_0 = \{0\} \times [0, M_{\mathrm{tar}}/G]$, its second component evolves under the increasing scalar map $\Phi(q) = qg + a(qG)$, with*

$$\Phi(q) - q = qG\big(R(qG) - \Gamma\big).$$

Then:

(a) if $R_{\max} < \Gamma$, the orbit remains in E_0, decreases strictly for $q > 0$ and converges to $(0,0)$;

(b) if $R_{\max} > \Gamma$ and $M_{\mathrm{tar}} \ge M_{\mathrm{emp}}$, the orbit remains in E_0 and converges to $(0, p_{\mathrm{emp}})$ for every $q > 0$;

(c) if $R_{\max} > \Gamma$ and $M_{\mathrm{tar}} < M_{\mathrm{emp}}$, the orbit leaves E_0 after finitely many steps for every $q > 0$.

Proof. For $(0,q) \in E_0$, $F(0,q) = (0, \Phi(q))$, and Φ is increasing because a is increasing. The identity above shows that the sign of $\Phi(q) - q$ is exactly the sign of $R(qG) - \Gamma$.

(a) If $R_{\max} < \Gamma$, then $R(qG) < \Gamma$ for every $q > 0$, so $\Phi(q) < q$ for every $q > 0$. Thus E_0 is forward invariant and the orbit decreases to a fixed point, necessarily $(0,0)$.

(b) If $M_{\mathrm{tar}} \ge M_{\mathrm{emp}}$, then E_0 contains $(0, p_{\mathrm{emp}})$ and is forward invariant by Lemma 8.5(i), since $R_{\mathrm{tar}} \le \Gamma$. By the strict decrease of R, $\Phi(q) > q$ below p_{emp} and $\Phi(q) < q$ above it. Hence every positive orbit in E_0 converges monotonically to $(0, p_{\mathrm{emp}})$.

(c) If $M_{\mathrm{tar}} < M_{\mathrm{emp}}$, then $R(qG) > \Gamma$ throughout the positive part of E_0, so $\Phi(q) > q$. If a positive orbit remained in E_0 forever, it would increase to a fixed point in E_0, but no such positive fixed point exists. Hence it leaves E_0 after finitely many steps. □

Proof of Thm. 3.1. Remember that for $T > 0$ it holds that $R_{\max} > \Gamma \iff T < T_{\mathrm{crit}}$.

Proof. **Fixed points.** A fixed point in E has $m = 0$ and, for $p > 0$, satisfies $R(pG) = \Gamma$. By the assumed shape of R, there is no positive solution for $R_{\max} < \Gamma$ and exactly one, $p = p_{\mathrm{emp}}$, for $R_{\max} > \Gamma$; it is admissible in E exactly when $M_{\mathrm{tar}} \ge M_{\mathrm{emp}}$. A fixed point outside E must be $z_{\mathrm{tar}} = (m_{\mathrm{tar}}, p_{\mathrm{tar}})$ of (13); it is admissible exactly when $R_{\mathrm{tar}} > \Gamma$, i.e. when $M_{\mathrm{tar}} < M_{\mathrm{emp}}$. This gives the stated fixed points.

Stability. Since $a'(0) = R(0) = R_{\max}$, the nonzero eigenvalue at z_0 is

$$g + Ga'(0) = g + (1-g)\frac{R_{\max}}{\Gamma},$$

so z_0 is stable for $R_{\max} < \Gamma$ and unstable for $R_{\max} > \Gamma$. Since R is strictly decreasing, $R'(M_{\text{emp}}) < 0$, so by Lemma 8.4(i) the positive p-axis state is stable whenever it lies in the interior of E. The interior target-met state is stable by Lemma 8.4(ii).

Global convergence. For $R_{\max} < \Gamma$, one has $R_{\text{tar}} < \Gamma$, so Lemma 8.5(i) sends every orbit into E_0, after which Lemma 8.6(a) gives convergence to z_0.

Now let $R_{\max} > \Gamma$ and $z \neq z_0$. If $M_{\text{tar}} > M_{\text{emp}}$ then $R_{\text{tar}} < \Gamma$ and Lem. 8.5(i) sends every orbit into E_0, after which Lem. 8.6(b) gives convergence to $z_2 = (0, p_{\text{emp}})$ (see Fig. 3(b), orbits (1) and (2)).

Finally, for $R_{\max} > \Gamma$, $z \neq z_0$ and $M_{\text{tar}} < M_{\text{emp}}$ there are two routes: Either the orbit stays in E^{c}, in which case Lem. 8.5(ii) gives convergence to $z_2 = z_{\text{tar}}$ directly (see Fig. 3(a), orbits (2)). If the orbit enters E, its next iterate is $(0, q)$ with $q > 0$ (q cannot be 0 since $F^{-1}(\{z_0\}) = \{z_0\}$). If $q \geq M_{\text{tar}}/G$, it dominates z^* and Lem. 8.3 applies directly. If $0 < q < M_{\text{tar}}/G$, Lem. 8.6(c) implies that the orbit leaves E_0 after finitely many iterations, thereby producing a point $(0, \tilde{q})$ with $\tilde{q} > M_{\text{tar}}/G$. Lem. 8.3 then gives convergence to z_{tar} (see Fig. 3(a), orbits (1)).
Hence in both cases $B(z_2) = X \setminus \{z_0\}$. □

Dynamics on the p-axis: unimodal-efficiency case. As in the decreasing-efficiency case, only the scalar dynamics on the p-axis is specific to the response class; the remaining ingredients are Lemmas 8.1–8.3. We note for later use that $M_{\text{tar}} > M_{\text{sep}}$ gives $a_{\text{tar}} > a(M_{\text{sep}}) = p_{\text{sep}}(1 - g)$, hence

$$p_{\text{tar}} > p_{\text{sep}}. \tag{56}$$

Lemma 8.7 (Dynamics on the p-axis, unimodal-efficiency)**.** *Let $q \in [0, M_{\text{tar}}/G]$ and assume $0 < T < T_{\text{crit}}$ and $M_{\text{tar}} > M_{\text{sep}}$. While the orbit of $(0, q)$ remains in E_0, its first component vanishes and its second evolves under the increasing scalar map $\Phi(q) = qg + a(qG)$, which satisfies*

$$\Phi(q) - q = qG\,(R(qG) - \Gamma)\,.$$

Consequently:

(a) if $q < p_{\text{sep}}$, the orbit remains in E_0, decreases strictly when $q > 0$ and converges to z_0;

(b) if $q > p_{\text{sep}}$ and $M_{\text{tar}} \geq M_{\text{emp}}$, the orbit remains in E_0 and converges to $z_2 = (0, p_{\text{emp}})$;

(c) if $q > p_{\text{sep}}$ and $M_{\text{tar}} < M_{\text{emp}}$, the orbit leaves E_0 after finitely many steps.

Proof. For $(0, q) \in E_0$, $F(0, q) = (0, \Phi(q))$, and Φ is increasing because a is increasing. The identity above shows that the sign of $\Phi(q) - q$ is exactly the sign of $R(qG) - \Gamma$. The assumed unimodal shape of R makes this difference negative on $(0, p_{\text{sep}})$, positive on $(p_{\text{sep}}, p_{\text{emp}})$ and negative on (p_{emp}, ∞).

(a) If $0 < q < p_{\text{sep}}$ then $\Phi(q) < q$ and, since Φ is increasing with fixed point p_{sep}, also $\Phi(q) < p_{\text{sep}}$. As $p_{\text{sep}} < M_{\text{tar}}/G$ the orbit stays in E_0; being decreasing and bounded below it converges to a fixed point of Φ in $[0, p_{\text{sep}})$, necessarily 0.

(b) Here $M_{\text{tar}}/G \geq p_{\text{emp}}$, so $E_0 \supseteq \{0\} \times [0, p_{\text{emp}}]$, and E_0 is forward invariant by Lemma 8.5(i), whose hypothesis $R_{\text{tar}} \leq \Gamma$ holds by (21) since $M_{\text{tar}} \geq M_{\text{emp}}$. The orbit is monotone by the sign of $R(qG) - \Gamma$ (increasing if $q < p_{\text{emp}}$, decreasing if $q > p_{\text{emp}}$) and bounded, hence converges to a fixed point of Φ in $(p_{\text{sep}}, M_{\text{tar}}/G]$, which must be p_{emp}.

(c) Now $M_{\text{tar}}/G < p_{\text{emp}}$, so Φ has no fixed point in $(p_{\text{sep}}, M_{\text{tar}}/G]$ and $\Phi(q) > q$ there. The orbit therefore increases strictly while it remains in E_0; were it to remain in E_0 for all time it would converge to a fixed point of Φ in that interval, a contradiction. Hence some iterate exceeds M_{tar}/G.

□

Additional statement about the shape of the separatrix. It holds that,

$$\Sigma = \bigcup_{k=1}^{N} \Sigma_k,$$

where the Σ_k are strictly decreasing arcs, consecutive arcs share an endpoint, the first arc lies in E, and subsequent arcs are obtained by successive inverse images under the affine target-met map. The number of non-degenerate arcs is

$$N = \left\lceil \frac{\log\bigl(1 - (1-g)\, p_{\text{sep}}/a_{\text{tar}}\bigr)}{\log g} \right\rceil. \tag{57}$$

In particular, $N = 1$ if and only if

$$M_{\text{tar}} \geq M_c, \qquad M_c := a^{-1}(p_{\text{sep}}),$$

where a^{-1} denotes the inverse of the strictly increasing stimulation function on its range, with $a^{-1}(y) = +\infty$ when $y \geq a_{\max}$.

Proof of Thm. 3.2 and Additional Statement about Separatrix.

Proof. **(i)** Let $z = (m, p)$ be a fixed point.
If $z \in E$ then the first component of (11) forces $m = 0$, so $x = pG \leq M_{\text{tar}}$ and $p = pg + a(pG)$, i.e. $R(pG) = \Gamma$ for $p > 0$; by the unimodal-efficiency assumption the solutions are $p \in \{0, p_{\text{sep}}, p_{\text{emp}}\}$, admissible precisely when $pG \leq M_{\text{tar}}$. This retains $p = 0$ always, $p = p_{\text{sep}}$ by the hypothesis $M_{\text{sep}} < M_{\text{tar}}$, and $p = p_{\text{emp}}$ exactly when $M_{\text{tar}} \geq M_{\text{emp}}$.
If instead $z \notin E$ then F is affine near z, and (13) gives $z = z_{\text{tar}}$; this is admissible iff $m_{\text{tar}} > 0$, i.e. iff $R_{\text{tar}} > \Gamma$, which by (21) means $M_{\text{tar}} < M_{\text{emp}}$. The two cases are complementary, so there are exactly three fixed points, as claimed.

For stability we apply Lemma 8.4. At z_0 we have $a'(0) = 0$, so the non-zero eigenvalue is $g < 1$. Since R is unimodal with $R(M_{\text{sep}}) = R(M_{\text{emp}}) = \Gamma$ and $M_{\text{sep}} < M_{\text{emp}}$, we have $R'(M_{\text{sep}}) > 0$ and $R'(M_{\text{emp}}) < 0$; by Lemma 8.4(i), $z_1 = (0, p_{\text{sep}})$ is therefore unstable, and $(0, p_{\text{emp}})$ is stable whenever it lies in the interior of E (i.e. for $M_{\text{tar}} > M_{\text{emp}}$); and $z_2 = (m_{\text{tar}}, p_{\text{tar}})$ is stable by Lemma 8.4(ii).

(ii) Let $z \in X$ and apply Lemma 8.5.

Case $R_{\text{tar}} < \Gamma$. In this case Lem. 8.5(i) shows that every orbit will enter E in finite time. Then, at the next iteration the orbit enters E_0 at some point $(0, q)$ with $q \leq M_{\text{tar}}/G$. Now Lem. 8.7(a) and (b) assert convergence to z_0 if $q < p_{\text{sep}}$ (see Fig. 5(b), orbit (1)), or convergence to $z_2 = (0, p_{\text{emp}})$ for $q > p_{\text{sep}}$ (see Fig. 5(b), orbits (2) and (3)). For $q = p_{\text{sep}}$ the orbit will be fixed at $z_1 = (0, p_{\text{sep}})$.

Case $R_{\text{tar}} > \Gamma$. We follow analogous arguments as in the proof of Thm. 3.1: Suppose $z \neq z_0$ and the orbit never enters E. Then Lem. 8.5 shows convergence to $z_2 = z_{\text{tar}} \in E^c$ (see Fig. 5(a), orbit (3)). If the orbit enters E, its next iterate is $(0, q)$ with $q > 0$ (since $F^{-1}(\{z_0\}) = \{z_0\}$). If $q \geq M_{\text{tar}}/G$, it dominates z^* and Lemma 8.3 applies directly. If $0 < q < M_{\text{tar}}/G$, Lemma 8.7(a) and (c) imply that for $q < p_{\text{sep}}$, the orbit converges to z_0 (see Fig. 5(a), orbit (1)), and for $q > p_{\text{sep}}$ the orbit will leave E_0 after finitely many iterations, thereby producing a point $(0, \tilde{q})$ with $\tilde{q} > M_{\text{tar}}/G$. Lemma 8.3 then gives convergence to z_{tar} (see Fig. 5(a), orbit (2)). Finally, for $q = p_{\text{sep}}$ the orbit will be fixed at $z_1 = (0, p_{\text{sep}})$.

Hence every orbit converges to z_0, z_1 or z_2. Let

$$\Sigma := \{z \in X : F^n(z) \to z_1\},$$

then $X = B(z_0) \sqcup \Sigma \sqcup B(z_2)$.

The preceding case distinction also shows that every orbit in Σ reaches z_1 in finitely many iterations. By definition $\Sigma = W^s(z_1)$. The sets $B(z_0)$ and $B(z_2)$ are open because z_0 and z_2 are asymptotically stable and F is continuous. $B(z_0)$ is a lower set: if $z \leq w \in B(z_0)$ then $0 \leq F^n(z) \leq F^n(w) \to z_0$, using Lemma 8.1. $B(z_2)$ is an upper set: if $z \geq w \in B(z_2)$ then $F^n(z) \geq F^n(w) \to z_2$, and since $F^n(z)$ converges to one of the three fixed points, its limit is $\geq z_2$ and hence equals z_2.

(iii) By the proof of part (ii), $z \in \Sigma$ if and only if the orbit of z enters E for the first time at some step $k - 1 \geq 0$ with entry value p_{sep}. We define the *entry map* by

$$\Psi(m, p) = p\, g + a\big(x(m, p)\big). \tag{58}$$

Points with $k = 1$ are those in E with $\Psi(z) = p_{\text{sep}}$. Hence

$$\Sigma_1 = \{z \in E : \ \Psi(z) = p_{\text{sep}}\}.$$

Solving $\Psi(m, p) = pg + a(x) = p_{\text{sep}}$ for p in terms of x and substituting into $x = md + pG$ gives

$$p(x) = \frac{p_{\text{sep}} - a(x)}{g}, \qquad m(x) = \frac{1}{d}\left(x - \frac{G}{g}\big(p_{\text{sep}} - a(x)\big)\right), \tag{59}$$

for $x \in \big[M_{\text{sep}},\, \min\{M_{\text{tar}}, a^{-1}(p_{\text{sep}})\}\big]$.
At $x = M_{\text{sep}}$ one gets $(p, m) = (p_{\text{sep}}, 0)$ so Σ_1 starts at z_1. Differentiating,

$$p'(x) = -\frac{a'(x)}{g} < 0, \qquad m'(x) = \frac{1}{d}\left(1 + \frac{G}{g}a'(x)\right) > 0,$$

so Σ_1 is a strictly decreasing arc. The admissible range of x is bounded above by M_{tar}, to remain in E, and by $a^{-1}(p_{\text{sep}})$, to keep $p \geq 0$.

Points whose first entry occurs after further affine steps are obtained by pulling the preceding arc back through F. For the geometric arc construction we include the boundary $x = M_{\text{tar}}$ so that consecutive arcs share endpoints; boundary points themselves are already contained in the earlier arc. Inverting (12) gives

$$p = \frac{p' - a_{\text{tar}}}{g}, \qquad m = \frac{1}{d}\Big(m' + M_{\text{tar}} - pG\Big). \tag{60}$$

The constraint $p \geq 0$ is $p' \geq a_{\text{tar}}$. For such a preimage,

$$x = md + pG = m' + M_{\text{tar}}.$$

Hence it lies strictly outside E whenever $m' > 0$, and on ∂E when $m' = 0$. The latter case is precisely the shared-endpoint convention just described.

The map (60) is increasing in p' and, along an arc traversed with p' decreasing and m' increasing, produces p decreasing and m increasing. Hence every Σ_k is a strictly decreasing arc.

Let

$$\pi_k := \max\{p : (m, p) \in \Sigma_k\}.$$

Since Σ_{k+1} is obtained by pulling back Σ_k through F, its maximal-p endpoint is the inverse image of the maximal-p endpoint of Σ_k. Thus

$$\pi_1 = p_{\text{sep}}, \qquad \pi_{k+1} = \frac{\pi_k - a_{\text{tar}}}{g},$$

and therefore

$$\pi_k = p_{\text{tar}} - (p_{\text{tar}} - p_{\text{sep}})g^{-(k-1)}.$$

The corresponding inverse-image point is the common endpoint of Σ_k and Σ_{k+1}. The pullback can be continued as a non-degenerate arc precisely while $\pi_k > a_{\text{tar}}$.

Using the expression for π_k, this condition is equivalent to

$$g^k > 1 - \frac{(1-g)p_{\text{sep}}}{a_{\text{tar}}}.$$

By (56), the right-hand side lies in $(0, 1)$, so this inequality fails for all sufficiently large k and the chain of arcs is finite. Consequently,

$$N = \left\lceil \frac{\log\bigl(1 - (1-g)p_{\text{sep}}/a_{\text{tar}}\bigr)}{\log g} \right\rceil,$$

as stated in (57). If the logarithmic quotient is an integer, equality corresponds to a degenerate pullback consisting only of the terminal endpoint already contained in Σ_N, so the ceiling formula still counts the non-degenerate arcs correctly.

Finally, $N = 1$ is equivalent to

$$g \leq 1 - \frac{(1-g)p_{\text{sep}}}{a_{\text{tar}}},$$

or equivalently $a_{\text{tar}} \geq p_{\text{sep}}$. Since a is strictly increasing, this is equivalent to

$$M_{\text{tar}} \geq a^{-1}(p_{\text{sep}}) = M_c.$$

Geometrically, this means that Σ_1 reaches the m-axis before leaving E.

Each Σ_k is a continuous, strictly decreasing arc, consecutive arcs meet only at their common endpoints, and the final arc terminates on the m-axis. Hence their union is the graph of a continuous, strictly decreasing function

$$\sigma : [0, \bar{m}_{\text{sep}}] \to [0, p_{\text{sep}}],$$

with $\sigma(0) = p_{\text{sep}}$ and $\sigma(\bar{m}_{\text{sep}}) = 0$. □

Remark 8.8. The junction $\Sigma_1 \cap \Sigma_2$ lies on ∂E, at $x = M_{\mathrm{tar}}$, whereas every later junction lies strictly outside E. Accordingly Σ_1 is the only arc whose extent is constrained by the geometry of E; the remaining arcs are determined by (60) alone.

The branch count N has a natural reading in terms of how far back the history matters. When $N = 1$, one session suffices to decide which side of the unstable production level the trajectory enters. When $N \geq 2$, the target caps the stimulation below p_{sep}, and the outcome can depend on the accumulated effect of several successive sessions. The criterion $M_{\mathrm{tar}} \geq M_c$ is exactly the statement that one maximal session is sufficient.

Proof of Cor. 3.3

Proof. In both cases $R(M) < \Gamma$ for $0 < M \leq M_{\mathrm{tar}}$: if $T > T_{\mathrm{crit}}$ because $R \leq R_{\max} < \Gamma$, and if $M_{\mathrm{tar}} < M_{\mathrm{sep}}$ by (21). Hence there is no fixed point $(0, p)$ with $0 < pG \leq M_{\mathrm{tar}}$ and, since $R_{\mathrm{tar}} < \Gamma$, no target-met fixed point, so z_0 is the unique fixed point; it is locally asymptotically stable by Lemma 8.4(i), since $a'(0) = 0$. By Lemma 8.5(i) every orbit enters E and thereafter remains in E_0, where $\Phi(q) - q = qG\big(R(qG) - \Gamma\big) < 0$ for $q > 0$; hence every orbit decreases to 0. □

8.2 Amount-dependent stimulation, set-duration protocol: Auxiliary results and proofs

Throughout this subsection we assume $0 < \tau < \tau_{\mathrm{emp}}$, and hence $0 < h < 1$. The map $F : X \to X$ is given by (23),

$$F(m, p) = \Big(x\,h,\;\; p\,g + a\big(x(1-h)\big)\Big), \quad x = md + pG.$$

Auxiliary results. We start by noting that F is globally injective, and its inverse on the image $F(X)$ is explicit:

$$x = \frac{m'}{h}, \qquad p = \frac{p' - a\big(x(1-h)\big)}{g}, \qquad m = \frac{x - pG}{d}. \tag{61}$$

Lemma 8.9. *The map* (23) *is order-preserving on X. Moreover, if $z \leq \tilde{z}$ componentwise and $z \neq \tilde{z}$, then both components of $F(z)$ are strictly smaller than the corresponding components of $F(\tilde{z})$. The map is injective, with inverse* (61) *defined on $F(X)$, and every orbit is bounded, with*

$$\limsup_{n\to\infty} p_n \leq \frac{a_{\max}}{1-g}, \qquad \limsup_{n\to\infty} m_n \leq \frac{a_{\max}\,h}{\Gamma(1-dh)}.$$

Moreover, for every $z \in X \setminus \{0\}$ the image $F(z)$ has both coordinates strictly positive.

Proof. If $z \leq \tilde{z}$ and $z \neq \tilde{z}$, then $x(z) < x(\tilde{z})$ since $d, G > 0$. Hence the first components are strictly ordered; the second components are also strictly ordered because a is strictly increasing. Inverting (23) in the order x, then p, then m gives (61). For the bounds, $p_{n+1} \leq p_n g + a_{\max}$ gives the first, and $m_{n+1} \leq m_n dh + p_n Gh$ then gives the second on iterating. Finally $z \neq 0$ gives $x(z) > 0$, hence $m' = xh > 0$ and $p' \geq a(x(1-h)) > 0$. □

Lemma 8.10 (Global convergence)**.** *Every orbit of the set-duration map F converges to a fixed point.*

Proof. By Lem. 8.9, every orbit is bounded and F is injective. Moreover, $X = \mathbb{R}^2_+$ is convex, F is C^1, and $DF(z)$ is entrywise nonnegative for every $z \in X$, with

$$\det DF(z) = dhg > 0.$$

Thus F satisfies the cooperative analogue of the hypotheses $(H+)$ in (Smith 1998). By Smith (1998, Corollary 4.4), every orbit with compact closure converges to a fixed point. Since X is closed and every orbit is bounded, its closure is compact and contained in X. Hence every orbit converges to a fixed point. □

Lemma 8.11 (Linearisation)**.** *For $z = (m, p) \in X$, set*

$$M = (1 - h)x(z).$$

Then

$$DF(z) = \begin{pmatrix} dh & Gh \\ a'(M)\, d(1-h) & g + a'(M)\, G(1-h) \end{pmatrix}, \qquad \det DF(z) = dhg.$$

At a fixed point with production rate p_* and removed amount $M_* = Grp_*$, the eigenvalues of DF are real and positive, with product $dhg \in (0, 1)$. Moreover,

$$\det(I - DF) = G(1-h)\big(\Gamma_\tau - a'(M_*)\big). \tag{62}$$

(i) At the zero fixed point $z_0 = (0, 0)$, the state is locally asymptotically stable if

$$a'(0) < \Gamma_\tau,$$

and unstable if $a'(0) > \Gamma_\tau$.

(ii) At a positive fixed point, where $R(M_*) = \Gamma_\tau$,

$$\det(I - DF) = -G(1-h)M_* R'(M_*). \tag{63}$$

Hence the fixed point is locally asymptotically stable if $R'(M_*) < 0$, whereas if $R'(M_*) > 0$ it is a hyperbolic saddle.

In the equality cases $a'(0) = \Gamma_\tau$ or $R'(M_*) = 0$, one eigenvalue equals 1.

Proof. The Jacobian and its determinant follow by direct computation. Its characteristic discriminant is

$$\big(dh - g - a'(M_*)G(1-h)\big)^2 + 4Gh\, a'(M_*)d(1-h) \geq 0,$$

so the eigenvalues are real. Their product is $dhg > 0$ and their sum is positive, hence both eigenvalues are positive. Since $\det(I - DF) = 1 - \operatorname{tr} DF + \det DF$, we obtain

$$\begin{aligned} \det(I - DF) &= (1 - dh)(1 - g) - a'(M_*)G(1-h) \\ &= G(1-h)\big(\Gamma_\tau - a'(M_*)\big), \end{aligned}$$

where we used $\Gamma_\tau = (1 - g)(Gr)$.

Because the two eigenvalues are positive and have product $dhg < 1$, they both lie in $(0, 1)$ if and only if $\det(I - DF) > 0$. This gives part (i).

At a positive fixed point, $R(M_*) = \Gamma_\tau$, and

$$a'(M_*) = R(M_*) + M_* R'(M_*),$$

so

$$\det(I - DF) = -G(1-h)M_* R'(M_*).$$

Thus $R'(M_*) < 0$ implies that both eigenvalues lie in $(0, 1)$. If $R'(M_*) > 0$, then $\det(I - DF) < 0$, so one eigenvalue lies below 1 and the other above 1; hence the fixed point is a hyperbolic saddle.

If $\det(I - DF) = 0$, one eigenvalue is 1. □

Proof of Thm. 3.4.

Proof. **Fixed points and stability.** A positive fixed point is equivalent to a solution of $R(M) = \Gamma_\tau$. For decreasing R there is no positive solution when $R_{\max} < \Gamma_\tau$ and exactly one, M_{lac}, when $R_{\max} > \Gamma_\tau$. Since $a'(0) = R_{\max}$, Lemma 8.11 shows that z_0 is stable for $R_{\max} < \Gamma_\tau$ and unstable for $R_{\max} > \Gamma_\tau$. At the positive root, $a'(M_{\mathrm{lac}}) - \Gamma_\tau = M_{\mathrm{lac}} R'(M_{\mathrm{lac}}) < 0$, so Lemma 8.11 gives stability of z_2.

(i) Since z_0 is the unique fixed point, Lemma 8.10 implies that every orbit converges to z_0.

(ii) Since $a'(0) = R_{\max} > 0$ and $h < 1$, all four entries of $DF(0)$ are positive, so $DF(0)$ has a strictly positive eigenvector v for its spectral radius ρ, and $\rho > 1$ because z_0 is unstable. As F is C^1 with $F(0) = 0$,

$$F(\varepsilon v) = \varepsilon \rho v + o(\varepsilon) \qquad (\varepsilon \downarrow 0),$$

and since $v > 0$ strictly and $\rho > 1$, there is $\varepsilon_0 > 0$ with $F(\varepsilon v) \geq \varepsilon v$ for all $\varepsilon \in (0, \varepsilon_0]$. For such ε the orbit of εv is nondecreasing and bounded, hence converges to a fixed point $\geq \varepsilon v > 0$, necessarily z_2.

Now let $z \in X \setminus \{0\}$. By Lem. 8.9, $F(z)$ has both coordinates strictly positive, so $F(z) \geq \varepsilon v$ for some $\varepsilon \in (0, \varepsilon_0]$. Hence

$$F^{n+1}(z) \geq F^n(\varepsilon v) \longrightarrow z_2.$$

By Lem. 8.10, the orbit of z converges to a fixed point. Since the only fixed points are z_0 and z_2, the above inequality excludes convergence to z_0. Thus $F^n(z) \to z_2$. Hence $B(z_2) = X \setminus \{z_0\}$. □

Proof of Thm. 3.5.

Proof. Under the hypotheses $0 < T < T_{\mathrm{crit}}$ and $\tau > \tau_{\min}(T)$, one has $R_{\max} > \Gamma_\tau$.

(i) The positive fixed points are in one-to-one correspondence with the positive solutions of $R(M) = \Gamma_\tau$. Since $R_{\max} > \Gamma_\tau$ and R is unimodal, these are precisely M_{sep} and M_{lac}. Together with z_0, this gives exactly the three fixed points stated above.

Since $R(0) = a'(0) = 0$, the eigenvalues at z_0 are dh and g, so z_0 is locally asymptotically stable. Since $R'(M_{\mathrm{sep}}) > 0$, Lem. 8.11(ii) shows that z_1 is a hyperbolic saddle, whereas $R'(M_{\mathrm{lac}}) < 0$ implies that z_2 is locally asymptotically stable.

(ii) By Lem. 8.10, every orbit converges to a fixed point. Since z_0, z_1, z_2 are the only fixed points,

$$X = B(z_0) \sqcup W^s(z_1) \sqcup B(z_2).$$

The basins $B(z_0)$ and $B(z_2)$ are open because z_0 and z_2 are locally asymptotically stable. If $z \leq w \in B(z_0)$, then order preservation gives

$$0 \leq F^n(z) \leq F^n(w) \longrightarrow z_0,$$

hence $z \in B(z_0)$. Thus $B(z_0)$ is a lower set. Similarly, if $z \geq w \in B(z_2)$, then $F^n(z)$ converges to one of the three fixed points, while

$$F^n(z) \geq F^n(w) \longrightarrow z_2.$$

Since no fixed point lies strictly above z_2, the limit must be z_2. Hence $B(z_2)$ is an upper set.

(iii) Let $0 < \lambda_s < 1 < \lambda_u$ denote the eigenvalues of $DF(z_1)$. Since $\lambda_s \lambda_u = dhg$,

$$\lambda_s = \frac{dhg}{\lambda_u} < dhg < dh.$$

By the stable manifold theorem, z_1 has a one-dimensional local stable manifold $W^s_{\mathrm{loc}}(z_1)$. An eigenvector associated with λ_s may be chosen as

$$(v, w) = (Gh, \lambda_s - dh).$$

Its slope is negative, since $\lambda_s < dh$. Hence, near z_1, $W^s_{\mathrm{loc}}(z_1)$ is a strictly decreasing C^1 curve.

Since F is injective and $\det DF = dhg > 0$, it is a C^1 diffeomorphism onto its image. By the global stable-manifold construction, $W^s(z_1)$ is obtained by backward continuation of $W^s_{\mathrm{loc}}(z_1)$ and is a connected one-dimensional curve.

Next we show that this curve cannot fold in either coordinate direction. Suppose that Σ contained two distinct points

$$z = (m_1, p_1), \qquad \widetilde{z} = (m_2, p_2)$$

with $m_1 \le m_2$ and $p_1 \le p_2$. By Lem. 8.9, both components of $F(z)$ are then strictly smaller than the corresponding components of $F(\widetilde{z})$. Since F is injective, the two iterates remain distinct, and repeated application of Lem. 8.9 gives the same strict componentwise ordering for every positive iterate. On the other hand, both z and $\widetilde{z}$ belong to $W^s(z_1)$, so

$$F^n(z) \longrightarrow z_1, \qquad F^n(\widetilde{z}) \longrightarrow z_1.$$

For all sufficiently large n, both iterates therefore lie on $W^s_{\mathrm{loc}}(z_1)$. This is impossible, since the local stable manifold is a strictly decreasing curve and hence cannot contain two distinct points whose two coordinates are ordered in the same direction.

Consequently, every vertical line intersects Σ in at most one point. Let

$$I_\Sigma := \{m \ge 0 : \text{ there exists } p \ge 0 \text{ with } (m, p) \in \Sigma\}.$$

Since Σ is connected, I_Σ is an interval, and there is a function $\sigma : I_\Sigma \to [0, \infty)$ such that

$$\Sigma = \{(m, \sigma(m)) : m \in I_\Sigma\}.$$

If $m_1 < m_2$ are in I_Σ, the argument above rules out $\sigma(m_1) \le \sigma(m_2)$. Hence

$$\sigma(m_1) > \sigma(m_2),$$

so σ is strictly decreasing. Finally, connectedness of Σ excludes jump discontinuities of the monotone function σ, and therefore σ is continuous. Thus Σ is the graph of a continuous, strictly decreasing function, as claimed. □

Proof of Cor. 3.6.

Proof. Under either hypothesis of Cor. 3.6, one has $\Gamma_\tau > R_{\max}$, equivalently $R_{\max} < \Gamma_\tau$. Hence there is no positive solution of $R(M) = \Gamma_\tau$. Hence z_0 is the unique fixed point, and Lem. 8.11(i) gives local asymptotic stability, while Lem. 8.10 gives convergence of every orbit to z_0. □

8.3 Duration-dependent stimulation, set-duration protocol: Auxiliary results and proofs

Proof of Thm. 3.7

Proof. The linear part L in (32) is upper triangular with diagonal entries dh and g, both in $(0,1)$, so its spectral radius is $\max\{dh, g\} < 1$ and $I - L$ is invertible. Hence F has the unique fixed point $z_{\mathrm{lac}} = (I-L)^{-1}b$, and $z_n - z_{\mathrm{lac}} = L^n(z_0 - z_{\mathrm{lac}}) \to 0$ for every z_0, which is global asymptotic stability. Solving $(I-L)z = b$ componentwise gives $p_{\mathrm{lac}}(1-g) = a(\tau)$ and $m_{\mathrm{lac}}(1-dh) = p_{\mathrm{lac}}Gh$, that is (33); the removed amount is $M_{\mathrm{lac}} = x(z_{\mathrm{lac}})(1-h) = Grp_{\mathrm{lac}}$. Rewriting L^n we can see the convergence for $dh \neq g$ more explicitly from

$$p_n = g^n\big(p_0 - p_{\mathrm{lac}}\big) + p_{\mathrm{lac}}, \qquad m_n = (dh)^n\big(m_0 - m_{\mathrm{lac}}\big) + Gh\,\frac{(dh)^n - g^n}{dh - g}\big(p_0 - p_{\mathrm{lac}}\big) + m_{\mathrm{lac}}. \quad (64)$$

The case $dh = g$ follows by taking the limit $dh \to g$. In either case the convergence is exponential. Finally $F(0,0) = (0, a(\tau)) \neq (0,0)$, so the origin is not fixed. □

8.4 Duration-dependent stimulation, set-target protocol: Auxiliary results and proofs

Proof of Thm. 3.8.

Proof. **Existence of fixed points.** We have already established in Sec. 3.4 that for $0 < M_{\mathrm{tar}} < M_{\mathrm{emp}}(T)$ there exists a unique target-met fixed point as defined in (39) with τ the unique solution to (37). We have also shown that if $M_{\mathrm{tar}} > M_{\mathrm{emp}}(T)$, there exists a unique emptying fixed point given by (35). At $M_{\mathrm{tar}} = M_{\mathrm{emp}}(T)$ the two branches meet. Furthermore, $F(0,0) = (0, a(\tau_{\mathrm{emp}}))$, so the origin is not a fixed point.

Stability of the target-met fixed point. To determine local stability, we apply the Jury conditions (Elaydi 2005; Jury 1974) for a two-dimensional discrete map. For the Jacobian

$$J = \begin{pmatrix} d & G \\ -cd & g - cG \end{pmatrix}, \qquad c := \frac{\tau a'(\tau)}{x_{\mathrm{tar}}} > 0,$$

we have

$$\det J = dg, \qquad \mathrm{Tr}J = d + g - cG.$$

Local asymptotic stability requires

$$1 - \det J > 0, \qquad 1 - \mathrm{Tr}J + \det J > 0, \qquad 1 + \mathrm{Tr}J + \det J > 0.$$

The first two conditions are automatically satisfied, since

$$1 - \det J = 1 - dg > 0, \qquad 1 - \mathrm{Tr}J + \det J = (1-d)(1-g) + cG > 0.$$

Hence stability is determined entirely by the remaining condition

$$1 + \mathrm{Tr}J + \det J = (1+d)(1+g) - cG > 0.$$

The second Jury condition excludes a stability loss through $\lambda = +1$, while $\det J = dg < 1$ excludes a complex-conjugate pair crossing the unit circle. Hence the only possible local stability loss is through $\lambda = -1$.

Using the definitions of E_a and E_{crit} in (40) and using (39), we can write

$$cG = (1-g)(1-dh)E_a(\tau),$$

so that the remaining Jury condition is equivalent to

$$E_a(\tau) < E_{\text{crit}}(T, \tau).$$

At equality, one eigenvalue is $\lambda = -1$ and the other is $\lambda = -dg \in (-1, 0)$.

Stability of the emptying fixed points. For $M_{\text{tar}} > M_{\text{emp}}(T)$ the emptied fixed point lies strictly inside the emptying region, where

$$DF = \begin{pmatrix} 0 & 0 \\ 0 & g \end{pmatrix}.$$

Its eigenvalues are 0 and $g \in (0, 1)$, so it is locally asymptotically stable. □

Proof of Cor. 3.9.

Proof. Since $a(\tau) = \tau R_d(\tau)$, we have

$$E_a(\tau) = 1 + \frac{\tau R_d'(\tau)}{R_d(\tau)}.$$

Because $E_{\text{crit}}(T, \tau) > 1$, any τ with $R_d'(\tau) \leq 0$ gives $E_a(\tau) \leq 1 < E_{\text{crit}}(T, \tau)$ and therefore a stable target-met fixed point.

Conversely, suppose $R_d'(\tau_0) > 0$ for some $\tau_0 \in (0, \tau_{\text{emp}})$. Then $E_a(\tau_0) > 1$. For fixed τ_0, $E_{\text{crit}}(T, \tau_0)$ decreases continuously and strictly from ∞ to 1 as T increases from 0 to ∞. Hence there is a unique $T_{\text{thresh}}(\tau_0)$ such that

$$E_{\text{crit}}(T_{\text{thresh}}, \tau_0) = E_a(\tau_0),$$

and the corresponding target-met fixed point is unstable for $T > T_{\text{thresh}}(\tau_0)$. Choosing

$$M_{\text{tar}} = \frac{r(T, \tau_0) a(\tau_0)}{\Gamma(T)}$$

produces the required set-target schedule. □

Explicit instability boundary for the Hill response. For

$$a(\tau) = a_{\max} \frac{\tau^2}{\tau^2 + \mu_\tau^2},$$

one has

$$E_a(\tau) = \frac{2\mu_\tau^2}{\tau^2 + \mu_\tau^2}.$$

Substitution into $E_a(\tau) = E_{\text{crit}}(T, \tau)$, using $h = 1 - \tau/\tau_{\text{emp}}$, gives after rearrangement

$$(1 + d)(1 + g)\tau^2 - 2\mu_\tau^2 d(1 - g)\tau/\tau_{\text{emp}} + \mu_\tau^2(-1 + 3d + 3g - dg) = 0. \tag{65}$$

Small target approximation We derived the small target limit as follows: 1. the exact target-met recurrence for x_n is

$$x_{n+1} = (d+g)x_n - d\,g x_{n-1} - d(1-g)M_{\text{tar}} + Ga\left(\frac{M_{\text{tar}}}{x_n}\tau_{\text{emp}}\right).$$

Rescaling $x_n = M_{\text{tar}}^{2/3} z_n$ and letting $M_{\text{tar}} \to 0$ gives

$$z_{n+1} = (d+g)z_n - d\,g z_{n-1} + Ga_{\max}\left(\frac{\tau_{\text{emp}}}{\mu_\tau z_n}\right)^2.$$

After $z_n = y_n\left[Ga_{\max}\left(\frac{\tau_{\text{emp}}}{\mu_\tau}\right)^2\right]^{1/3}$, the leading order map is simply

$$y_{n+1} = (d+g)y_n - d\,g y_{n-1} + \frac{1}{y_n^2}.$$

For sufficiently long wait times $dg = e^{-(\delta+\gamma)T}$ is small, hence the limiting recurrence is close to

$$y_{n+1} = (d+g)y_n + \frac{1}{y_n^2},$$

which with $q_n = (d+g)^{-1/3} y_n^{-1}$ is equivalent to

$$q_{n+1} = \frac{\lambda q_n}{1+q_n^3}, \qquad \lambda = \frac{1}{d+g}.$$

This is the Maynard Smith-Slatkin population model (Smith and Slatkin 1973), which has the same structure as the right-hand side of the logistic map $q_{n+1} = rq_n(1-q_n)$: A unimodal shape with unique maximum. Thus, in the combined small-target and strongly dissipative regime, the lactation map approaches a one-dimensional smooth unimodal map with a quadratic critical point, providing a natural explanation for the numerically observed period-doubling cascade and apparent chaotic behaviour.

8.5 Protocol Comparison: Auxiliary results and proofs

Proof of Lem. 3.11

Proof. Let $h_* = h(\tau_*)$ and let x_* denote the amount available immediately before removal. At a steady state,

$$M_* = (1-h_*)x_*, \qquad m_* = h_* x_*.$$

Using $x_* = dm_* + Gp_*$ gives

$$Gp_* = x_*(1-dh_*) = M_*\frac{1-dh_*}{1-h_*} = \frac{M_*}{r(T,\tau_*)}.$$

The steady-state production balance is

$$(1-g)p_* = a_*.$$

Since $\Gamma(T) = (1-g)/G$, combining the two relations yields

$$\frac{a_*}{M_*} = \frac{\Gamma(T)}{r(T,\tau_*)}.$$

At complete emptying $h_* = 0$ and hence $r(T,\tau_*) = 1$. □

8.6 Daily Milk Output: Auxiliary results and proofs

The following calculations are used in the below proofs. For r as defined in (25), we have before emptying

$$\partial_\tau r(T,\tau) = -h'(\tau)\frac{(1-d(T))}{(1-d(T)h(\tau))^2} > 0 \tag{66}$$

$$\partial_T r(T,\tau) = d'(T)\frac{h(\tau)(1-h(\tau))}{(1-d(T)h(\tau))^2} < 0 \tag{67}$$

Proof of Lem. 4.1.

Proof. Recall that $\Gamma(T)$ is strictly increasing in T.

For set-duration removal with amount-dependent stimulation, the steady-state balance is

$$R(M_*) = \frac{\Gamma(T)}{r(T,\tau)}.$$

Along a stable positive branch $R'(M_*) < 0$. Using (66) and (67), one has

$$\partial_T\left(\frac{\Gamma}{r}\right) > 0, \qquad \partial_\tau\left(\frac{\Gamma}{r}\right) < 0,$$

implicit differentiation therefore gives $\partial_T M_* < 0$ and $\partial_\tau M_* > 0$ before complete emptying. For duration-dependent stimulation,

$$M_* = \frac{r(T,\tau)a(\tau)}{\Gamma(T)}.$$

Using (66), (67), $\Gamma'(T) > 0$ and $a'(\tau) > 0$, we again obtain $\partial_T M_* < 0$ and $\partial_\tau M_* > 0$.

Finally, for $\tau \geq \tau_{\text{emp}}$ one has $r = 1$. Hence under amount-dependent stimulation the steady-state condition $R(M_*) = \Gamma(T)$ is independent of τ, whereas under duration-dependent stimulation

$$M_* = \frac{a(\tau)}{\Gamma(T)}$$

continues to increase with τ. This completes the proof. □

Proof of Lem. 4.2.

Proof. Fix $0 < T < T_{\text{crit}}$. Along a stable positive steady state,

$$R(M_*) = \frac{\Gamma(T)}{r(T,\tau)}, \qquad R'(M_*) < 0.$$

Implicit differentiation with respect to τ gives

$$R'(M_*)\,\partial_\tau M_* = -\frac{\Gamma(T)\partial_\tau r}{r^2}.$$

Defining

$$E_R(M) := \frac{MR'(M)}{R(M)}, \tag{68}$$

we obtain

$$Q(T,\tau) = (T+\tau)\frac{\partial_\tau M_*}{M_*} = -(T+\tau)\frac{\partial_\tau r}{r}\frac{1}{E_R(M_*)}.$$

Before complete emptying, $r(T,\tau) > 0$ and $\partial_\tau r(T,\tau) > 0$. Moreover, as $\tau \downarrow \tau_{\min}(T)$,

$$\frac{\Gamma(T)}{r(T,\tau)} \longrightarrow R_{\max}.$$

For a decreasing-efficiency response, this implies $M_*(T,\tau) \to 0$. Since $a(0) = 0$, a is differentiable at zero, and $R_{\max} = a'(0) > 0$, we have

$$E_R(M) = \frac{Ma'(M)}{a(M)} - 1 \longrightarrow 0 \qquad \text{as } M \to 0^+.$$

For a unimodal-efficiency response, the stable steady state satisfies $M_* > M_{\text{peak}}$ and approaches M_{peak} as $\tau \downarrow \tau_{\min}(T)$. Since $R'(M_{\text{peak}}) = 0$, it follows that

$$E_R(M_*) \longrightarrow 0^-.$$

Thus, we have $E_R(M_*) \longrightarrow 0^-$ in both cases, whereas

$$(T+\tau)\frac{\partial_\tau r}{r}$$

approaches a finite positive value. Consequently,

$$Q(T,\tau) \longrightarrow +\infty \qquad \text{as } \tau \downarrow \tau_{\min}(T).$$

Hence $Q(T,\tau) > 1$ for all $\tau > \tau_{\min}(T)$ sufficiently close to $\tau_{\min}(T)$. By (50), $M_{\text{DAY}}(T,\tau)$ is strictly increasing for $\tau > \tau_{\min}(T)$ sufficiently close to $\tau_{\min}(T)$, as claimed. □

Proof of Prop. 4.3.

Proof. Fix $T \in (0, T_{\text{crit}})$ and suppress the dependence on T. For $\tau_{\min} < \tau < \tau_{\text{emp}}$, define

$$\sigma(\tau) := (T+\tau)\partial_\tau M_*(T,\tau) - M_*(T,\tau).$$

Then

$$\partial_\tau M_{\text{DAY}}(T,\tau) = \frac{24}{(T+\tau)^2}\sigma(\tau),$$

while the concavity assumption gives

$$\sigma'(\tau) = (T+\tau)\partial_\tau^2 M_*(T,\tau) < 0.$$

Thus σ, and hence the sign-determining numerator of $\partial_\tau M_{\text{DAY}}$, is strictly decreasing before complete emptying.

By Lem. 4.2, $M_{\text{DAY}}(T,\tau)$ is strictly increasing for τ sufficiently close to $\tau_{\min}(T)$, so $\sigma(\tau) > 0$ there. At the other end of the interval, (50) and the definition of $Q_A^{\text{pre}}(T)$ imply that the sign of the left limit of $\partial_\tau M_{\text{DAY}}$ at τ_{emp} is the sign of $Q_A^{\text{pre}}(T) - 1$.

If $Q_A^{\text{pre}}(T) < 1$, then $\sigma < 0$ for τ sufficiently close to τ_{emp}. Since σ is strictly decreasing, it has exactly one zero $\tau_{\text{opt}} \in (\tau_{\min}, \tau_{\text{emp}})$. At this point M_{DAY} changes from increasing to decreasing, so

τ_{opt} is the unique maximum before complete emptying. By (50), it is equivalently characterized by $Q(T, \tau_{\mathrm{opt}}) = 1$.

If $Q_A^{\mathrm{pre}}(T) \geq 1$, strict monotonicity of σ, together with $\sigma > 0$ near $\tau_{\min}$, implies $\sigma(\tau) > 0$ for all $\tau_{\min} < \tau < \tau_{\mathrm{emp}}$; in the case $Q_A^{\mathrm{pre}}(T) = 1$, σ approaches zero only at τ_{emp}. Hence M_{DAY} increases up to complete emptying.

Finally, for $\tau \geq \tau_{\mathrm{emp}}$, complete emptying has already been reached and, under amount-dependent stimulation, $M_*(T, \tau)$ is independent of τ. Therefore $M_{\mathrm{DAY}}(T, \tau) = 24 M_*(T, \tau_{\mathrm{emp}})/(T+\tau)$ is strictly decreasing for $\tau > \tau_{\mathrm{emp}}$. Thus the unique maximum is attained at τ_{emp} whenever $Q_A^{\mathrm{pre}}(T) \geq 1$. □

Proof of Cor. 4.4.

Proof. At complete emptying, $R(M_{\mathrm{emp}}(T)) = \Gamma(T)$. Hence defining $E_R(M)$ as in (68), we have

$$Q_A^{\mathrm{pre}}(T) = -\left(1 + \frac{T}{\tau_{\mathrm{emp}}}\right) \frac{1 - d(T)}{E_R(M_{\mathrm{emp}}(T))}.$$

As $T \to 0^+$, we have $d(T) \to 1$ and $\Gamma(T) \to \gamma < R_{\max}$. Therefore $M_{\mathrm{emp}}(T)$ converges to the stable solution of $R(M) = \gamma$, for which $E_R(M) < 0$ is finite. Since $1 - d(T) \to 0$, it follows that

$$Q_A^{\mathrm{pre}}(T) \longrightarrow 0 \qquad \text{as } T \to 0^+.$$

Thus $Q_A^{\mathrm{pre}}(T) < 1$ for all sufficiently small $T > 0$.

Next let $T \to T_{\mathrm{crit}}^-$. Since $\Gamma(T) \to R_{\max}$, the stable solution $M_{\mathrm{emp}}(T)$ approaches the point at which R attains its maximum. For a decreasing-efficiency response this is $M = 0$, and $E_R(M_{\mathrm{emp}}(T)) \to 0^-$. For a unimodal-efficiency response, $M_{\mathrm{emp}}(T) \to M_{\mathrm{peak}}$, where $R'(M_{\mathrm{peak}}) = 0$, and again $E_R(M_{\mathrm{emp}}(T)) \to 0^-$. Meanwhile, $(1 + T/\tau_{\mathrm{emp}})\,(1 - d(T))$ approaches a finite positive value. Hence

$$Q_A^{\mathrm{pre}}(T) \longrightarrow +\infty \qquad \text{as } T \to T_{\mathrm{crit}}^-.$$

Therefore $Q_A^{\mathrm{pre}}(T) > 1$ for $T < T_{\mathrm{crit}}$ sufficiently close to T_{crit}.

Finally, $Q_A^{\mathrm{pre}}(T)$ is continuous for $0 < T < T_{\mathrm{crit}}$. By the intermediate value theorem, there exists at least one $T_{\mathrm{reach}} \in (0, T_{\mathrm{crit}})$ satisfying $Q_A^{\mathrm{pre}}(T_{\mathrm{reach}}) = 1$. The location of the daily-output maximum then follows directly from Prop. 4.3. □

Proof of Lem. 4.5.

Proof. For duration-dependent stimulation,

$$M_*(T, \tau) = \frac{r(T, \tau) a(\tau)}{\Gamma(T)}.$$

Hence, for fixed T,

$$\frac{\partial_\tau M_*}{M_*} = \frac{\partial_\tau r}{r} + \frac{a'(\tau)}{a(\tau)},$$

and therefore

$$Q(T, \tau) = \left(1 + \frac{T}{\tau}\right)\left(E_a(\tau) + E_r(T, \tau)\right), \qquad E_r(T, \tau) := \frac{\tau \partial_\tau r(T, \tau)}{r(T, \tau)}.$$

Before complete emptying, the linear removal law gives

$$r(T, \tau) = \frac{\tau/\tau_{\mathrm{emp}}}{1 - d(T) + d(T)\tau/\tau_{\mathrm{emp}}},$$

and hence

$$E_r(T,\tau) = \frac{1-d(T)}{1-d(T)+d(T)\tau/\tau_{\text{emp}}}.$$

Thus $E_r(T,\tau) > 0$ and is strictly decreasing in τ. Since $E_a(\tau) > 0$ is also strictly decreasing, both factors in the expression for $Q(T,\tau)$ are positive and strictly decreasing. Hence $Q(T,\tau)$ is strictly decreasing for $0 < \tau < \tau_{\text{emp}}$.

For $\tau > \tau_{\text{emp}}$, one has $r(T,\tau) = 1$ and therefore $E_r(T,\tau) = 0$. Thus $Q(T,\tau) = (1+T/\tau)E_a(\tau)$, which is again strictly decreasing.

As $\tau \to 0^+$, $E_r(T,\tau) \to 1$, while $1+T/\tau \to \infty$, and hence $Q(T,\tau) \to \infty$. As $\tau \to \infty$, $1+T/\tau \to 1$ and $E_a(\tau) \to 0$, so $Q(T,\tau) \to 0$.

Finally, at complete emptying, $E_r(T,\tau_{\text{emp}}^-) = 1-d(T)$ and $E_r(T,\tau_{\text{emp}}^+) = 0$. Therefore

$$Q_D^{\text{pre}}(T) = \left(1+\frac{T}{\tau_{\text{emp}}}\right)\left[E_a(\tau_{\text{emp}}) + 1 - d(T)\right],$$

whereas

$$Q_D^{\text{post}}(T) = \left(1+\frac{T}{\tau_{\text{emp}}}\right)E_a(\tau_{\text{emp}}).$$

Since $0 < d(T) < 1$ for $T > 0$, it follows immediately that $Q_D^{\text{post}}(T) < Q_D^{\text{pre}}(T)$. □

Proof of Prop. 4.6.

Proof. Fix $T > 0$. By (50), the sign of $\partial_\tau M_{\text{DAY}}(T,\tau)$ is determined by whether $Q(T,\tau)$ is larger or smaller than one. By Lem. 4.5, $Q(T,\tau)$ is strictly decreasing on each side of τ_{emp}, with

$$\lim_{\tau\to 0^+} Q(T,\tau) = \infty, \qquad \lim_{\tau\to\infty} Q(T,\tau) = 0,$$

and one-sided values $Q_D^{\text{pre}}(T) > Q_D^{\text{post}}(T)$ at complete emptying.

Suppose first that $Q_D^{\text{pre}}(T) < 1$. Since Q decreases from infinity to $Q_D^{\text{pre}}(T)$ on $0 < \tau < \tau_{\text{emp}}$, there is a unique $\tau_{\text{opt}} < \tau_{\text{emp}}$ such that $Q(T,\tau_{\text{opt}}) = 1$. Thus M_{DAY} increases before τ_{opt} and decreases afterwards. Since $Q_D^{\text{post}}(T) < Q_D^{\text{pre}}(T) < 1$, it continues to decrease for all $\tau > \tau_{\text{emp}}$. Hence τ_{opt} is the unique global maximum.

Next suppose that $Q_D^{\text{post}}(T) \le 1 \le Q_D^{\text{pre}}(T)$. Strict monotonicity of Q implies $Q(T,\tau) > 1$ for every $0 < \tau < \tau_{\text{emp}}$, while $Q(T,\tau) < 1$ for every $\tau > \tau_{\text{emp}}$. Hence M_{DAY} increases up to complete emptying and decreases afterwards, so its unique maximum is attained at $\tau = \tau_{\text{emp}}$.

Finally, suppose that $Q_D^{\text{post}}(T) > 1$. Then also $Q_D^{\text{pre}}(T) > 1$, so M_{DAY} is increasing throughout $0 < \tau \le \tau_{\text{emp}}$. For $\tau > \tau_{\text{emp}}$, Q decreases strictly from $Q_D^{\text{post}}(T) > 1$ to zero. Therefore there is a unique $\tau_{\text{opt}} > \tau_{\text{emp}}$ satisfying $Q(T,\tau_{\text{opt}}) = 1$, with M_{DAY} increasing before and decreasing after this point. Thus τ_{opt} is the unique global maximum.

This proves all three cases. Whenever the maximum lies away from complete emptying, its unique location is characterized by $Q(T,\tau_{\text{opt}}) = 1$. □

Proof of Cor. 4.7.

Proof. By Lem. 4.5,

$$Q_D^{\mathrm{pre}}(T) = (1 + T/\tau_{\mathrm{emp}}) \left[E_a(\tau_{\mathrm{emp}}) + 1 - d(T)\right], \qquad Q_D^{\mathrm{post}}(T) = (1 + T/\tau_{\mathrm{emp}}) E_a(\tau_{\mathrm{emp}}),$$

where $d(T) = e^{-\delta T}$. Since $T > 0$, we immediately have $Q_D^{\mathrm{post}}(T) < Q_D^{\mathrm{pre}}(T)$.

Moreover,

$$\frac{d}{dT} Q_D^{\mathrm{post}}(T) = E_a(\tau_{\mathrm{emp}})/\tau_{\mathrm{emp}} > 0,$$

while

$$\frac{d}{dT} Q_D^{\mathrm{pre}}(T) = \left[E_a(\tau_{\mathrm{emp}}) + 1 - d(T)\right]/\tau_{\mathrm{emp}} + (1 + T/\tau_{\mathrm{emp}}) \delta d(T) > 0.$$

Hence both quantities are strictly increasing with T.

Since $d(T) \to 1$ as $T \to 0^+$, both $Q_D^{\mathrm{pre}}(T)$ and $Q_D^{\mathrm{post}}(T)$ converge to $E_a(\tau_{\mathrm{emp}})$. As $T \to \infty$, the factor $1 + T/\tau_{\mathrm{emp}}$ diverges, while $E_a(\tau_{\mathrm{emp}}) > 0$; hence both quantities tend to infinity.

Suppose first that $E_a(\tau_{\mathrm{emp}}) < 1$. By continuity and strict monotonicity, there exist unique $T_{\mathrm{reach}} > 0$ and $T_{\mathrm{pass}} > 0$ satisfying $Q_D^{\mathrm{pre}}(T_{\mathrm{reach}}) = 1$ and $Q_D^{\mathrm{post}}(T_{\mathrm{pass}}) = 1$, respectively. Since $Q_D^{\mathrm{post}}(T_{\mathrm{reach}}) < Q_D^{\mathrm{pre}}(T_{\mathrm{reach}}) = 1$, strict monotonicity of Q_D^{post} implies $T_{\mathrm{reach}} < T_{\mathrm{pass}}$. The three regimes for the location of the maximum then follow directly from Prop. 4.6.

Finally, if $E_a(\tau_{\mathrm{emp}}) \geq 1$, then for every $T > 0$, $Q_D^{\mathrm{post}}(T) = (1 + T/\tau_{\mathrm{emp}}) E_a(\tau_{\mathrm{emp}}) > 1$. Hence Prop. 4.6 implies that the maximum lies after complete emptying for every $T > 0$. □

Proof of Lemma 4.8.

Proof. Before complete emptying, $M_{\mathrm{tar}} = M_*(T, \tau)$ is strictly increasing with τ. Hence the maximum at $M_{\mathrm{tar},opt}$ corresponds to a pre-emptying maximum at a unique removal duration $\tau_{\mathrm{opt}} < \tau_{\mathrm{emp}}$.

At such a maximum, $Q(T, \tau_{\mathrm{opt}}) = 1$, and therefore

$$E_a(\tau_{\mathrm{opt}}) = \frac{\tau_{\mathrm{opt}}}{T + \tau_{\mathrm{opt}}} - \tau_{\mathrm{opt}} \frac{\partial_\tau r(T, \tau_{\mathrm{opt}})}{r(T, \tau_{\mathrm{opt}})} < 1.$$

On the other hand, a target-met fixed point can lose stability only when

$$E_a(\tau) = E_{\mathrm{crit}}(T, \tau),$$

with $E_{\mathrm{crit}}(T, \tau) > 1$. Hence the fixed point corresponding to $M_{\mathrm{tar},opt}$ is locally asymptotically stable. □

References

S. Agudelo-Pérez, D. Botero-Rosas, L. Rodríguez-Alvarado, J. Espitia-Angel, and L. Raigoso-Díaz. Artificial intelligence applied to the study of human milk and breastfeeding: A scoping review. *Int Breastfeed J*, 19:79, 2024. https://doi.org/10.1186/s13006-024-00686-1.

J. Azarnoosh and F. Hassanipour. Fluid-structure interaction modeling of lactating breast. *J Biomech*, 103:109640, 2020. https://doi.org/10.1016/j.jbiomech.2020.109640.

C. W. Clark. *Mathematical Bioeconomics: The Optimal Management of Renewable Resources*. Wiley-Interscience, New York, 2 edition, 1990.

D. B. Cox, R. A. Owens, and P. E. Hartmann. Blood and milk prolactin and the rate of milk synthesis in women. *Exp Physiol*, 81(6):1007–1020, 1996. https://doi.org/10.1113/expphysiol.1996.sp003985.

S. E. Daly, J. C. Kent, R. A. Owens, and P. E. Hartmann. Frequency and degree of milk removal and the short-term control of human milk synthesis. *Exp Physiol*, 81(5):861–875, 1996. https://doi.org/10.1113/expphysiol.1996.sp003982.

J. Dijkstra, J. France, M. S. Dhanoa, J. A. Maas, M. D. Hanigan, A. J. Rook, and D. E. Beever. A model to describe growth patterns of the mammary gland during pregnancy and lactation. *J Dairy Sci*, 80(10):2340–2354, 1997. https://doi.org/10.3168/jds.S0022-0302(97)76185-X.

S. Elaydi. *An Introduction to Difference Equations*. Springer, New York, 3 edition, 2005. https://doi.org/10.1007/0-387-27602-5.

K. R. Faulkner. Modeling milk production in the lactation period and the effect of feeding frequency on milk production. Master's thesis, University of British Columbia, 2019. URL https://open.library.ubc.ca/cIRcle/collections/ubctheses/24/items/1.0380624.

L. Gatti. Maternal perceptions of insufficient milk supply in breastfeeding. *J Nurs Scholarsh*, 40 (4):355–363, 2008. https://doi.org/10.1111/j.1547-5069.2008.00234.x.

N. Haiden and E. E. Ziegler. Human milk banking. *Ann Nutr Metab*, 69(Suppl. 2):8–15, 2016. https://doi.org/10.1159/000452821.

X. Jin, C. T. Lai, S. L. Perrella, X. Zhou, G. M. Hassan, J. L. McEachran, Z. Gridneva, N. L. Taylor, M. E. Wlodek, and D. T. Geddes. Milk composition is predictive of low milk supply using machine learning approaches. *Diagnostics (Basel)*, 15(2):191, 2025. https://doi.org/10.3390/diagnostics15020191.

E. I. Jury. *Inners and Stability of Dynamic Systems*. John Wiley & Sons, New York, 1974.

J. C. Kent, L. R. Mitoulas, D. B. Cox, R. A. Owens, and P. E. Hartmann. Breast volume and milk production during extended lactation in women. *Exp Physiol*, 84(2):435–447, 1999. https://doi.org/10.1111/j.1469-445X.1999.01808.x.

J. C. Kent, L. R. Mitoulas, M. D. Cregan, D. T. Ramsay, D. A. Doherty, and P. E. Hartmann. Volume and frequency of breastfeedings and fat content of breast milk throughout the day. *Pediatrics*, 117(3):e387–e395, 2006. https://doi.org/10.1542/peds.2005-1417.

J. C. Kent, D. K. Prime, and C. P. Garbin. Principles for maintaining or increasing breast milk production. *J Obstet Gynecol Neonatal Nurs*, 41(1):114–121, 2012. https://doi.org/10.1111/j.1552-6909.2011.01313.x.

V. Lakshmikantham and P. S. Simeonov. *Theory of impulsive differential equations*, volume 6. World scientific, 1989.

J. Lawson and E. Braverman. Optimality and sustainability of delayed impulsive harvesting. *Comm Nonlin Science Num Sim*, 117:106914, 2023. https://doi.org/10.1016/j.cnsns.2022.106914.

A. S. McNeilly, I. C. Robinson, M. J. Houston, and P. W. Howie. Release of oxytocin and prolactin in response to suckling. *Br Med J (Clin Res Ed)*, 286(6361):257–259, 1983. https://doi.org/10.1136/bmj.286.6361.257.

P. P. Meier, A. L. Patel, R. Hoban, and J. L. Engstrom. Which breast pump for which mother: An evidence-based approach to individualizing breast pump technology. *J Perinatol*, 36(7):493–499, 2016. https://doi.org/10.1038/jp.2016.14.

S. N. Mortazavi, F. Hassiotou, D. T. Geddes, and F. Hassanipour. Mathematical modeling of mammary ducts in lactating human females. *J Biomech Eng*, 137(7):071009, 2015. https://doi.org/10.1115/1.4028967.

S. N. Mortazavi, D. Geddes, and F. Hassanipour. Lactation in the human breast from a fluid dynamics point of view. *J Biomech Eng*, 139(1):011009, 2017. https://doi.org/10.1115/1.4034995.

M. Peaker and C. J. Wilde. Feedback control of milk secretion from milk. *J Mammary Gland Biol Neoplasia*, 1(3):307–315, 1996. https://doi.org/10.1007/BF02018083.

M. Rios-Leyvraz and Q. Yao. The volume of breast milk intake in infants and young children: A systematic review and meta-analysis. *Breastfeed Med*, 18(3):188–197, 2023. https://doi.org/10.1089/bfm.2022.0281.

H. L. Smith. Planar competitive and cooperative difference equations. *J Differ Equ Appl*, 3(5-6):335–357, 1998. https://doi.org/10.1080/10236199708808108.

J. M. Smith and M. Slatkin. The stability of predator-prey systems. *Ecology*, 54(2):384–391, 1973. https://doi.org/10.2307/1934346.

S. Truchet and E. Honvo-Houéto. Physiology of milk secretion. *Best Pract Res Clin Endocrinol Metab*, 31(4):367–384, 2017. https://doi.org/10.1016/j.beem.2017.10.008.

I. Vetharaniam, S. R. Davis, T. K. Soboleva, P. R. Shorten, and G. C. Wake. Modeling the interaction of milking frequency and nutrition on mammary gland growth and lactation. *J Dairy Sci*, 86(6):1987–1996, 2003. https://doi.org/10.3168/jds.S0022-0302(03)73787-4.

S. R. Weaver and L. L. Hernandez. Autocrine-paracrine regulation of the mammary gland. *J Dairy Sci*, 99(1):842–853, 2016. https://doi.org/10.3168/jds.2015-9828.

X. Zhang, Z. Shuai, and K. Wang. Optimal impulsive harvesting policy for single population. *Nonlin Analysis: Real World Appl*, 4(4):639–651, 2003. https://doi.org/10.1016/S1468-1218(02)00084-6.